UNIVERSITÄT ZU LÜBECK

From the Priority Research Area Infections
Research Center Borstel-Leibniz Lung Center
Director: Prof. Dr. Ulrich E. Schaible

Division of Microbial Interface Biology
PD Dr. Norbert Reiling

Identification and Characterisation of Novel Antimicrobials against *Mycobacterium tuberculosis*

Dissertation
for Fulfilment of Requirements
for the Doctoral Degree
of the University of Lübeck

from the Department of Natural Sciences

Submitted by

Vidhisha Vijay Sonawane

from Pune, India

Lübeck, 2024

First referee: PD Dr. Norbert Reiling

Second referee: Prof. Dr. Jan Rupp

Date of oral examination: 17 September 2024

Approved for printing.: Lübeck, 18 September 2024

Declaration

Hereby I declare that I have written this dissertation completely on my own. Furthermore, I confirm that no other sources have been used than those specified in the dissertation itself.

This dissertation, in the same or similar form, has not been submitted to any other doctoral degree committee yet.

Vidhisha Vijay Sonawane

Hamburg, 17/06/2024

Table of Contents

Chapter 1

Introduction

1.1 Tuberculosis

1.1.1 Overview

In 1882, Robert Koch made a groundbreaking discovery by identifying the tubercle bacillus, *Mycobacterium tuberculosis* (Mtb), as the causative agent of tuberculosis (TB) (2). Even today TB remains a persistent global health challenge continuing to spread across the globe. This highly contagious airborne disease is one of the leading causes of mortality worldwide (3).

While TB predominantly affects the lungs (pulmonary TB), it can also disseminate to other parts of the body and result in extrapulmonary TB (3). Moreover, Mtb can remain dormant in the human body for extended periods, causing no symptoms and leading many individuals to become asymptomatic carriers of the bacterium (Latent TB) (4). According to the 2022 report by the World Health Organization (WHO), approximately one-quarter of the global population, about 2 billion people, are latently infected with Mtb. For those with latent TB infections (LTBI), there is a 5-10% lifetime risk of reactivation, leading to active TB disease (3).

Early diagnosis and effective treatment are important in preventing the spread of TB and the development of drug-resistant strains (5). Several diagnostic methods are routinely used, including immunological tests like the QuantiFERON-TB Gold (QFT) and the Tuberculin skin test (Mantoux test), radiography (Chest X-rays), as well as microscopical, bacterial culture, and clinical methods (5). While immunological tests and radiography are valuable for screening and diagnosing active pulmonary TB, they fall short in detecting latent TB infections.

The clinical symptoms of active pulmonary TB can include pleuritic chest pain, low-grade fever, prolonged productive cough, haemoptysis, fatigue, loss of appetite, night sweats, and weight loss (5, 6). Currently, there is no effective vaccine to prevent TB in adults (3). The bacille Calmette-Guérin (BCG) vaccine, developed nearly a century ago, remains the only licensed TB vaccine. It provides moderate protection in infants and children, particularly against severe forms of TB such as TB meningitis (3)

In summary, to tackle the global TB epidemic it is critical to develop better diagnostic tools, effective vaccines and improved treatment therapies. Furthermore, a comprehensive understanding of TB pathogenesis is essential for improving TB treatment strategies. Such knowledge will facilitate the development of innovative host-directed therapeutic approaches, which can be used alongside antibiotics to more effectively manage and eradicate TB.

1.1.2 TB pathogenesis

The pathogenic life cycle of Mtb is complex and critical for understanding its transmission and persistence. When a patient with active TB coughs, sneezes or talks, TB is spread through aerosol droplets to other healthy hosts (6). Once these droplets are inhaled by a new host, the bacteria travel through the respiratory tract and reach the lungs of the host. The host's innate immune system attempts to fight the infection by phagocytosing the tubercle bacilli by alveolar macrophages. However, if the macrophages fail to eliminate the bacteria, Mtb multiplies within the macrophages, is released, and subsequently phagocytosed by other macrophages, repeating the cycle (6).

At the infection site, neutrophils and lymphocytes are recruited, initiating a cell-mediated immune response where immune cells accumulate to contain the bacteria and limit its multiplication. During this phase, the host remains asymptomatic and the bacteria may either be eliminated or enter a latent state (7). In individuals with a weakened immune system, the disease can progress immediately to active TB, characterized by clinical symptoms.

If the bacteria are not eliminated, they enter latency inside a granuloma (8). The granuloma is a hallmark of pulmonary TB and it consists of macrophages and other immune cells that work to contain the bacteria. In immunocompetent individuals, while the granuloma does not eliminate Mtb, it restricts the bacteria and prevents progression to active disease. However, Mtb survives within the granuloma by blocking phagolysosome fusion thereby evading the host's immune response which allows it to persist in a non-replicating or slowly replicating state. This state of latency poses significant challenges for current TB therapies, which struggle to target the pathogen within the granuloma (8).

As the granuloma matures, macrophages differentiate into foamy macrophages and other cell types **(Figure 1).** The centre of the granuloma may undergo necrosis that results in a caseous granuloma characterized by a cheese-like accumulation of necrotic debris (9). Foamy macrophages are filled with lipid droplets and surround the necrotic core of the granuloma. Mtb disrupts host lipid metabolism which leads to the formation of these lipid-rich cells that support bacterial persistence and contribute to caseum accumulation (10, 11). Another factor reported to contribute to the differentiation of macrophages into foam cells is Mycolic acids. These are a component of the Mtb cell wall that are essential for mycobacterial growth (12, 13).

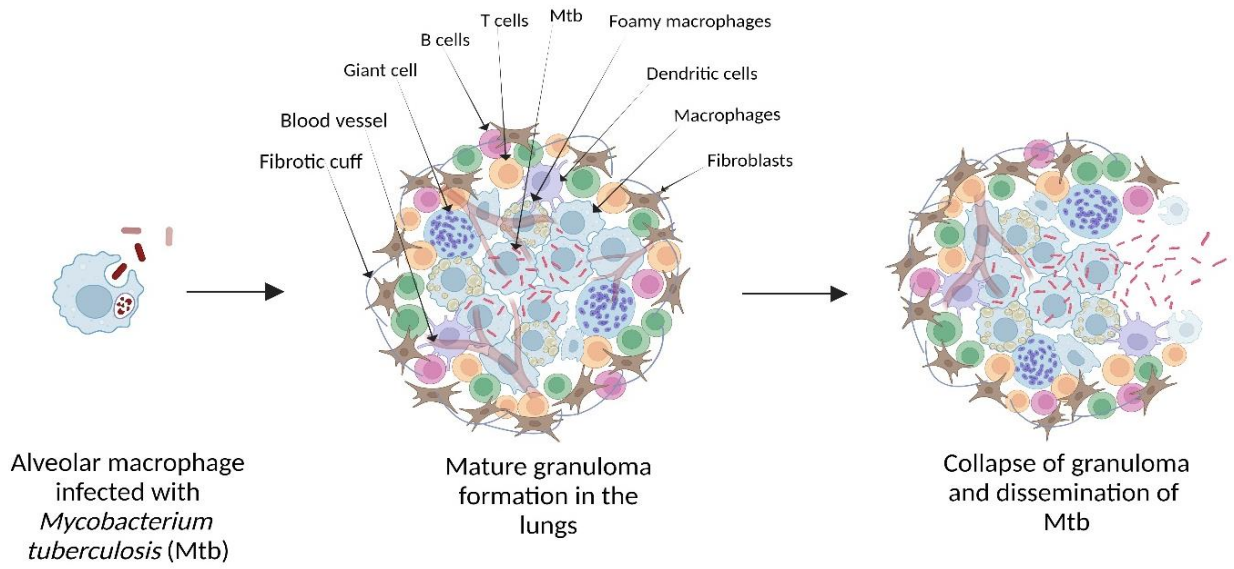

Figure 1: TB pathogenesis. *Mycobacterium tuberculosis* (Mtb) enters the lungs and is taken up by alveolar macrophages. This initial uptake triggers a local inflammatory response, recruiting additional macrophages and neutrophils to the infection site, forming an aggregate of innate immune cells. As the immune response progresses, a mature granuloma develops, characterized by the activation of acquired immunity. B and T cells are recruited to the granuloma and surround a central area that includes various macrophage subtypes, such as foamy macrophages and giant cells, all encased by a fibrous cuff. Disease reactivation causes bacterial replication, leading to the breakdown of the granulomatous structure and the dissemination of bacilli.

These caseous lesions within the granuloma serve as reservoirs for the bacteria, maintaining their dormancy. In advanced stages of the disease, the caseous core softens and cavitation occurs, leading to bacterial revival and the development of active TB (14). This revival leads to the spread of Mtb throughout the lungs and into the bloodstream finding their way for dissemination to other organs and also for transmission to other people.

1.1.3 TB treatment and challenges

Since the 1940s, significant progress has been made in developing effective drug treatments for tuberculosis (15). Currently, the recommended course for drug-susceptible TB (DS-TB) involves a six-month regimen containing four primary drugs: isoniazid (INH), rifampicin (RIF), ethambutol (EMB), and pyrazinamide (PZA) **(Figure 2).** Success rates of at least 85% have been consistently reported for cases treated with these first-line drugs (3, 16). However, the situation shifts when dealing with drug-resistant strains. When one or more first-line drugs fail, second-line drugs such as bedaquiline (BDQ), pyrazinamide (PZA), levofloxacin (LVX), linezolid (LZD), and clofazimine (CFZ) are implemented to treat resistant TB.

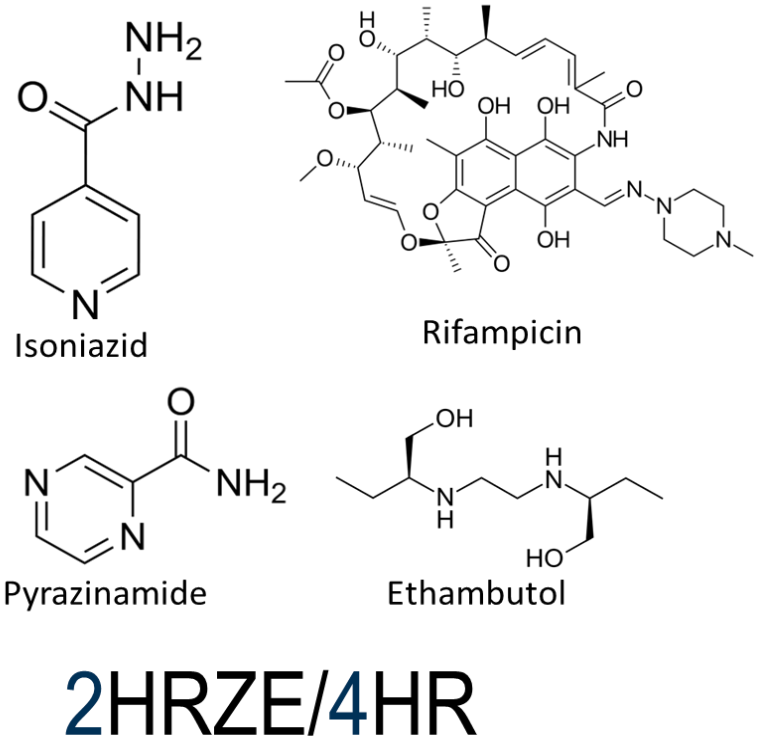

Figure 2: Standard drug regimen for fully susceptible Tuberculosis. 2HRZE/4HR regimen stands for initial phase of 2 months of isoniazid (H), rifampicin (R), pyrazinamide (Z) and ethambutol (E), followed by a continuation phase of 4 months of isoniazid and rifampicin.

According to the WHO Global TB Report 2022, the global incidence of tuberculosis (TB) rose to an estimated 10.6 million cases in 2022, marking an increase from 10.3 million in 2021 and 10.0 million in 2020. This upward trend contradicts the consistent decline observed in previous years leading up to 2020. These increases in TB cases for 2021 and 2022 are primarily attributed to disruptions in TB diagnosis and treatment caused by the COVID-19 pandemic. During the pandemic, the number of newly diagnosed TB cases decreased from 7.1 million in 2019 to 5.8 million in 2020 and 6.4 million in 2021 (3).

Multidrug-resistant tuberculosis (MDR-TB) is developed when the bacteria become resistant to both RIF and INH (17). On the other hand, Rifampicin-resistant tuberculosis (RR-TB) refers specifically to resistance to RIF, with resistance to PZA and EMB not factored in. Since both RR-TB and MDR-TB share similar prognoses and treatment approaches, they are collectively termed MDR/RR-TB (17, 18). Amongst the 10.6 million new TB cases in 2022, approximately 410,000 of these were MDR/RR-TB patients. Despite rifampicin-resistant strains consisting of only about 5% of total TB cases, they contribute approximately 15-20% to global TB mortality (3). Alarmingly, only one-third of patients with MDR/RR-TB are typically diagnosed, leading to

delayed treatment initiation and increased morbidity. This underlines the urgency of improving detection and treatment strategies for drug-resistant TB to diminish its impact on global public health (19).

Treating these resistant strains presents its own challenges, with a spectrum of side effects. Side effects can range from mild gastrointestinal disturbances, including nausea, anorexia, diarrhoea, vomiting, and abdominal pain, to more severe manifestations such as headaches and insomnia. In some cases, patients may experience significant complications such as psychosis, seizures, heart rhythm abnormalities (prolongation of the QT interval), hypothyroidism, joint pain (arthralgia), kidney toxicity (nephrotoxicity), liver toxicity (hepatotoxicity), hearing impairment (ototoxicity), and adverse dermatologic reactions (20).

Furthermore, the effectiveness of therapies, both first and second-line, hinges heavily on patient compliance with the prescribed regimen. Failure to complete treatment not only jeopardizes individual health but also fuels the spread of drug-resistant strains (21). In healthy individuals, the bacteria may be cleared out by the immune system or turn into an active infection. Other times, the bacteria may stay dormant and give rise to latent TB infection. It's estimated that around 1.7 billion people globally harbour LTBI, posing a significant challenge in limiting transmission (22).

In light of these challenges, there's an urgent need for novel drugs, which are potent against Mtb, less toxic, easy to administer, show activity against dormant TB, and show lesser side effects, to combat the TB pandemic.

1.2 Drug development approaches

To address the challenges in TB treatment and the growing issue of antibiotic resistance, finding new active drugs is of utmost importance. The complete genome sequencing of Mtb in 1998 has been an important step in this effort (23). This has led to the identification of genes that are essential for Mtb, and therefore enabling the identification of targets for new drugs, hence making a significant advance in drug discovery. In the drug discovery pipeline understanding the target of the drug, is a valuable step that decides whether the drug can progress into clinical trials (24).

To search for such effective drugs for Mtb, the drug development process can be categorized into two approaches **(Figure 3):**
1) Phenotypic screening (Drug-to-target) (25) and
2) Target-based drug discovery (Target-to-drug) (26).

Compounds identified through both these approaches undergo a rigorous pipeline involving multiple assays. Initially, the compound hits are evaluated to determine their suitability as leads for further development. These lead compounds then undergo optimization to enhance their efficacy, safety, and pharmacokinetic properties. Once optimized, the selected compounds advance to preclinical studies, where they undergo thorough testing in animal models to assess their safety and efficacy. Following

successful preclinical evaluation, the compounds progress to clinical trials, where their safety and efficacy are evaluated in patients. This cascade of drug development for both approaches is depicted in **Figure 4**, illustrating the sequential stages from compound identification to clinical trials (27, 28).

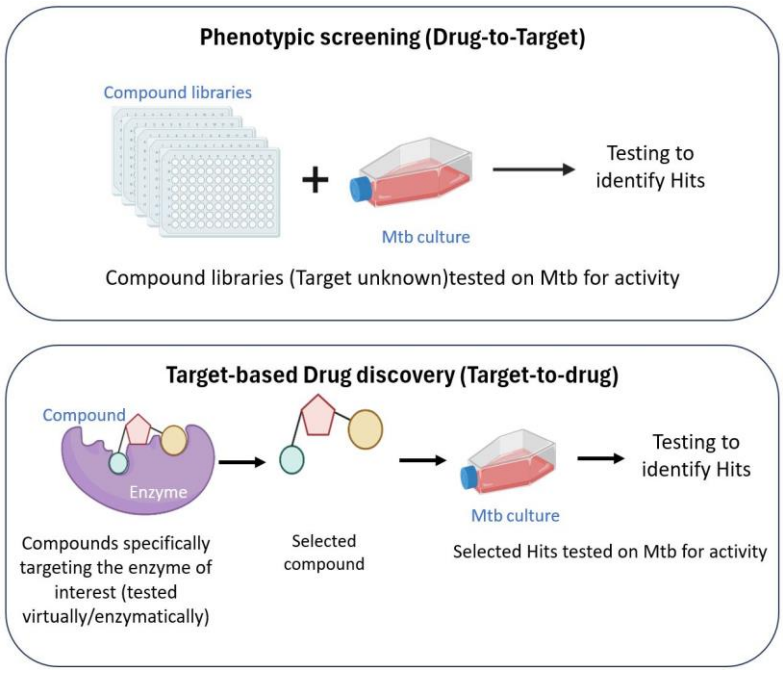

Figure 3: Illustration of drug development approaches. Phenotypic screening (Drug-to-target): Compound libraries with unknown targets are screened on bacterial culture and active compounds are selected for further development. This process starts with finding an active compound and proceeding further with the actives to identify its target, hence also called a Drug-to target-based approach. Target-based drug discovery (Target-to-drug): compounds are first tested against a specific target protein, and identified hits are subsequently further tested for activity on whole cells. Hence this approach is the target to drug-based approach, where the process starts with finding an ideal target.

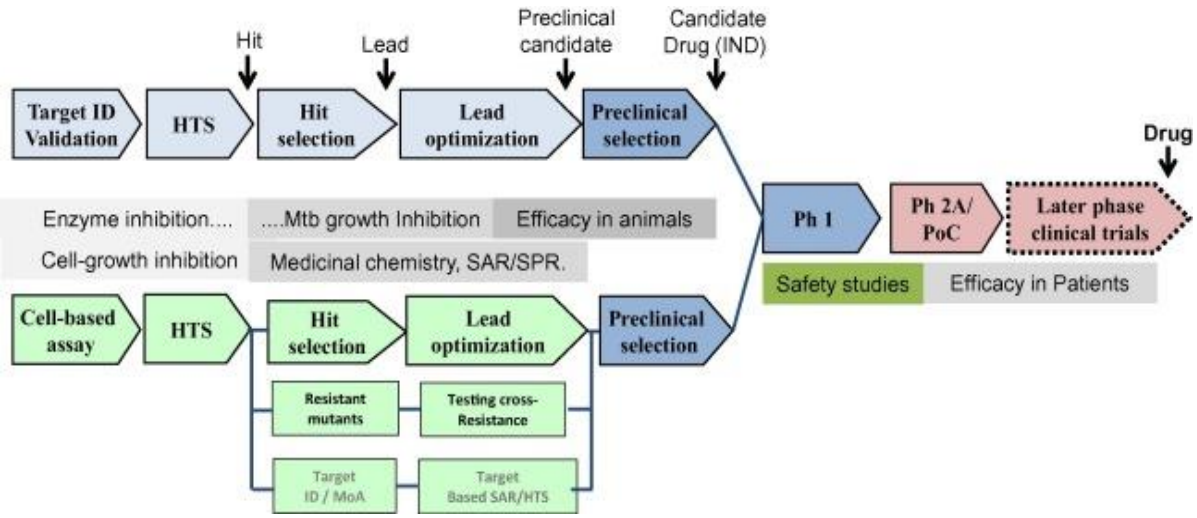

Figure 4: TB drug discovery cascade for phenotypic and target-based screening. This figure has been obtained from Ujjini H. Manjunatha, Paul W. Smith, 2014 (28). (SAR, structure-activity relationship; SPR, structure-activity relationship; HTS, high through-put screen; PoC, proof-of-concept in patients.)

1.2.1 Phenotypic screening (Drug-to-target)

Phenotypic drug screening is an approach where test compounds of interest are screened against whole-cell organisms and activity is assessed through a change in phenotype. For most infectious disease phenotypic screening, including Mtb, this traditionally means testing compounds for their ability to inhibit the growth of the disease organism under actively replicating conditions. The process involves screening small or large libraries of novel compounds against the organism to observe the antimicrobial activity of the compound **(Figure 4)** (29, 30). New methods, such as screening using 384-well plates, have been developed to facilitate the screening of large compound libraries, thereby efficiently identifying active compounds (31). This process starts with finding an active compound and proceeding further with the actives to identify its target, hence also called a Drug-to target-based approach.

The drugs approved until now for clinical use against Mtb and other organisms have seen more success through this approach, resulting in most pharmaceutical companies and research institutes focusing on phenotypic screening as the primary tool for drug discovery (32). This effort has certainly proven helpful in Mtb drug development as it gave rise to many active drugs that are now clinically used, or currently in clinical trials, for the treatment of Mtb and drug-resistant Mtb **Table 1** provides a list of new drugs in clinical trials and those approved. Some of these drugs and their mode of action are described below. These drugs mark the successes of Mtb drug development achieved in recent years.

Table 1: Global Pipeline of Medicines in Clinical Development for Tuberculosis. Table based on treatment Action Group Tuberculosis treatment report 2023 (33).

Phase 1	Phase 2	Phase 3	Regulatory Market Approvals
TBAJ-587	TBAJ-876	Sudapyridine(WX-081)	Bedaquiline
MK-7762 (TBD09)	TBI-223	Sitafloxacin	Delamanid
GSK-286	Delpazolid	Contezolid	Pretomanid
SPR720	Sutezolid		Linezolid
	Tedizolid		Clofazimine
	BTZ-043		Moxifloxacin
	Macozinone(PBTZ-169		Levofloxacin
	TBA-7371		
	Quabodepistat(OPC-167832)		
	Pyrifazimine (TBI-166)		
	Ganfeborole (GSK-656)		
	Telacebec (Q203)		
	Alpibectir (BVL-GSK098)		
	Sanfetrinem		
	SQ-109		

New drugs for TB treatment

1) Bedaquiline:

Bedaquiline was discovered in the early 2000s and was approved by the US Food and Drug Administration (FDA) as an anti-TB medication. Its approval for treating MDR-TB occurred in 2013, becoming the first novel antitubercular drug in nearly half a century of drug discovery research (34). Bedaquiline operates by diminishing the cellular ATP reservoir and targets the e subunit of ATP synthase. Additionally, studies indicate that bedaquiline disrupts the proton gradient across the Mtb cell membrane, functioning as an uncoupler of the proton motive force (35, 36). Demonstrating bactericidal properties against Mtb in both replicating and nonreplicating hypoxic environments, bedaquiline holds promise for combating tuberculosis effectively (37).

2) Pretomanid and delamanid

These two drugs belong to the class of nitroimidazole compounds and exhibit potent bactericidal properties against both replicating and nonreplicating Mtb. Pretomanid received approval from FDA for Extensively drug-resistant TB (XDR-TB) and MDR TB treatment in 2019 (38, 39); while Delamanid received approval from

the European Medicines Agency (EMA) in 2014 (40). Pretomanid and Delamanid rely on activation by a nitroreductase enzyme, leading to the generation of Reactive nitrogen species (RNS) that effectively eliminate Mtb (41, 42). Moreover, they also disrupt cell wall synthesis and interfere with cellular respiration (40, 43-47).

3) Benzothiazinones

Compounds from the Benzothiazinones class inhibit decaprenyl-phosphoribose epimerase (DprE1), which disrupts the final stages of arabinogalactan biosynthesis (48). This unique mechanism targets cell wall biogenesis, providing a distinct method to target Mtb (49). Several derivatives of benzothiazinones have been evaluated in preclinical and clinical settings for their efficacy and safety in TB treatment (50). Notably two compounds, BTZ043 and PBTZ169, showed MIC90 values lower than 0.004uM against whole cell Mtb *in vitro*. Moreover, both these compounds showed synergistic activity with the first-line TB drugs and are also active against clinical MDR and XDR strains. These compounds are now being assessed in Phase II clinical trials.

4) Q203

Q203 belongs to the class of imidazopyridine amides and works by inhibiting the cytochrome bc1 complex in the mycobacterial respiratory chain, which hinders the proliferation of Mtb (51). It has successfully moved through preclinical development and is currently undergoing clinical trials to evaluate its use in anti-TB regimen (52).

5) SQ109

SQ109 is a diamine compound now in Phase II clinical trials. It targets the MmpL3 transporter, crucial for cell wall biosynthesis among other functions. By disrupting MmpL3, SQ109 interferes with the transport of essential lipids and molecules needed for building the cell wall (53, 54). SQ109 shows good synergistic activity with bedaquiline and also improves the drug efficacy of the current four first-line TB drugs (53).

Repurposed Drugs for TB Treatment

1) Linezolid

Linezolid, originally used for treating Gram-positive bacterial infections, has been repurposed as an antimycobacterial agent for TB. It works by targeting 23S rRNA, which inhibits protein synthesis in Mtb. Linezolid has shown bacteriostatic activity in MDR-TB and XDR-TB as demonstrated *in vitro* (55).

2) Clofazimine

Clofazimine, once used against leprosy, has become significant in the fight against drug-resistant TB. It is thought to be reduced by mycobacterial type II nicotinamide adenine dinucleotide (NADH) quinone oxidoreductase, leading to the production of reactive oxygen species (ROS) upon non-enzymatic reoxidation

(56). Clofazimine tends to accumulate in host macrophages and tissues, particularly in pulmonary macrophages. While these traits might seem undesirable, they could enhance the drug's effectiveness against leprosy and TB (57). Its promising results in murine TB infection models have spurred efforts to develop new analogues with fewer side effects, improving its potential as a TB drug (58).

3) Moxifloxacin

Moxifloxacin is an 8-methoxy-fluoroquinolone and is considered to be the most potent fluoroquinolone for the treatment of MDR-TB. It was found to be bactericidal in mouse models against Mtb (59, 60). Moxifloxacin acts by inhibiting an enzyme called DNA gyrase and stops DNA synthesis (61). It has been tested in multiple phase 3 trials for the treatment of DS-TB and MDR-TB (62, 63).

In 2022, the WHO Global TB Report highlighted new guidelines for treating MDR-TB, based on the results of the Phase 3 clinical trial TB-PRACTECAL (64). The new recommended treatment is a 6-month BPaLM regimen, consisting of bedaquiline (B), pretomanid (Pa), linezolid (L), and moxifloxacin (M), for patients with MDR/RR-TB and those with additional resistance to fluoroquinolones (pre-XDR-TB). The BPaLM regimen demonstrated an improved success rate of 89% in the Phase 3 trial, compared to the previous standard of care, which had a success rate of 52% and reduced the treatment time to 6 months.

In summary, phenotypic-based drug discovery has proven valuable for Mtb drug development, with new drugs currently being tested in clinical trials. However, in nearly half a century, only three new drugs (bedaquiline, pretomanid and delamanid) have been approved for treating resistant TB strains. The persistent rise in TB cases necessitates increased efforts and the development of more effective drugs to combat this infection.

1.2.2 Target-based drug discovery (Target-to-drug)

With the complete genome sequence of Mtb available (23), researchers gained the ability to explore the entire Mtb genome for potential targets in antibiotic development. This helped in finding new enzyme/protein targets which could be crucial for the survival of Mtb. Such drug targets have been further assessed in target-based drug discovery approaches where compounds are first tested against a specific target protein, for example using in silico modelling or *in vitro* biochemical assays, and identified hits are subsequently further tested for activity on whole cells (65). Hence this approach is the target to drug-based approach, where the process starts with finding an ideal target.

However, to maximize the chances of developing *in vivo* efficacious drugs using this approach, it is crucial to first identify a promising target.

An ideal target for antibiotic development should meet several criteria, with the most important being target essentiality, target vulnerability, target selectivity and target Accessibility to chemical inhibition. These criteria are described in further detail below.

Target essentiality:

An ideal target needs to be essential for the survival of bacteria. This essentiality can be checked by knocking down the essential gene and observing the bacterial growth phenotype (66, 67). Another way to test the gene essentiality is by using transposon mutagenesis and insertion sequencing (Tn-seq) (68). If a gene doesn't contain any transposons after subjecting a population to Tn-mutagenesis, it's considered essential. This can further be studied in a macrophage model (69) or mouse model (70) to assess the essentiality of genes in different models. This is crucial because a target may be essential for Mtb's growth or survival under different environmental conditions and replication states which makes it necessary to study the essentiality of genes in these different infection scenarios (71).

Despite genetic studies demonstrating a gene to be essential for bacterial survival under test conditions, the activity of a drug targeting the gene product may result in a different response. This is because, along with being essential, the target protein also needs to be vulnerable (72).

Target vulnerability:

Target vulnerability is a quantifiable trait that relates to the degree of target inhibition required to affect cell viability and achieve bactericidal effects (72). Essential genes with high vulnerability can be effectively targeted by drugs, even if the drug does not occupy the protein target completely in the cell. To more accurately assess target vulnerability, methods have been developed to evaluate the extent to which the target protein must be deactivated in the cell (73). Moreover, in 2021, CRISPRi based genomics methods were first used to quantify gene vulnerability in Mtb and provide a vulnerability score for each gene [Vulnerability Index (VI)] (72). CRISPRi was used to titrate gene expression across the entire genome and by monitoring the fitness of the bacteria VIs for all essential genes could be determined. These approaches provide valuable insights into the feasibility of targeting specific genes for drug development in TB (72).

Target selectivity:

The target selected should ideally be absent in human cells or at least maintain sufficient structural distinction from its human homolog(s). This assists in alleviating the drug cytotoxicity on host cells and further side effects (74).

Accessible to chemical inhibition:

The target must be accessible to chemical inhibition, meaning it should have the ability to bind a small molecule other than its natural substrate. Inhibiting or activating the protein's function, with achievable concentrations of a small molecule, should result in cellular dysfunction resulting in impaired growth or cell death (75).

In conclusion, selecting an ideal target is critical in target-based drug discovery. Once an appropriate target is identified, compounds can be screened against it and further developed. Understanding the target before developing an active drug significantly saves time and effort, streamlining the process from discovery to clinical trials. The efforts to obtain Mtb drugs through Target-based drug discovery are currently still in process. Unfortunately, no new drug has been successfully cleared in clinical trials through a target-based drug development approach for Mtb treatment as of yet. Hence, more research and efforts are needed in target-based discovery to make it successful.

1.3 Targets studied in the current work

For the target-based drug discovery approach, the current thesis focused mainly on three different targets in Mtb. Compounds for these targets were obtained from collaborator institutes and further studied for their activity against Mtb. To understand the activity of these compounds, understanding their target is of utmost importance. The three targets explored in the thesis are described below.

1.3.1 Aspartate transcarbamoylase (ATCase)

The *de novo* pyrimidine nucleotide synthesis pathway is crucial for producing pyrimidine nucleotides in organisms, comprising six catalytic steps mediated by three distinct enzymes in Mtb **(Figure 5).** Aspartate transcarbamoylase (ATCase; *pyrB*; Rv1380) is involved in the second step of the pathway catalysing the conversion of L-aspartate (L-ASP) and carbamoyl phosphate (CP) into carbamoyl-aspartate (CP-ASP) (76, 77). ATCase enzyme is also present in other organisms such as Plasmodium, *E. coli* and also in humans. However, the catalytic site of MtbATCase is different from these organisms including humans. This is supported by the minimum sequence identify of the ATCases of these organisms to Mtb (47 % Mtb: E. coli; 37 % Mtb: Human) (77).

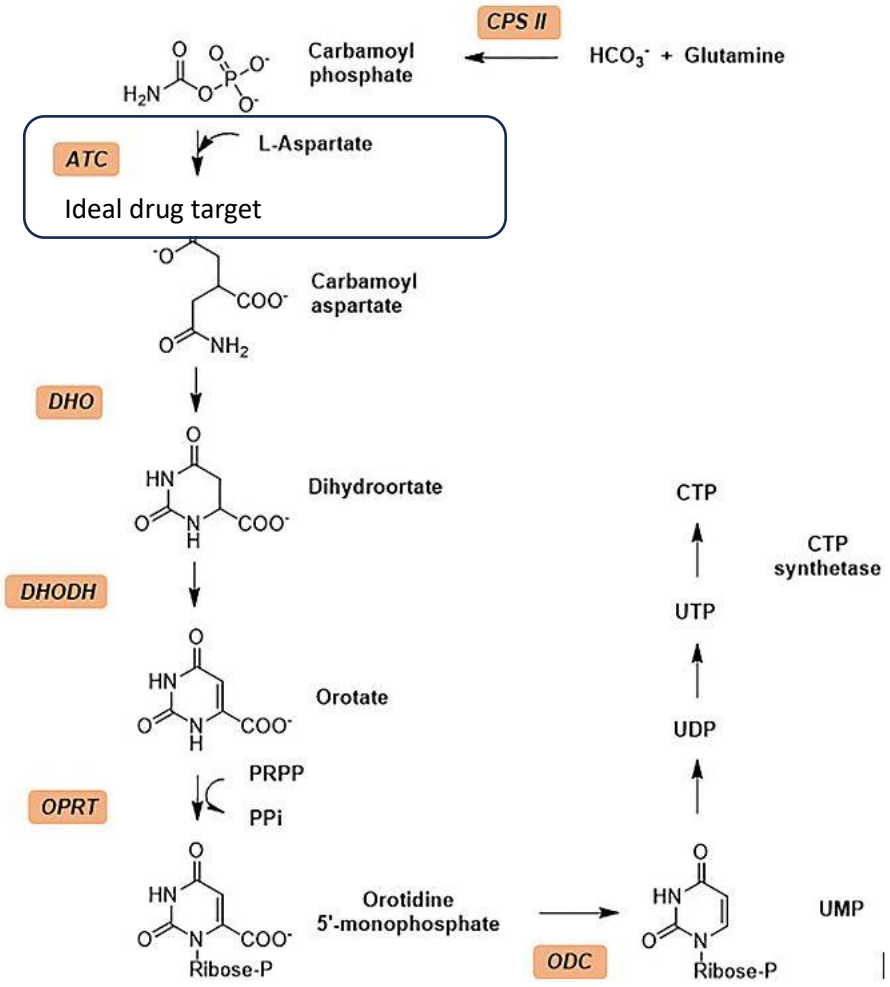

Figure 5: The *de novo* Pyrimidine nucleotide synthesis pathway in *Mycobacterium tuberculosis* (Mtb)

ATCase from *Plasmodium falciparum* (Pf ATCase) has been identified as a potential drug target due to the malaria parasite's sole reliance on the *de novo* pyrimidine biosynthesis pathway for proliferation (78). This discovery led to the development of a series of compounds with inhibition against PfATCase, advancing anti-malarial drug discovery (79, 80)

MtbATCase and PfATCase were identified to have similarities in their compound binding pockets (77). In Mtb, ATCase is an essential enzyme, with a VI of -5.5 (72), indicating that it is highly druggable and could serve as a promising drug target (76).

1.3.2 InhA/KatG (Terpenoid derivatives)

For more versatile approaches to yield effective drugs in TB drug discovery, existing Mtb drugs have been studied and further modified to develop new, potent treatment options. Isoniazid (INH), one of the most

effective drugs against Mtb, was chosen and further linked to terpenoid molecules. By covalently linking INH and terpenoids, the aim was to generate compounds that leverage INH's strong anti-mycobacterial properties and the beneficial characteristics of terpenoids. To study these novel compounds, understanding the mode of action of INH and the properties of terpenoids is vital and hence described below.

Mechanism of action of Isoniazid (INH)

INH is one of the most potent antibiotics for Mtb treatment and hence chosen for the development of these novel compounds. For the mechanism of action of INH multiple approaches have been discovered that may additively or synergistically add to the exceptional and highly selective potency of isoniazid (INH) against Mtb. Two important mechanisms, relevant to the current study, have been described below:

A) INH activation by KatG

INH gains entry into the mycobacterial cell via passive diffusion (81). INH itself does not exert toxicity on the bacterial cell but serves as a prodrug, meaning it requires activation by the mycobacterial enzyme Catalase–Peroxidase (KatG) (82). KatG, a multifunctional catalase-peroxidase, also exhibits other activities such as peroxynitritase (83) and NADH oxidase (84). Aligned with its peroxidase activity, KatG activates INH through peroxidation in the presence of NADH, generating intracellular INH-derived damaging species (83). Various oxidants facilitate KatG oxidation of INH, including superoxide (85), hydrogen peroxide (86) and simple alkyl hydroperoxides (87). Even in the absence of added oxidants, the *in vitro* auto-oxidation of INH and NADH can provide sufficient oxidants to enable INH activation by KatG (86).

B) Targeting mycolic acids:

Followed by KatG activation and the oxidation of INH in the presence of NADH results in the formation of covalent INH-NADH adducts, which have been identified as potent inhibitors of enoyl acyl carrier protein reductase (InhA) enzyme (*inhA*; Rv1484) (88). InhA is crucially involved in the biosynthesis of mycolic acids, which are unique and essential components of the mycobacterial cell wall (89). Therefore, the inhibition of InhA aligns with the distinctive sensitivity of mycobacteria to INH. This elucidates a key aspect of INH's mechanism of action and its efficacy against Mtb.

Terpenoid derivatives

Terpenoids, also known as isoprenoids, constitute a class of naturally occurring organic compounds derived from the 5-carbon compound isoprene and its derivatives, commonly referred to as terpenes, diterpenes, and so forth (90). Many terpenoids exhibit significant pharmacological activity, rendering them of considerable interest to medicinal chemists.

Terpenes and derivatives are proven to be potent against pathogenic bacteria and are not toxic (91). Given these properties, terpenoids were covalently linked with INH for this class of compounds.

The terpenoids can be classified according to the number of isoprene units that comprise the parent terpene. In this study, monoterpenoids with 2 isoprene units namely, carvone, thymol, menthol etc. were used (92).

Hence, given the potent activity of INH and the pharmacological activity of terpenoids, these two were covalently linked and the resulting synthesized compounds were analysed for their antitubercular activities and modes of action.

1.3.3 The 2C-methyl-D-erythritol 4-phosphate (MEP) Pathway

Isoprenoids consist of a large class of natural products found in fungi, bacteria, plants, and mammals. Over 35,000 isoprenoids have been identified until now that show remarkable structural diversity and contain a wide range of biologically relevant functions (93) such as protein degradation, apoptosis, regulation of transcription, and post-translational processes (94).

Despite the structural and functional diversity of isoprenoids, they all originate from two common five-carbon (C5) building blocks: isopentenyl diphosphate (IPP) and its isomer, dimethylallyl diphosphate (DMAPP) (95). Two known pathways for the biosynthesis of these precursors in different organisms are the mevalonate (MVA) pathway and the methylerythritol phosphate (MEP) pathway (96).

Until the early 1990s, it was believed that the MVA pathway, which uses acetyl-CoA as a starting material and is named after its central intermediate, was the sole metabolic pathway for the biosynthesis of IPP and DMAPP in all organisms (97, 98). However, later a completely different pathway was discovered for the synthesis of these compounds using pyruvate and D-glyceraldehyde 3-phosphate (G3P) as building blocks (99, 100). This alternative pathway initially called the non-mevalonate pathway, is now referred to as the 2C-methyl-D-erythritol 4-phosphate (MEP) pathway (101).

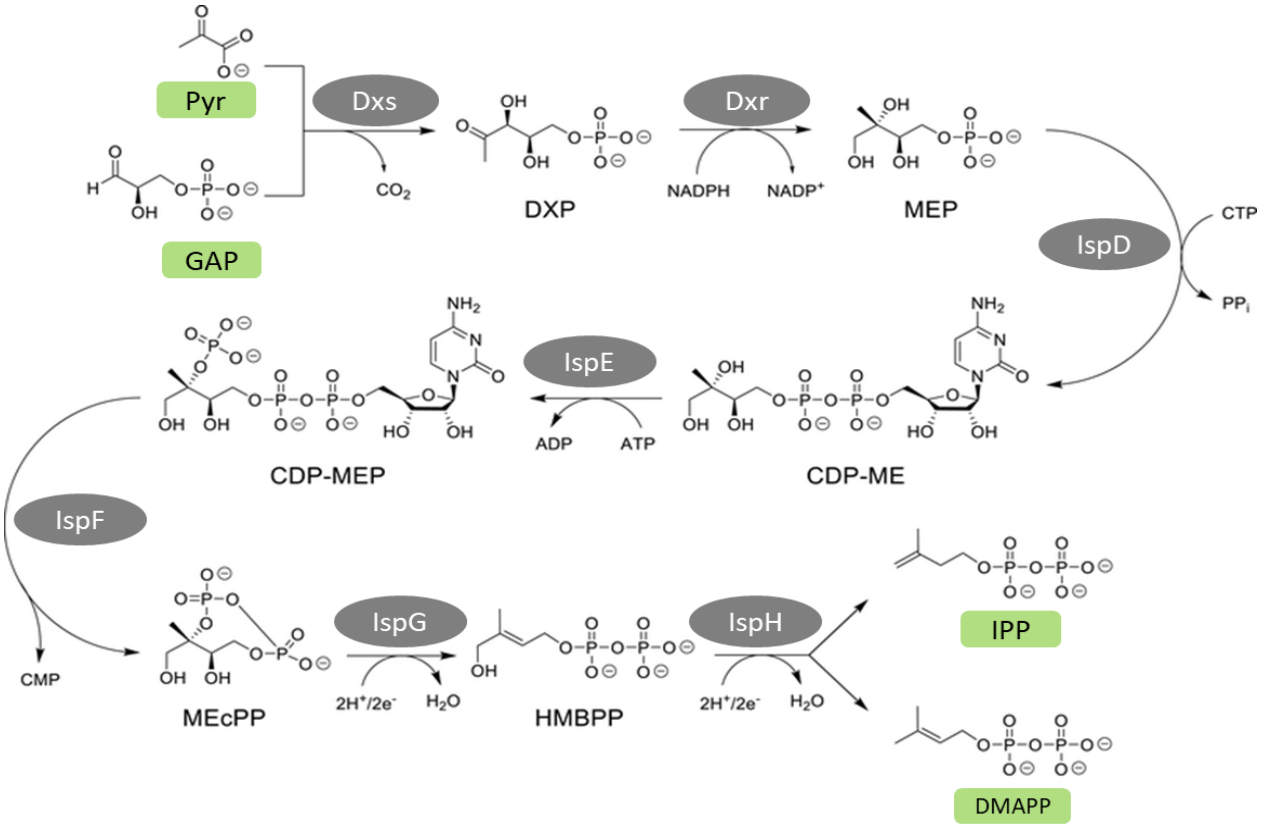

Figure 6: 2C-methyl-D-erythritol 4-phosphate (MEP) Pathway in *Mycobacterium tuberculosis* (Mtb). The end products of the pathway are isopentenyl diphosphate (IPP) and its isomer, dimethylallyl diphosphate (DMAPP) which are building blocks for isoprenoid synthesis. The first two enzymes 1-Deoxy-D-xylulose-5-phosphate Synthase (Dxs) and 1-Deoxy-D-xylulose-5-phosphate Reductoisomerase (Dxr) of the pathway are the focus of this thesis. Figure based on (102).

The MEP pathway is utilized by a variety of organisms, including:

- Plants such as Tobacco (*Nicotiana tabacum*) and Rice (*Oryza sativa*) (103).
- Algae such as *Chlamydomonas reinhardtii* (104).
- Many parasites, including *Toxoplasma gondii*, *Plasmodium falciparum*, Babesia species, and Cryptosporidium species (105-107).
- Microorganisms such as Chlamydia species, *Escherichia coli*, *Streptococcus pneumoniae, Pseudomonas aeruginosa, Campylobacter jejuni,* Salmonella species, *Mycobacterium leprae, Staphylococcus aureus,* and *Mycobacterium tuberculosis* (108, 109).

In Mtb, the synthesis of isoprenoids, carried out solely by the MEP pathway, is crucial for both cell wall construction and oxidative phosphorylation (108). Moreover, this pathway and its enzymes are absent from all mammalian genomes (humans); hence, the enzymes involved in the MEP pathway are potential targets for new drugs (95, 109).

The MEP pathway in Mtb is illustrated in **Figure 6**. This pathway begins with a thiamin diphosphate-dependent condensation of D-glyceraldehyde 3-phosphate and pyruvate, resulting in the formation of DXP. DXP is then reductively isomerized to MEP by DXP reducto-isomerase (DXR/IspC). Next, MEP combines with cytidine 5'-triphosphate (CTP) through the catalytic action of CDP-ME synthetase (IspD), producing methylerythritol cytidyl diphosphate (CDP-ME). The C2 hydroxyl group of CDP-ME is then phosphorylated by an ATP-dependent enzyme (IspE), forming 4-diphosphocytidyl-2-C-methyl-D-erythritol-2-phosphate (CDP-MEP). CDP-MEP is subsequently cyclized by IspF to 2-C-methyl-D-erythritol-2,4-cyclodiphosphate (MEcPP). IspG then catalyzes the ring-opening of the cyclic pyrophosphate and the C3-reductive dehydration of MEcPP to 4-hydroxy-3-methyl-butenyl 1-diphosphate (HMBPP). The final step of the MEP pathway, catalyzed by IspH, converts HMBPP to both IPP and DMAPP.

The first two enzymes of the MEP pathway in Mtb 1-Deoxy-D-xylulose-5-phosphate Synthase (Dxs) and 1-Deoxy-D-xylulose-5-phosphate Reductoisomerase (Dxr or IspC) are studied in the present thesis and are described below in detail.

Dxs (*dxs1* gene; Rv2682c)**:**

Dxs catalyses the first and rate-limiting step of the MEP pathway, converting pyruvate and G3P into 1-deoxy-D-xylulose 5-phosphate (Dxp). Dxp is an important intermediate in the biosynthesis of isoprenoids and in certain bacteria it is also used in the production of thiamine (vitamin B1), and pyridoxal (vitamin B6) (110, 111) which makes the Dxs-catalysed reaction important in bacterial metabolism (107, 112).

In Mtb, there are two genes encoding the Dxs orthologues, *dxs1* (Rv2682c) and *dxs2* (Rv3379c). Research has shown that *dxs1* is essential for the Mtb's survival and that *dxs2* cannot compensate for the functional loss of *dxs1* (112). Moreover, *dxs1* has a VI of -11.29 (72). This is in line with the VI of target genes of the front-line anti-TB drugs like INH (gene*: inhA*; VI: -9.9) and Rifampicin (RIF) (gene: *rpoB*; VI: -9.56) (72). This highlights the importance of *dxs1* for the metabolic processes and viability of Mtb and suggests it to be a promising drug target (107, 112).

Dxr (*dxr* gene; Rv2870c)**:**

Dxr, also known as IspC is one of the most extensively studied enzymes in the MEP pathway (96). Numerous protein (co)crystal structures of IspC from various organisms have been reported (113-115). This enzyme catalyses the second step in the pathway, which is also the first committed step in the formation of IPP and DMAPP. In its catalytic process, Dxr utilizes NADPH, and the presence of a divalent cation such as Mg2+ or Mn2+ is important for its activity (96). Moreover, the Mtb *dxr* gene (Rv2870c), is essential with a VI of -7.04, hence making it a promising drug target (72).

Comprehending the importance of the MEP pathway enzymes as a drug target in several microorganisms, an international consortium, MepAnti (https://mepanti.hips-wordpress.helmholtz-hzi.de.), was set up focusing on the discovery and development of anti-infectives targeting MEP pathway enzymes. The present study is a part of this consortium. MepAnti was funded by the European Commission-Innovative Training

Networks, Horizon 2020 Projects and led by Prof. Dr Anna Hirsch from Helmholtz-Institut für Pharmazeutische Forschung Saarland (HIPS) (Saarbrücken, Germany).

1.4 Target Validation

In target-based drug discovery, compounds are usually selected based on virtual screening using multiple bioinformatic tools and further moved to biochemical assays such as enzymatic screening (116). In the enzymatic screen, these compounds are tested for their affinity for a specific enzyme of interest (117). Followed by a strong binding they are further tested on whole-cell organisms, in this case, Mtb. Hence, these compounds are developed to potentially target the protein of interest. However, the bacterial cell is complex and the physiological conditions inside the cell cannot be imitated by virtual screening or by enzymatic assays. Hence, a biological confirmation using live bacteria is crucial to validate the activity and target of these compounds (116).

Multiple approaches to achieving biological target validation have been studied throughout the years (73, 118-121). The techniques involving the regulation of a target gene using molecular biology tools have proven among the most successful of the approaches available. These techniques comprise generating conditional mutants where the expression of the target is regulated, either downregulated or upregulated, using anti-sense interference or inducible promoters. Regulating the levels of the target results in a corresponding change in the sensitivity of the mutant to compounds that act on the specific target. Hence, a shift in the MIC90 of a compound against the mutant is observed only when the compound is targeting the product of the regulated gene (118, 122).

To validate the target of the MEP pathway inhibitors (obtained from the MepAnti consortium), we aimed to generate conditional mutants for the first two genes of the pathway *dxs1* and *dxr* in Mtb.

To generate these conditional mutants, two genetic modification approaches were used:
1) Promoter replacement mutants (123)
2) CRISPRi mutants (124)

Both these approaches are described below.

1.4.1 Promoter replacement mutants

To validate the MEP pathway genes *dxs1* and *dxr* as targets of the novel compounds, promoter replacement mutants were generated. This method has been previously published and several genes have been successfully studied for their essentiality and as promising drug targets (73, 123, 125-127). In this method, the native promoter of the target gene is replaced by a tet operator (tetO)-containing promoter (pmyc1tetO) using a single homologous recombination technique. These mutants are expected to have a growth phenotype similar to unmodified bacteria *in vitro* (128), as the psmyc1tetO promoter leads to constitutive

expression of downstream genes in the absence of a tet repressor protein. These mutants are further transformed with plasmids expressing either tet repressor (TetR) or reverse tet repressor (rev TetR) proteins. These proteins have an affinity to Anhydrotetracycline (Atc) supplemented in the media. Depending on the protein present, either TetR or RevTetR, the addition of Atc leads to target gene upregulation (Tet ON) or downregulation (Tet OFF) respectively **(Figure 7).** This gene manipulation is expected to occur in an Atc dose-dependent manner (122, 128).

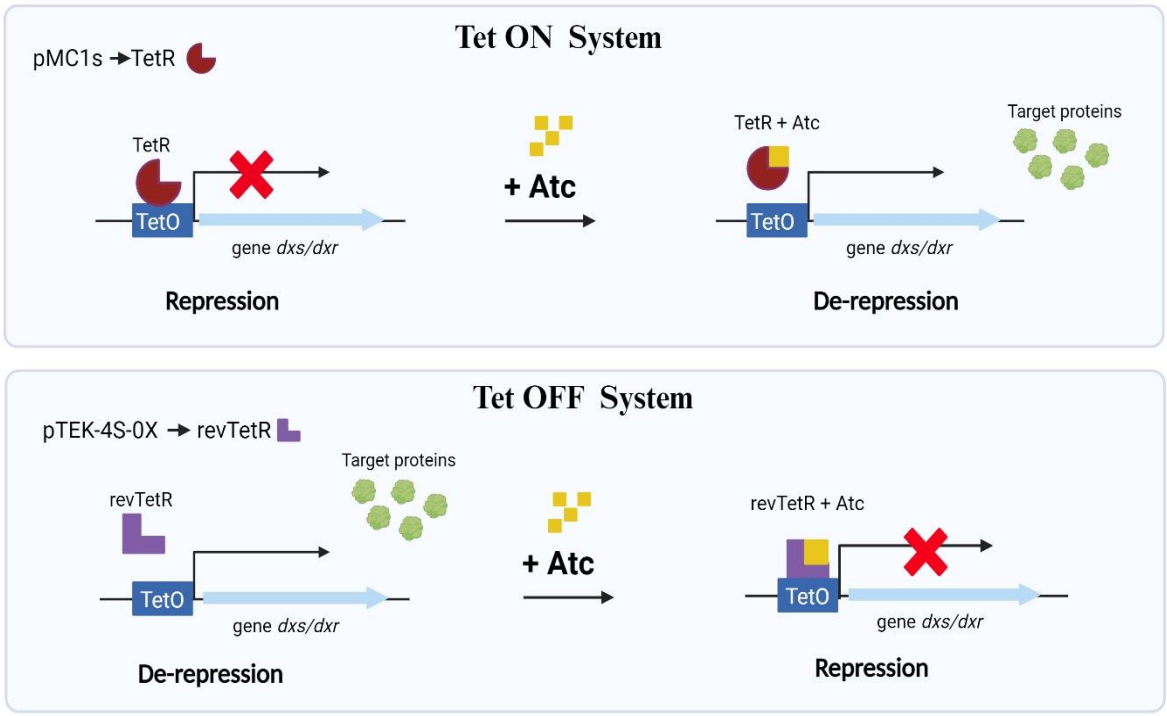

Figure 7: Promoter replacement mutants. These mutants are generated by replacing the mycobacterial promoter of the gene of interest with a tetO-containing promoter. These mutants are further introduced with TetR (Tet ON) or revTetR proteins (Tet OFF). These proteins have an affinity to Atc supplemented in a dose-dependent concentration in the growth media. In Tet ON, TetR binds to Atc and induces the gene expression of the target gene. In Tet OFF, revTetR binds to Atc and has an affinity to tetO, hence repressing the target gene.

Tet ON mutants

In Tet ON mutants, plasmids expressing the tetR proteins are introduced in the mutants carrying the tetO-containing promoter upstream of the gene of interest (129). The TetR proteins have DNA-binding domains and have a strong affinity to the tetO region, leading to blockage of transcription of the gene of interest. If the gene is essential, bacterial growth will cease. When Atc enters the cell, it binds to TetR and induces a conformational change that results in the dissociation of TetR from tetO and thus expression of the TetR-controlled gene of interest commences. Hence, the more Atc supplemented in the growth media, the more the release of transcriptional repression, leading to gene upregulation in a growth culture of Mtb mutant (128).

Tet OFF mutants

In Tet OFF mutants, plasmids expressing the revTetR proteins are introduced in the mutants with tetO-controlled gene of interest (129). In the presence of Atc, the revTetR proteins bind with a strong affinity to the tetO. This results in the transcription repression of the gene of interest leading to gene downregulation. Hence, the more Atc is supplemented in the growth media, the more transcription repression of the gene is observed in a growth culture of Mtb mutant (128).

1.4.2 CRISPRi mutants

Using an independent approach to validate the MEP pathway genes *dxs1* and *dxr* as targets of the novel compounds, conditional mutants were generated using the Clustered Regularly Interspaced Short Palindromic Repeats (CRISPR) interference (CRISPRi) system.

The Promoter replacement mutant technique described above, though successful in multiple studies, requires months to target a single protein. Additionally, the multiple steps involved increase the potential for errors, making it difficult to optimize if the desired phenotype is not observed (123). Consequently, newer techniques were needed to generate conditional mutants. In 2017, CRISPR interference was established, achieving gene downregulation in just one cloning step and overcoming other limitations observed in the promoter replacement technique (124). This system was also utilized in the current study for target validation

The widely known CRISPR/Cas9 system is commonly used for specific gene modifications *in vitro* and *in vivo* (130). This system uses the Cas9 protein to make target-specific DNA modifications in the host genome, as Cas9 is a double helicase endonuclease. A modification of this system is CRISPR interference (CRISPRi) where a mutated Cas9 is used. This is a catalytically-dead Cas9 (dCas9) protein which while still able to bind to targeted DNA sequences is unable to cleave the DNA strands and therefore acts as via steric hindrance to block transcription of the target gene (124).

The CRSIPRi system for Mtb comprises of 3 main components:

1. catalytically dead Cas9 variant from *Streptococcus thermophilus* (Sth1 dCas9).
2. a gene-of-interest specific targeting small guide RNA (sgRNA)
3. protospacer adjacent motif (PAM)

The dCas9 protein, when transcribed, is guided to the specific gene of interest by a chimeric RNA called sgRNA. The target specificity here is determined by the gene-targeting sequence of the sgRNA, which should be complementary to the precise desired target genomic DNA location. Along with sgRNA, the target specificity is also assisted by a protospacer adjacent motif (PAM). PAMs are 2-8 base pair sequences located immediately downstream of a sgRNA target sequence. Recognition of the target base pairs is the first

important step in the successful binding of dCas9. Recognition of PAM by the dCas9 protein leads to destabilisation of the DNA duplex and successfully allows the dCas9 and sgRNA to bind. This binding creates a steric hindrance on the target gene where the promoter access is blocked which leads to transcription repression of the target gene (120). The CRISPRi system is illustrated in **Figure 8.**

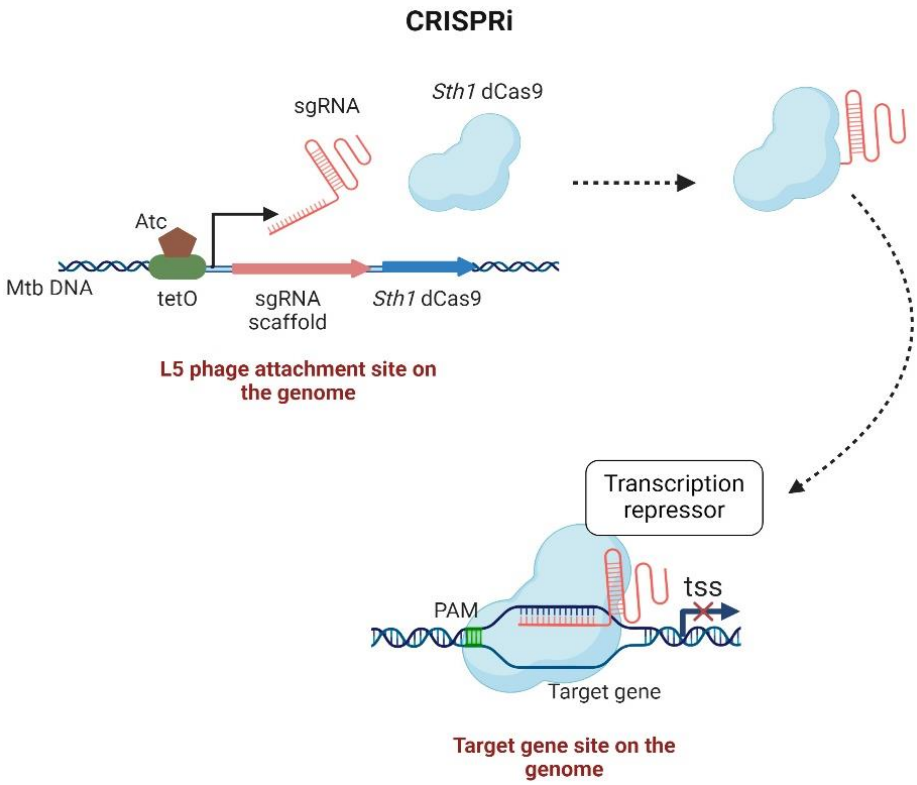

Figure 8: CRISPRi system for gene knockdown. A plasmid containing a sgRNA scaffold and the Sth1 dCas9 under the transcriptional control of a tetO-containing promoter, as well as a constitutively expressed TetR gene, is integrated into the Mtb genome at the L5 phage attachment site. Atc supplementation of the growth media initiates the transcription of target-specific sgRNA and dCas9. The dCas9 binds to the target gene and prevents gene transcription through a steric hindrance mechanism. The magnitude of gene repression is dose-dependent with respect to Atc.

The CRISPRi system is inducible by using Atc. This works similarly to the Tet ON mutants. The plasmid encodes for the TetR proteins which bind to the tetO within the psmyc1tetO promoter (located on the CRISPRi plasmid) preventing the expression of the dCas9 and sgRNA until Atc is added. Atc supplementation is then followed by target-specific binding of dCas9 and transcription repression. Hence, the higher the Atc supplemented to the bacteria, the higher the gene repression observed in a growing Mtb culture.

Moreover, the gene repression in this system is tunable, meaning the transcriptional repression can be achieved strongly or weakly (72). This depends on the use of different PAM sequences (124), varying lengths of sgRNA (131) and the GC content of sgRNA (132).

Once these mutants are generated, they can be further used to validate the target of novel compounds. If the compound targets the product of the gene of interest which is being downregulated, a shift in the susceptibility of the compound against the mutant will be observed, relative to wildtype bacteria. This shift indicates that the target of the compound is indeed likely to be the enzyme associated with the gene of interest (133).

Collectively, target validation studies are a crucial step in the drug discovery pipeline. Knowing the target of the compound maximizes its potential for rapid progression in animal testing and clinical trials.

Chapter 2

Objective

Effective clinical treatment of TB requires the administration of multiple drugs over extended periods. Due to the frequent development of resistance to antitubercular drugs by Mtb, global MDR and XDR cases remain high, with approximately 410,000 new cases reported in 2022 (3). Therefore, new drugs that target novel essential functions of the bacteria, have the potential to shorten TB treatment duration, and generate fewer side effects, are necessary to improve tuberculosis treatment outcomes. This doctoral study intends to address these needs with the specific objective of:

- **Identification of novel compounds with *in vitro* anti-TB activity, low cytotoxicity, and intracellular activity within macrophages, the primary host cell of Mtb.**

Secondly, as a part of an international consortium, the 2C-methyl-D-erythritol 4-phosphate (MEP) pathway, which is essential in Mtb for the biosynthesis of isoprenoids, was selected as a promising source of drug targets for a target-based anti-tubercular drug discovery programme (95). A key consideration with hit compounds identified via this approach is target validation at the whole cell level. Thus, another key objective was:

- **Setting up a conditional mutant system for *M. tuberculosis dxs1* and *dxr* genes of the MEP pathway and successfully validating the targets of novel compounds using these mutants.**

By focusing on these objectives, the study aims to contribute to the key initial steps of identifying novel chemotherapeutic options for TB and establishing robust *in vitro* methods for drug target validation.

Chapter 3

Materials and Methods

3.1 Materials

Table 2: List of reagents and disposals

Materials	Manufacturer
26G needle	Becton, Dickinson, Heidelberg, Germany
50ml Luer Lock Spritzen	Becton, Dickinson, Heidelberg, Germany
96-well-plates; flat bottom	Sarstedt, Nümbrecht, Germany
96-well-plates; round bottom	Sarstedt, Nümbrecht, Germany
Absolut ethanol for molecular biology	APPLICHEM, Darmstadt, Germany;
Albumin (BSA) Fraction V (pH7,0)	APPLICHEM, Darmstadt, Germany;
Anhydrotetracycline	Thermo Scientific, Waltham, USA
Aqua B. Braun	Braun, Melsungen, Germany
BCA Protein Assay Kit	Thermo Scientific, Waltham, USA
Blunt needle	M+W Dental, Illnau, Swizzerland;
Bovine serum albumin	Sigma-Aldrich, St. Louis, USA
Calcium Chloride	Sigma-Aldrich, St. Louis, USA
Calf Serum	Serana Europe GmbH, Pessin, Germany;
Cell scrapper	VWR, Radnor, USA
Corning costar Stripette (5ml, 10ml, 25ml)	Corning, New York, USA
Corning® 96 well microplates	Sigma-Aldrich, St. Louis, USA
Corning® PET 30ml inkwell bottles	Sigma-Aldrich, St. Louis, USA
Costar Stripette™, 10ml	Corning, New York, USA
Costar Stripette™, 25ml	Corning, New York, USA
Costar Stripette™, 5ml	Corning, New York, USA
Cuvette for electroporation	BioRad California, United States
Cuvette for spectrophotometer	Sarstedt, Nümbrecht, Germany
Cuvette for Zetasizer	Sarstedt, Nümbrecht, Germany
Deckel für Küvetten	Th.Geyer GmbH, Renningen, Germany

D-glucose, cell culture grade	Applichem, Darmstadt, Germany;
DifcoTM Middlebrook 7H10 Agar	Becton Dickinson, Heidelberg, Germany;
DifcoTM Middlebrook 7H9 Broth	Becton Dickinson, Heidelberg, Germany;
DIG High Prime DNA labelling and detection kit I	Roche, Basel, Switzerland;
DIG wash and block buffer	Roche, Basel, Switzerland;
Dimethylsulfoxide for cell culture	APPLICHEM, Darmstadt, Germany;
Direct-zolTM RNA MiniPrep	Zymo Research, Irvine, Canada;
Dulbecco's PBS (10x)	Biochrom, Berlin, Germany;
E-plate for xCELLigence	ACEA Biosciences, California, USA
Eppendorf® Safe-Lock microcentrifuge tubes (1.5ml, 2ml)	Sigma-Aldrich, St. Louis, USA
Eppendorf®Combitips advanced 0.25ml	VWR, Radnor, USA; #0030089413
Eppendorf®Combitips advanced 0.5ml	Eppendorf, Hamburg, Germany; #0030089421
Ethanol non-denatured	Walther CMP GmbH, Kiel, Germany
Ethylenediamine tetraacetic acid disodium (Na2-EDTA)	Carl-Roth, Karlsruhe, Germany;
Falcon® 5ml polystyrene round-bottom	Corning, New York, USA
FCS Standard South America sterile filtered	Pan-Biotek, Aidenbach, Germany
Filter Tip 10-1000µl	Nerbe plus, Winsen, Germany;
Filtropur S 0.2 syringe filter	Sarstedt, Nümbrecht, Germany
GeneRuler 1kb ladder	Thermo Scientific, Waltham, USA
Gloves, powder-free nitrile	VWR, Radnor, USA;
Glycerol	Carl-Roth, Karlsruhe, Germany;
Glycine, analytical grade	Serva Electrophoresis GmbH, Heidelberg, Germany;
HBSS	Pan-Biotek, Aidenbach, Germany
High-Fidelity (HF®) restriction enzymes	New England Biolabs, Massachusetts, USA
Illumina Nextera XT kit	Illumina, California, United States
InnuPREP DNA mini kit	Analytik Jena, Jena, Germany;
Inoculation loop with needle	Brand, Wertheim, Germany; #BRA452210
LB Broth (Miller)	Sigma-Aldrich, St. Louis, USA;
L-Glutamine	Pan-Biotek, Aidenbach, Germany
LightCycler®480 multiwell plate 96, white	Roche, Basel, Switzerland;
LightCycler®480 sealing foil	Roche, Basel, Switzerland;
LightCycler®480 SYBR Green I Master	Roche, Basel, Switzerland;
Luria-Bertani broth	Sigma-Aldrich, St. Louis, USA
Lysing Matrix tubes with beads	MP Biomedicals, California, USA
lysozyme	Thermo Scientific, Waltham, USA;
Magnesium chloride	Sigma-Aldrich, St. Louis, USA
Methanol	MERCK MILLIPORE, Darmstadt, Germany
Microtube 1.5ml	Sarstedt, Nümbrecht, Germany

Microtube 1.5ml with lid	Sarstedt, Nümbrecht, Germany
Multiply®PCR strips, 0.2ml chain	Sarstedt, Nümbrecht, Germany
Multiply®-Pro tube 0.5ml	Sarstedt, Nümbrecht, Germany
NunclonTM Delta surface Petri dish	Thermo Scientific, Waltham, USA;
NunclonTM Delta surface, 24-well	Thermo Scientific, Waltham, USA;
NunclonTM Delta surface, 6-well	Thermo Scientific, Waltham, USA;
NuncTM 48 and 96 well multi dishes	Thermo Scientific, Waltham, USA;
NuncTM cell culture Petri dish	Thermo Scientific, Waltham, USA;
OADC (oleic acid, albumin,	Becton Dickinson, Heidelberg, Germany
Oleic acid	APPLICHEM, Darmstadt, Germany;
Pancoll	Pan-Biotek, Aidenbach, Germany
Penicillin-Streptomycin	Pan-Biotek, Aidenbach, Germany
Petri dish	Sarstedt, Nümbrecht, Germany
Petridish 92x16mm	Sarstedt, Nümbrecht, Germany
Phenol-chloroform-isoamyl alcohol	Roth, Karlsruhe Germany
Pipette tip, 1000µl	Sarstedt, Nümbrecht, Germany
Pipette tip, 20µl	Sarstedt, Nümbrecht, Germany
Pipette tip, 200µl	Sarstedt, Nümbrecht, Germany
Pipette tips, no filter; 10 - 1000 µl	Sarstedt, Nümbrecht, Germany
Plate seal air permeable	Porvair Sciences, Wrexham, UK
polyethersulfone (PES) membrane 0.2uM filter	Sigma-Aldrich, St. Louis, USA
Proetin low bind tubes 1.5ml	Eppendorf, Hamburg, Germany
Protease Inhibitor Cocktail Tabletten	Roche, Basel, Switzerland
Proteinase K solution	Roth, Karlsruhe Germany
QIAGEN DNA gel purification kit	QIAGEN, Venlo, The Netherlands
Rapid DNA Ligation Kit	Thermo Scientific, Waltham, USA
rCutSmart™ Buffer	New England Biolabs, Massachusetts, USA
Resazurin	Cayman chemicals, Michigan, USA
RNA purification and isolation kit	Zymo Research, Irvine, Canada;
Roller bottles	Corning, New York, USA
RPMI 1640 VLE	Pan-Biotek, Aidenbach, Germany
SafeSeal microtube 2ml	Sarstedt, Nümbrecht, Germany
Screw Cap tube, 15ml	Sarstedt, Nümbrecht, Germany
Screw Cap tube, 50ml	Sarstedt, Nümbrecht, Germany
Sodium chlorid 99,9%	APPLICHEM, Darmstadt, Germany;
Sodium hydrogen carbonate	MERCK MILLIPORE, Darmstadt, Germany
Staurosporin	Sigma-Aldrich, St. Louis, USA
SYBR Safe DNA Gel Stain	Thermo Scientific, Waltham, USA
Syringe, 1ml	Becton Dickinson, Heidelberg, Germany
T4 DNA Ligase Reaction Buffer	New England Biolabs, Massachusetts, USA
T4 DNA Ligase Reaction Enzyme	New England Biolabs, Massachusetts, USA

Taq PCR polymerase	Qiagen, Venlo, The Netherlands
Tissue culture flask T25, stand. vent. cap	Sarstedt, Nümbrecht, Germany
Tissue culture plate 96well Standard F	Sarstedt, Nümbrecht, Germany
Tissue culture plate 96well Standard R	Sarstedt, Nümbrecht, Germany
TritonTM X-100	Sigma-Aldrich, St. Louis, USA
TriTrack DNA Loading Dye	Thermo Scientific, Waltham, USA
TRIzol™ Reagent	Thermo Scientific, Waltham, USA;
Tween® 20 molecular biology grade	ChemSolute®; Renningen, Germany
TWEEN®80	Sigma-Aldrich, St. Louis, USA;
UltraPureTM agarose	Carl-Roth, Karlsruhe, Germany;
Vue life cell culture bags	Cellgenix, Freiburg, Germany
x-gal fluorescent dye	Sigma-Aldrich, St. Louis, USA
XTT dye	Serva, Heidelberg, Germany
ZymoPURE™ 96 Plasmid Miniprep Kit	Zymo Research, Irvine, Canada;

Table 3: List of buffers and solutions

Name	Ingredients
7H9 broth	4.7 g Difco Middlebrook 7H9 broth
	900 ml ddH_2O
	2 ml glycerol
	100 ml bovine serum
	500ul Tween-20
7H10 agar plates	19 g Difco Middlebrook 7H10 Agar
	900 ml ddH_2O
	5 ml glycerol
	100 ml bovine serum
50x TAE (Tris-acetate-EDTA) buffer	242 g tris base
	57.1 ml glacial acetic acid
	100 ml of 500 mM EDTA (pH 8.0) solution
	bring up to 1 litre with ddH2O
	Adjust to pH8
1xTBS-T	100ml TBS (10x)
	900ml ddH_2O
	0.1% Tween-20
10xTBS	24.2g TRIS base
	80.0g NaCl
	in 1l ddH_2O
	pH adjusted to 7.6 using 1M HCl

8x SDS Lysis Buffer	16%SDS,
	1M Tris
	160mM DTT (added freshly)
	in ddH_2O
	pH adjusted to 7.8 using 1M HCl
20x SSC	175.3 g NaCl
	88.2 g sodium citrate
	in 1L of ddH2O
2x SSC	10x dilution of 20xSSC
Antibody solution (ABS) (DIG detection kit I)	Anti-DIG-AP, diluted 1:5000 in 1% Blocking solution
Annealing Buffer Composition (1X)	10 mM Tris
	50 mM NaCl.
	1 mM EDTA
	Adjust to pH8
Blocking solution 1% (BS) (DIG detection kit I)	10% Blocking solution diluted to 1x Maleic acid buffer
Cell culture medium	VLE-RPMI (1640)
	+10% FCS
	+1% L-Glutamine
Colour-substrate solution (CSS) (DIG detection kit I)	NBT/BCIP solution diluted 50x in Detection buffer
Detection buffer (DB)	12.1 g Tris-HCl
	5.85 g NaCl
	in 1L water
	Adjust to pH9.5
DNB Denaturation buffer	87 g NaCl
	20 g NaOH
	in 1L ddH2O
DPB Depurination Buffer	200 ml of 0.2M HCL
	800ml of ddH2O
DS-LB Broth	50g of LB Broth (Miller) broth
	1 L of dH2O
HSB High Stringency Buffer	2 x SSC
	0.1% SDS
LB Broth	25g of LB Broth (Miller) broth
	1 L of dH2O
LSB Low Stringency Buffer	0.5 x SSC
	0.1% SDS

Maleic acid buffer	22.2 g maleic acid
	17.6 g NaCl
	in 1L water
	Adjust to pH7.5
NB Neutralization buffer	600ml of 3M NaCl
	500ml of 0.5M Tris HCl
	Adjust to pH7.5
SET lysis buffer	20% sucrose
	50mM EDTA
	50mM tris HCL
	Adjust to pH8
TE buffer	10mM Tris HCl
	1mM EDTA
	Adjust to pH8
Washing buffer (WB)	0.3% Tween-20 in Maleic acid buffer

Table 4: List of instruments and devices

Instrument	Manufacturer
Autoclave Systec DX-150	Systec GmbH, Münster, Germany
Axiovert 35M, light microscope	Carl Zeiss AG, Oberkochen, Germany
Balance	Sartorius AG, Göttingen, Germany
Block Thermostat QBD1	Grant Instruments, Shepreth, UK
Centrifuge 5430R	Eppendorf, Hamburg, Germany
Eppendorf Multipette®Xtream	Eppendorf, Hamburg, Germany
Eppendorf Research Pro multichannel pipette	Eppendorf, Hamburg, Germany
FastPrep™-24 Classic Bead-Beating device	MP Biomedicals, California, USA
GeneTouch Thermocycler	BIOER Technology, Binjiang, China
Hera Freeze HFU T Series -80°C freezer	Thermo Scientific, Waltham, USA
HeraCell 240 Incubator	Thermo Scientific, Waltham, USA
HeraeusFresco™ 21 benchtop centrifuge	Thermo Scientific, Waltham, USA
Herasafe safety cabinet	Heraeus Instruments, Hanau, Germany
Hettich® Rotanta 460R	Hettich, Tuttlingen, Germany
Illumina NextSeq 500	Illumina, California, United States
Julbalo TW12 waterbath	Julabo, Seelbach, Germany
LightCycler 480	Roche, Basel, Switzerland
MicroPulser Electroporator	BioRad California, United States
MiniSpin® centrifuge	Eppendorf, Hamburg, Germany
NanoDropTM 1000	Thermo Scientific, Waltham, USA
Pipetboy acu	Integra Bioscience, Zizers, Switzerland
Pipettes (10, 100, 200, 1000µl)	Eppendorf, Hamburg, Germany

Q Exactive Plus mass spectrometer	Thermo Scientific, Waltham, USA
S1 Pipet Filler Pipetbpy	Thermo Scientific, Waltham, USA
ScanLaf Mars Safety Class 2, biosafety cabinet	Labogene, Lynge, Denmark
ScotsmanTM AF-10 Ice Flake Maker	Thermo Scientific, Waltham, USA
Spectrophotometer	DeNovix Inc., Wilmington, USA
SynergyTM 2 plate reader	BIOTEK, Vermont, USA
Transferpette®-8	Brand, Wertheim, Germany
Vortex	VWR, Radnor, USA
xCELLigence Real-Time Cell Analyzer (RTCA)	Roche Applied Sciences, Indianapolis, IN
ZetaSizer Nano ZS	Malvern Pananalytical, Worcestershire, UK

3.2 Methods

3.2.1 Drug testing

3.2.1.1 Bacterial growth, media and strains

Frozen aliquots of the bacteria were prepared according to Brandenburg *et al*. (134). In brief, the bacteria were grown in Middlebrook 7H9 broth (Difco, Detroit, USA) supplemented with 10% Middlebrook Oleic albumin-dextrose-catalase (OADC) enrichment medium (Becton Dickinson, Heidelberg, Germany), 0.2% Glycerol (Carl-Roth, Karlsruhe, Germany), and 0.05% Tween 80 (Sigma-Aldrich, St. Louis, USA), henceforth referred to as "growth media", in 490 cm2 Corning roller bottles (New York, USA). If antibiotics were needed for their growth maintenance of transformed recombinant DNA (either replicating plasmids or genome-integrated DNA), in the case of the mutant, kanamycin (kan) or/and hygromycin (hyg) was supplemented at a concentration of 25ug/ml. The culture was further harvested at the mid-log phase (OD600 0.3-0.6) and aliquoted and frozen at −80 °C. These aliquots were thawed, centrifuged and resuspended in the growth media prior to every experiment. A detailed list of bacterial strains used in this study is presented in **Supplementary Table 1.**

3.2.1.2 Dynamic light scattering (DLS) assay

Compounds were analysed for solubility in the bacterial growth media using the Dynamic Light Scattering (DLS) assay using a Zetasizer Nano ZS90 (Malvern Instruments Ltd, Worcestershire, UK). Experiments were performed in 100 microliter (ul) volumes, using disposable cuvettes (Sarstedt AG & Co, Nümbrecht, Germany). Compounds were diluted in a growth medium to reach the desired test concentrations. Media with dimethyl sulfoxide (DMSO) alone was used as control. The derived count rate (DCR) values obtained from the analyses indicated the degree of aggregation formation. These values were compared to the DMSO control which allowed the determination of the sample concentration at which the respective compound was entirely soluble, with no detectable aggregate formation.

3.2.1.3 Activity assays/Minimum Inhibition Concentration assays

Anti-tubercular tests were performed as previously described (135, 136). In brief, the frozen bacterial aliquots of Mtb mCherry strain, if not stated otherwise, were thawed and then passed through a syringe with a 26-gauge needle (Becton Dickinson, Heidelberg, Germany) to disperse bacterial clumps. 100 ul aliquots of a culture diluted to 2×10^5 CFU/ml were then transferred in triplicate to pre-prepared test compound-containing 96 well plates, to test the non-precipitating compounds for anti-tubercular activity at the concentrations indicated. For these assays, 96-well flat clear bottom black polystyrene microplates (Corning® CellBIND®, Merck, New York, USA) were used unless mentioned otherwise. Each plate had RIF (at 1ug/ml and 0.1ug/ml) (National Reference Center, Borstel) as a reference compound. Plates were sealed

with an air-permeable membrane (Porvair Sciences, Wrexham, UK) in a 37 °C incubator with mild agitation (TiMix5, Edmund Bühler, Germany). The activity of compounds was determined after 7 days by measuring the bacterial growth as Relative fluorescence units (RFU) from the fluorescence intensity obtained at an excitation wavelength of 575 nm and an emission wavelength of 635 nm in a microplate reader (Synergy™ 2 plate reader, BioTek Instruments, Vermont, USA). Two independent experiments (each in triplicates) were performed, and all values were normalized to untreated control wells (100 %) in each experiment. The graphs were obtained by the average of both experiments using GraphPad Prism version 9.4.1 for Windows (GraphPad Software, San Diego, California USA, www.graphpad.com). The first concentration of compounds at which 90 % Mtb inhibition was observed was considered to be MIC90.

MIC90 using Alamar blue assay: 96 well plates were prepared as stated above. On day 7, 30ul of a 0.02 % (w/v) Resazurin (Cayman Chemicals, #14322) was added to each well and further incubated for 24 hours at 37 °C. Plates were measured for fluorescence of the reduced resazurin (resorufin) dye at an excitation wavelength of 540nm and emission wavelength of 635nm, and graphs were plotted by normalising the data to the 100% of growth control using GraphPad Prism version 9.4.1. Alamar blue assay was used for MIC determination using the Mtb H37Rv strain and the mutants. If the Mtb mCherry strain was used, then the plates were only visually observed for a colour change to determine the MIC90 since the mCherry fluorescence overlaps with the resazurin fluorescence.

3.2.1.4 Obtaining Human Monocyte-derived Macrophages (HMdM)

Isolation of monocytes was done using density gradient centrifugation and subsequent counterflow centrifugation as described in Brandenburg *et al.* (134). In brief, either human heparinized peripheral blood from healthy donors (Borstel, approved by the Ministry of Agriculture, Environment and Rural Areas in Kiel, Germany) or buffy coats from UKSH Lübeck (Ethics application: file reference 19-367) were used for this process. In brief, pre-warmed Phosphate Buffered Saline (PBS; Biochrom, Berlin, Germany) was used to dilute the blood (1:2 ratio) or buffy coats (1:6 ratio). 40 ml of this was layered carefully on a 10ml poly sucrose solution (Pancoll; Pan-Biotek, Aidenbach, Germany) of a density of 1.077 g/ml. This was followed by centrifugation [160 relative centrifugal force (rcf); 45mins; 21°C] and the interphase peripheral blood mononuclear cell (PBMC) layer was carefully transferred in a new 50ml tube. These PBMCs were washed twice with 50ml PBS and re-suspended in 100ml Hank's buffered salt solution (HBSS; Pan-Biotek, Aidenbach, Germany) containing 0.1% Bovine serum albumin (BSA; Sigma-Aldrich, St. Louis, USA) and mounted onto the elutriation chamber. Here, the counterflow centrifugal elutriation (CCE) method was used to separate the mixed cell population depending on their different size and density. Hence the lymphocytes, monocytes and thrombocytes from the PBMCs were separated. The CCE was disinfected thoroughly using ethanol and followed by the pumping of the PBMCs into the chamber. Due to the centrifugal outward force and the inward counterflow of the elutriator in an increasing flow rate, a cell gradient of increasing size is generated **(Table 5)**. The centrifuge was stopped at a flow rate of 39 ml/min and the monocyte fraction was collected in a 50ml tube. The monocyte fraction with a purity of minimum 93% determined using the Casy29 cell counter, was further centrifuged and the pellet was resuspended in Roswell Park Memorial Institute Medium (RPMI) 1640 containing 2% human serum, 10ng/ml recombinant human macrophage colony-

stimulating factor (M-CSF), 100ug/ml Streptomycin and 100ug/ml Penicillin (P/S) and 4mM L-glutamine at a cell density of 5 x 10^5 cells/ml. To differentiate the monocytes from the macrophages the suspension was transferred in Teflon-coated cell culture bags and incubated for 7 days at 37°C and 5% CO_2

On the day of the experiment, the human monocyte-derived macrophages (HMdMs) were removed from the Teflon bags by incubating them on ice for 1 h. Further, they were centrifuged (10 mins; 160 rcf; 4°C) and re-suspended in RPMI 16040 containing 10% FCS and 4mM L-glutamine, herein referred to as cell culture medium. Cells were counted using a Neubauer chamber and trypan blue staining. The cell count formula used was as follows:

cell count=number of cells in 4 quadrants*dilution factor*10,000

For the experiments cells were seeded in 96 well plates or 48 well plates and incubated for 2 hours at 37°C and 5% CO_2 before the assay.

Table 5: Protocol for elutriation indicating the flow rates and expected fractions

Flow rate (ml/min)	Fraction
27	Thrombocytes
30	Small lymphocytes
33-35	Lymphocytes
36	Large lymphocytes
37-42	Washing
43	Monocytes
44 (stop)	Pure Monocytes

3.2.1.5 Cytotox assay

To determine the toxicity of the compounds on HMdM, XTT assay and xCELLigence system were used.

XTT assay

HMdMs were seeded in 96-well clear flat bottom plates (Nunclon™ Delta Surface, ThermoScientific, Denmark) at a density of 5×10^4 cells/well in a total volume of 100ul RPMI cell culture medium. After 2 hours of incubation (37°C and 5% CO2) 100ul of compound to be tested, diluted in cell culture media, were added at different concentrations (64uM to 1uM) in triplicate wells. The plates were incubated further for 24 hours (37°C and 5% CO2). As a positive control for the experiment, Triton™-X 100 (1%-3% dissolved in PBS) (Sigma-Aldrich, Missouri, USA) diluted in culture medium was used. After the incubation, the cell culture media was replaced with 200ul of Triton™-X 100 and incubated for 10 mins (37°C and 5% CO2). This was followed by the addition of XTT dye (Serva, Heidelberg, Germany) to all the wells resuspended thoroughly and further incubated for 3-4 hours before measuring the plates for absorbance at 490 nm on a multi-well plate reader

(Synergy 2, BioTek Instruments, Vermont, USA). Untreated cells were used as a negative control. The Cytotoxic Concentration 50 (CC50) was determined by plotting a curve or observing the 90% cell death using GraphPad Prism version 9.4.1.

xCELLigence system

xCELLigence Real-Time Cell Analyzer (RTCA) Single Plate (SP) instrument (Roche Applied Sciences, Indianapolis, USA) is used for this assay. The background was measured by adding 50ul of cell culture medium to the 96-well E-Plate (ACEA Biosciences, California, USA) which is coated with biosensors. After the background media reading, 50,000 cells in 50ul of media were added to the plates and measured for 3 hours until the cells were settled. Subsequently, 50ul of the compounds with respective concentrations to be measured are added to the cells and the analysis is run for 4 days to measure real-time cell death. Staurosporin from Streptomyces sp. (Sigma Aldrich) was diluted in the cell culture media (1:1000) and was used as a positive control for the assay. Untreated cells were used as the negative control. Cells treated with the highest concentration of DMSO used by the compounds served as DMSO control. The data was exported from the xCELLigence system for analysis.

3.2.1.6 Intracellular survival assay

To analyse the survival of Mtb within macrophages HMdM were first obtained like previously described. The cells were seeded in 48 well plates (Nunclon™ Delta Surface, Thermo Scientific) at a density of 0.2×10^6 cells/well in a total volume of 500 cell culture medium. After 2 hours of incubation at 37°C and 5% CO2, the wells were infected with Mtb H37Rv American Type Culture Collection (ATCC) 27294, (unless otherwise stated), with a multiplicity of infection (MOI) of 0.5 (unless otherwise stated). The plates were incubated for 4h (37°C and 5% CO2) followed by washing 3 times with 500ul pre-warmed Hanks' Balanced Salt Solution (HBSS) to remove extracellular bacteria. Dilutions of compounds to be tested were made in cell culture media and 500ul were added to the wells containing infected cells. 500ul of water was added to the outer wells of the plate and sealed with micropore and incubated (37°C and 5% CO2) for 7 days. On day 3, the culture media was replaced with fresh media containing the same compound concentration as before. On day 7, the media from the wells were discarded and 500ul of water containing 0.05% tween 80 was added to the wells and incubated for 10 mins at 37°C. For bacterial CFU quantification, the liquid from respective wells was further diluted 2-fold and 100ul was spread on 7h10 agar plates. The plates were incubated at 37°C and the colonies were counted after 3-4 weeks.

As a positive control and negative control for the experiment RIF and untreated cells (respectively) were used. Since compounds were dissolved in DMSO, the highest concentration of DMSO in the compounds used was also included in the assay. On the first day of the experiment, samples from the 4-hour post-infection timepoint were plated to calculate the starting number of bacteria taken up by the macrophages.

3.2.2 Cloning

3.2.2.1 Basic molecular biology techniques

PCR, Primers and Plasmids

Polymerase chain reaction (PCR) was performed for amplification of cDNA, plasmids and genomic DNA templates. Taq DNA polymerase (Qiagen, Venlo, The Netherlands) was used for the PCR. PCRs performed to amplify the *dxs1* and *dxr* gene fragments for generating promoter replacement mutants used primers with flanking SphI and NotI (New England Biolabs, Massachusetts, USA) restriction enzyme cleavage sites. These primers are listed in **Table 6.** The protocol used for PCR is stated in **Table 7**. All the plasmids used in this study are described in the **Supplementary Table 1.**

Table 6: Primers used for Polymerase Chain reaction (PCR)

Primers	Sequences
Dxs forward	*GCATGC* TACACTAGCGAAATGCTGC
Dxs reverse	*GCGGCCGC* GTAGCTGCGCCCATTGTC
Dxr forward	*GCATGC* GCACAATGATGAGGTGACC
Dxr reverse	*GCGGCCGC* AGCTTGGCGACCTCGT

(Base pairs in italics are the restriction enzyme sequences)

Table 7: Overview of PCR mixture and PCR thermocycler protocol used in this study.

Reagents	Volume (ul)
10xbuffer	5
5xenhancer	10
10x mM dNTPs	1
forward primer 10uM	2.5
reverse primer 10uM	2.5
Template	1
Enzyme	0.5
Nuclease free water	27.5

Thermocycler settings for PCR for 20-30 amplification cycles		
Denature template	94 °C	1 min
Anneal primers	55 °C	2 min
Extension	72 °C	3 min

Gel electrophoresis

Gel electrophoresis was performed as described previously (137). In brief, 1% agar (Becton Dickinson, Heidelberg, Germany) in Tris-acetate-EDTA (TAE) buffer was mixed with 0.005% of SYBR Safe DNA Gel Stain (Thermo Scientific). For the samples to be loaded on the gel, TriTrack DNA Loading Dye (Thermo Scientific) was added to the samples to 1 x final concentration. The gel was run at 80-100V until the TriTrack dye had visibly separated. GeneRuler 1kb ladder (Thermo Scientific) was also included in the run to compare and identify the size of the DNA bands. The gel was then placed under UV light to visualize the bands. For the purification of PCR products from the gel, the QIAGEN DNA gel purification kit was used. Plasmid DNA was isolated using ZymoPURE 96 Plasmid Miniprep Kit following the user manual.

Restriction enzyme digestion and ligation

For Restriction enzyme digestions (REDs) rCutSmart™ Buffer (New England Biolabs, Massachusetts, USA) and High-Fidelity (HF®) restriction enzymes (New England Biolabs) were used. The digestion proceeded at 37°C for 2 hours overnight following the user manual**.** Following the RED, ligation was performed using the Rapid DNA Ligation Kit (Thermo Scientific). This was set up for a minimum of 3 hours to a maximum of overnight following the user manual. The protocols for both these steps are described in **Table 8.**

Table 8: Protocol used in this study for Restriction enzyme digestion and ligation

Restriction enzyme digestion	
Components	**Volume**
Sample (fragments to be ligated)	2ul
Buffer	5 ul
Restriction enzyme 1	2 ul
Restriction enzyme 2	2 ul
N.F water	39 ul
Total volume	**50 ul**
Ligation	
Components	**Volume**
DNA fragment 1 (plasmid)	2 ul
DNA fragment 2 (Gene insert)	8 ul
Ligation master mix	10 ul
Total volume	**20 ul**

Transformation in *E. coli*: Heat shock method

E. coli DH5a was cultured in Double strength Luria-Bertani broth (DS-LB) (Sigma-Aldrich) with 0.2% glucose up to an OD600 of 0.3-0.4. The culture was then centrifuged (5000 rpm, 10mins, 4°C), the supernatant discarded, and the pellet resuspended in 40ml of pre-cooled 100mM $MgCl_2$. Subsequently, cultures were incubated on ice for 20-30, centrifuged further (rpm 4000, 10mins, 4°C) and finally resuspended in 4ml of ice cold 100mM CaCl2 +15% glycerol. To proceed with transformation, aliquots of competent cells were

mixed with a minimum of 10-50ng plasmid DNA and incubated on ice for 30 minutes. This was followed by heat shocking the cells for 10mins at 37°C followed by the addition of 800ul DS-LB broth and incubating for 30-60mins on a shaker at room temperature. The cells were then concentrated by centrifugation if required and plated on LB-agar plates containing the relevant antibiotic. Colonies were picked the next day and cultured in 5-10ml of LB broth.

Transformation in Mtb: Electroporation

Bacteria were grown in 10ml 7H9 growth media in 30 ml inkwell bottles (Sigma-Aldrich) up to the mid-log phase (OD600 of 0.6-1.0). The cultures were then expanded to larger flasks in 40ml of growth media and grown further to the mid-log phase (OD600 of 0.6 -1.0). Subsequently, the cultures were collected by centrifugation (4000rpm, 10mins, 25°C), the supernatant discarded, and the pellet resuspended in 1ml of pre-warmed glycerol buffer (10% glycerol, 0.05% Tween 80). Further, 40ml of glycerol buffer was added to the resuspended pellet and the step was repeated three times to ensure proper washing of the cells. After the final wash step, the cells were resuspended in 1ml of glycerol buffer and split into two vials of 500ul each. 5ul of plasmid (at least 100ng) was then added to respective vials and incubated for 30 minutes on a shaker. One aliquot of competent cells was used as a transformation negative control and had no plasmid added. The transformation was performed using a MicroPulser Electroporation device (BioRad California, United States). 400ul of cell plasmid mixtures were added to electroporation cuvettes (BioRad) and electroporated with the following settings: 1000 Ω resistance, Voltage 2.5KV. The bacteria were recovered by immediately adding 1ml of growth media to the cuvette and further transferring it to 4ml of growth media in an inkwell culture bottle. Bottles were incubated overnight on a shaker at 37°C. The following day the bacteria were diluted 2-fold and 100ul of each dilution was plated on 7H10 plates and incubated at 37°C until colonies were visible. The colonies were picked after 3 weeks and cultured in 15ml growth media with supplements if required [such as antibiotics or Anhydrotetracycline (Atc)]. At the mid-log phase (OD600 of 0.6 -1.0) 500ul aliquots of the cultures were made and frozen at -80°C for further assays.

gDNA isolation

10ml of Mtb H37Rv was cultured up to OD600 of 0.8 to 1.0. The pellet was obtained by centrifuging (3200xg, 10 mins, room temperature) the bacteria and resuspending in 250ul of Sucrose EDTA Tris (SET) lysis buffer and 50ul of lysozyme (Thermo Scientific). A detailed description of the buffers is provided in the materials section in **Table 3**. This mixture was incubated overnight at 37°C. 10ul of RNAse (10mg/ml) was then added and incubated at 37°C for 30mins followed by the addition of 250ul Proteinase K solution (Roth, Karlsruhe, Germany) and incubation at 55°C for 2 hours. An equal amount of Phenol-chloroform-isoamyl alcohol (Roth) in the concentration of ratio 25:24:1 was added to the sample, mixed vigorously and centrifuged (16000xg, 10min, room temperature) to recover the top aqueous layer. Subsequently, 0.1 times the volume of 3M sodium acetate (pH5.2) and 0.7 times the volume of isopropanol was added to the recovered layer and incubated at -20°C for 1 hour. The gDNA was precipitated by centrifugation (16000xg, 30min at 4°C) and the pellet was washed with 70% ethanol. The pellet was then resuspended in Nuclease free (NF) water and filtered using a polyethersulfone (PES) membrane 0.2uM filter (Sigma-Aldrich) to allow it to leave the Bio

safety level-3 (BSL-3) laboratory. The concentration of gDNA was measured using a Nanodrop device (Thermo Scientific).

RNA isolation

Bacterial cultures were grown in 10ml growth media (with antibiotics if applicable) in inkwell bottles starting from the frozen aliquots. The cultures were grown up to the mid-log phase (OD600 of 0.6 -1.0) and then subcultured in 10ml of growth media with supplements (as required) to a starting OD600 of 0.05. These cultures were further grown for 3 days and centrifuged (rpm 3500, 15mins, 4°C) to collect the pellet. The pellet was resuspended in 1 ml TRIzol™ Reagent (Thermo Scientific) using pasture pipettes and transferred to Lysing Matrix tubes with beads (MP Biomedicals, California, USA). All the tubes were subjected to bead beating for 30 seconds at 6 m/s. This step was repeated four times with 5 mins of cooling between runs. The tubes were then centrifuged to pellet the beads and the supernatant was transferred to a clean RNAse/DNAse free microfuge tube. The tubes were kept on ice throughout the process. The RNA isolation was performed using an RNA purification and isolation kit (Zymo) following the user manual. The RNA obtained was stored at -80 or immediately used for further assays. The concentration of RNA was measured using a Nanodrop device (Thermo Scientific).

Southern blotting

Southern blotting was performed as described previously (138). In brief, following gDNA isolation, restriction enzyme digestion was performed by using XbaI and PvuII for the SCO Dxs mutant and XbaI and AgeI for the SCO Dxr mutant. This was followed by gel electrophoresis. The gel was immersed in denaturing buffer (DNB), followed by immersion in neutralization buffer (NB) for 15-30min each. The details of all the buffers used for this assay are described in **Table 3**. The DNA from the neutralized gel was then transferred to a nylon membrane by following multiple steps. The gel was placed on a filter paper which was immersed in 20x Saline-sodium citrate (SSC) buffer. The nylon membrane was carefully placed on top of the gel and multiple Whatman filter paper pre-immersed in 2x SSC were placed on top of the membrane. The transfer was allowed to happen overnight followed by baking the membrane for 2 hours at 70-80°C in a vacuum oven. Next, the membrane was labelled using the DIG High Prime DNA labelling and detection kit I and the DIG wash and block buffer (Roche) following the user manual's instructions. Post labelling, the membrane was pre-hybridized at 65°C for 30-60 mins in the pre-hybridization buffer using a shaking water bath followed by snap cooling on ice/ethanol for 5 mins and then transferring to a hybridization buffer. This was further incubated at 65°C overnight in a shaking water bath.

The following day, the membrane was washed with High stringency buffer (HSB) at room temperature and then with low stringency buffer (LSB) at 65°C. Subsequently, the membrane was incubated in washing buffer (WB) for 2mins, in Blocking solution (BS) for 30mins, Antibody solution (ABS) for 30 mins and washed with WB. The membrane was then equilibrated in 20ml DB for 5 mins and placed in Colour substrate solution (CSS) protected from light until bands were visible. The reaction was stopped by washing the membrane with NF water.

Next generation sequencing (NGS)

For Next generation sequencing the gDNA extracted from the bacteria was sent to the NGS team of the research group Molecular and Experimental Mycobacteriology at the Research Center Borstel, at a concentration >0.05ng/ul. Short-read Illumina (San Diego, CA, US) data was generated as instructed by the manufacturer using a modified Nextera XT DNA library preparation protocol (139). Raw reads were stored and documented locally as per the institute's guidelines. First, a short read assembly was performed with shovill (https://github.com/tseemann/shovill) under the supervision of Prof. Matthias Merker, using the following parameters: –-depth 100 –-gsize 4.4M --trim --assembler spades –noreadcorr. The data obtained from de novo assembly in the form of contiguous sequences (contigs) was blasted against the generated plasmid construct to find the contigs where the genome of interest belongs. The contigs containing the gene of interest were further aligned (Pairwise alignment) with the sequences of the expected construct using the software Geneious v2023.1.1 (https://www.geneious.com) to ensure the integration of the plasmid in the Mtb genome.

RT-qPCR

For qPCR, primers and probes were obtained from Tib MolBiol (Berlin, Germany). The probes received were prelabelled with a fluorescent dye (3' 6-Carboxyfluorescein [6-FAM]) and a quencher (5' BlackBerry quencher [BBQ]). The list of primers used for *dxs1* and *dxr* are mentioned in the **Table 9**.

For the qPCR, Mtb *sigA* (Rv2703) was used as a housekeeping gene for all the experiments. A standard PCR mix contained NF water (1.9ul), Light cycler 480 probes Master Mix (5ul) primers (2ul) and probes (0.1ul). Into each required well of a LightCycler 480 Multiwell plate (Roche, Basel, Switzerland) 9ul of PCR mix was added along with 1ul of cDNA. A standard curve was made using the cDNA pooled together from all the samples of the experiment. Followed by loading of the samples and standards, the plate was sealed with LightCycler 480 sealing foil (Roche) and centrifuged (rpm 1200, 2mins, room temperature) and analysed using the Light cycler 480 device (Roche). The protocol shown in **Table 9** was followed for the qPCR. The ΔΔCt data received from the Light cycler software was used to determine the fold change of the gene of interest by comparing transcript levels of the target gene relative to the housekeeping gene (*sigA*).

Table 9: Primers, probes and protocol for RT-qPCR using the Light Cycler 480 device. The probes used were pre-labelled with fluorescent dye 6-Carboxyfluorescein [6-FAM]) and quencher (BlackBerry quencher [BBQ].

Primers for RT-qPCR	
Dxs forward	AACATCTTgTggACgTAggC
Dxs reverse	CTgggAgTggTggAACTCA
Dxs probe	6FAM--CCgCACgATCCgATCATCTTCgA--BBQ
Dxr forward	gTgACCATCgAATggATgATC
Dxr reverse	gATgAACACgCTgAATTCg
Dxr probe	6FAM—CAgCAggTgggTTTCgATgACCTC--BBQ

Protocol for RT-qPCR		
Step	**Temperature (°C)**	**Duration (min: sec)**
Pre-Incubation (1 cycle)	50	02:00
	95	10:00
	95	00:15
Amplification (40 cycles)	62	01:00
	62	00:01
	95	00:10
Melting Curve (1 cycle)	65	00:10
	Increase up to 97	

Proteomics

Mtb H37Rv ATCC 27294 was heat-inactivated. Cultures were grown in 10ml bottles up to mid-log phase and cells were harvested by centrifugation followed by resuspension in 1ml growth media in 1.5 ml non-protein binding eppies. These eppies were subjected to heat treatment of 90 °C for 20 mins followed by shipping them to the collaboration institute OmicScouts, Freising, Germany where further work was conducted. The cells were further lysed by sonication (Bioruptor Pico, Diagenode) performing 5 cycles of 60 s sonication and 90 s pause before every cycle at 4 °C. The cell lysate was then centrifuged for 20 min at 4 °C, 20000 × g and the supernatant were collected. The protein concentration was determined (Pierce™ BCA Protein Assay Kit, Thermo Fisher Scientific) and the cell lysate was stored at -80 °C until further use.

Sample Preparation for LC-MS/MS Analysis:

Disulfide bonds were reduced with 10 mM Dithiothreitol (DTT), and incubated for 30 min at 35 °C. Proteins were alkylated with 55 mM chloroacetamide for 30 min at room temperature in the dark. Samples were acidified with phosphoric acid to 2.5%, diluted with methanol, and transferred to an S-trap column (Protifi, New york, USA). Trypsin was added for digestion overnight at 37 °C. Peptides were eluted, dried, resuspended in 0.5% FA, desalted, dried, and stored at −80 °C.

LC-MS/MS Data Acquisition:

Samples were solubilized in 0.1% FA and injected (1ug) into a Dionex UltiMate 3000 nano system coupled to a Q Exactive Plus mass spectrometer (Thermo Scientific, Waltham, USA). Peptides were trapped, then separated on an analytical column with a 120 min gradient from 2% to 32% solvent B. The mass spectrometer was operated in data-independent acquisition (DIA) mode and full scan spectra (m/z 400−1000) were acquired.

Peptide and Protein Identification and Quantification:

Raw files were processed with DIA-NN (v1.8.1) using the UniProt FASTA file for Mtb H37Rv. Trypsin/P was selected for digestion, with up to two missed cleavages. Peptide length was 7-30 amino acids, and m/z range was 300-1800.

3.2.2.2 Conditional mutant generation and target validation

Construction of Promoter replacement mutants

Single Crossover organisms (SCO) were generated using the integrative plasmid pSE100 ((129) Addgene plasmid #17972). Prior to the construction of Dxs-SCO and Dxr-SCO, subcloning with plasmid pDrive was performed. The ribosomal binding region for each gene along with the first 554 bp of the gene *dxs1* (Rv2682c; position 2999988 to 2999454) and 537 bp of the gene *dxr* (Rv2870c; position 3183025 to 3182488) were amplified using PCR. The primers **(Table 6)** used for the PCR were tagged with cleavage sites for the restriction enzymes SphI (forward primer) and NotI (Reverse primer; New England BioLabs). The amplified products were subjected to restriction digestion, isolated using Gel electrophoresis, purified, and ligated into a similarly digested empty pDrive cloning vector. The pDrive+dxs and pDrive+dxr ligation reactions were transformed into *E. coli* and selected using kanamycin and a blue-white screening method. In this method, the LB plates were supplemented with the chromogenic beta-galactosidase substrate X-Gal (SigmaAldrich) and white colonies were picked, cultured in LB broth and frozen stocks were made using 15% glycerol. Further, plasmids were isolated from the cultures and sent for Sanger sequencing (Eurofins Genomics). Following confirmation of correct pDrive vector construction, restriction enzyme digestion was performed on the plasmids using SphI and NotI enzymes and the relevant fragments were separated and purified using gel electrophoresis. Simultaneously the plasmid pSE100 was also digested using the enzymes SphI and NotI and the fragment containing the tet operator (2614 bp) was purified and used for further ligation steps. The gene fragments cut from the pDrive plasmids and the tet operator fragment from the pSE100 plasmid were ligated as described above and transformed into *E. coli*. Hygromycin-resistant colonies were picked and frozen stocks were made. Plasmids (herein termed SCO plasmids) were isolated and sent for Sanger sequencing (Eurofins). Sequence-confirmed SCO plasmids were transformed into Mtb H37Rv ATCC 27294 using the method described above. Hygromycin-resistant colonies were picked and frozen stocks of SCO-Dxs and SCO-Dxr Mtb strains were made. To further generate Tet OFF and Tet ON conditional mutants, each SCO strain was individually electroporated with plasmids pTEK-4S-OX (Addgene plasmid #17974) and pMC2m (Addgene plasmid #17970) respectively. Post electroporation, colonies were cultured in growth media including kan and hyg. For TetON cultures, 50ng/ml Atc was also included in the growth media. Frozen stocks of the cultures were made for further assays.

Design of sgRNA and cloning for CRISPRi

The design of sgRNAs was followed as previously described For designing the sgRNAs the following web-based tool was referred to: https://pebble.rockefeller.edu/tools/sgrna-design/. A 21bp sequence was selected downstream of strong PAM sequences for all three target genes (*dxs1*, *dxr* and *rpoB*). Three sgRNA sequences for each gene were selected **(Table 10).** The template strand and non-template strand of the selected sequences were ordered as oligos with 'GGGA' and 'AAAC' overhangs respectively (to allow for BsmBI restriction enzyme cloning). For annealing of the oligos, oligo annealing buffer **(Table 3)** was mixed with top and bottom oligos and placed in the thermocycler at 95°C for 2 mins followed by keeping the samples at -0.1°C/s to 25°C before further use.

The dsDNA generated from the oligo annealing process was further used for ligation into the CRISPRi backbone. As controls, sgRNAs were also designed for *rpoB* (positive control; Rv0667) and nontargeting (NT) 'scrambled' sequence (negative control). The NT sgRNA sequences do not target anywhere in the genome of Mtb which was confirmed by blastn analysis (maximum of 11 bp of complementary sequence observed).

To ligate the sgRNAs into the CRISPR backbone pJR965, the plasmid was first digested using BsmBI restriction enzyme digestion. The digestion was run at 55°C for 4h overnight. This was followed by gel electrophoresis and the band migrating at approximately 8.6kb was extracted. The obtained digested plasmid DNA was then ligated with the oligos using the T4 DNA ligase buffer and T4 DNA ligase enzyme (New England Biolabs). The ligated product was then transformed into *E. coli* competent cells and the cells were plated on LB plates with 50ug/ml kan and colonies were picked and cultured in LB broth. Plasmid isolation was performed for a single colony and the plasmids were further sent for Sanger sequencing (Eurofins), using the sequencing primer 5'-TTCCTGTGAAGAGCCATTGATAATG-3'

Table 10: sgRNA sequences designed for CRISPRi mutants. Three sgRNA sequences were designed for *dxs1* and *dxr*. One sgRNA was designed for *rpoB* and non-targeting control.

Gene	sgRNA sequences
dxs1	F: GGGAGCCAGCTCCCGAAGCTGCGCC R: AAACGGCGCAGCTTCGGGAGCTGGC
dxs1	F: GGGAGTGGCCGGATCGATCGGGACC R: AAACGGTCCCGATCGATCCGGCCAC
dxs1	F: GGGAGTTCGCGCACACCGTCAGACA R: AAACTGTCTGACGGTGTGCGCGAAC
dxr	F: GGGAGTGGCGGCGTCGGATCCGTGGT R: AAACACCACGGATCCGACGCCGCCAC
dxr	F: GGGAGTTCATCGGGCCCATCGACCAC R: AAACGTGGTCGATGGGCCCGATGAAC
dxr	F: GGGAGAACTCCCAGCTCGACGCGGT R: AAACACCGCGTCGAGCTGGGAGTTC
rpoB positive control	F: GGGAGACATCGTCGAAACGAGGGTC R: AAACGACCCTCGTTTCGACGATGTC
Non-targeting negative control:	F: GGGAGCACGGCGTATATGACATGAG R: AAACCTCATGTCATATACGCCGTGC

Growth curves and Colony-forming Unit plating for CRISPRi mutants

CRISPRi mutants were grown to mid-log phase (OD600 of 0.5 to 1.0) in 10ml growth media containing kan (25ug/ml). They were further subcultured with a starting OD600 of 0.005 with and without Atc. Different concentrations of Atc ranging from 1000ng/ml to 37.5ng/ml were included for all the CRISPRi mutants. The bottles were then incubated at 37°C on a shaker and the OD600 was measured every alternate day for 17 days using a spectrophotometer. Along with OD600 measurements, the cultures were also diluted and plated on 7H10 plates for CFU counting at the 14-day time point. The CFU plates were incubated at 37°C for a further 15 days and the colonies were counted.

Subculturing of the regrown (Escape) mutants

Cultures of CRISPRi mutants were grown as described above with Atc 250ng/ml and without Atc, with a starting OD600 of 0.005. OD600 was measured periodically and on day 14 the cultures containing Atc were split into two separate bottles. The culture in one bottle was allowed to continue growing while the culture in the second bottle was centrifuged, the pellet was washed with growth media and further resuspended in media containing Atc at a concentration of 250ng/ml. All the cultures were monitored for OD600 values for 8 days. The CRISPRi mutant *rpoB* was freshly inoculated from frozen stock on day 14 using the same media as other cultures and served as a media control.

Target validation of compounds

CRISPRi mutants were grown in 10ml growth media containing kan (25ug/ml) from the prepared frozen aliquots until mid-log phase (OD600 of 0.5 to 1). Atc was diluted in 10ml of growth media with kan (25ug/ml) for a final concentration of 125ng/ml, 62.50ng/ml, and 31.25ng/ml. 80 ul of Atc-containing media was added to the rows of flat bottom transparent 96 well plates in duplicates. On the right-most wells the compound at its MIC90 value was added and serially diluted 2-fold from right to left **(Figure 9).** The plates were then inoculated with the CRISPRi mutants with a final bacterial concentration of 2×10^5 CFU per well. The plates were sealed and incubated for 24 hours at 37°C. The Alamar blue assay was used to measure bacterial growth. The fluorescence values obtained from the Synergy2 device were normalized to the value of the highest and lowest concentration of Atc and plotted using GraphPad prism.

Statistical tests

Data are presented as mean ± standard deviation and were analysed using GraphPad Prism v.9.1.2 (GraphPad Software, LaJolla, CA). For experiments performed in three independent assays or more, two-way analysis of variance (ANOVA) with Tukey's post hoc analysis was used to evaluate normally distributed data. Differences were considered statistically significant at $p < 0.05$, $p < 0.01$, $p < 0.001$, and $p < 0.0001$.

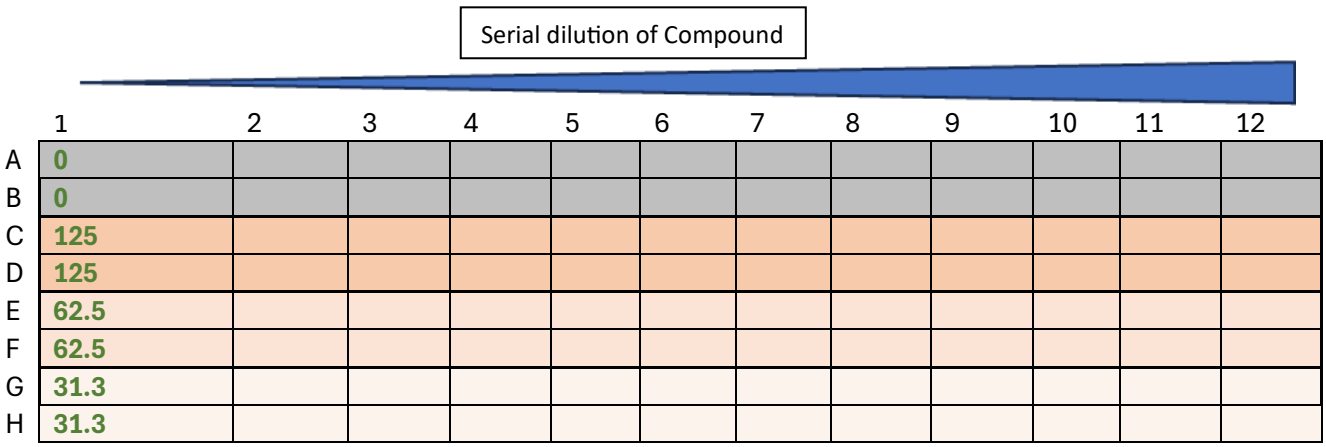

Figure 9: Plate layout for the target validation of compounds. The compound to be tested was serially diluted (2-fold) from right to left. Three different Anhydrotetracycline (Atc) concentrations were used, represented on the left most column of the layout. Mutants were added (2×10^5 CFU per well) after the plate setup and Alamar blue assay was used to identify the activity of the compounds.

Chapter 4

Results

4.1 Drug testing

Given the urgent need for drugs against TB, novel compounds/inhibitors were tested for phenotypic activity against Mtb. These compounds were synthesized and obtained from collaborative institutes, namely Helmholtz-Institut für Pharmazeutische Forschung Saarland (HIPS) (Saarbrücken, Germany), Ghent University (Ghent, Belgium), Specs (The Netherlands), or Groningen University (The Netherlands). This thesis is a part of the MepAnti consortium, funded by the EU commission; it was conducted to identify novel compounds targeting enzymes within the MEP pathway in Mtb (and other microorganisms).

The compounds obtained were aimed at either phenotypic-based drug discovery or target-based drug discovery. A flowchart representing the compound classes tested under phenotypic screening and target-based screening is shown in **Figure 10.**

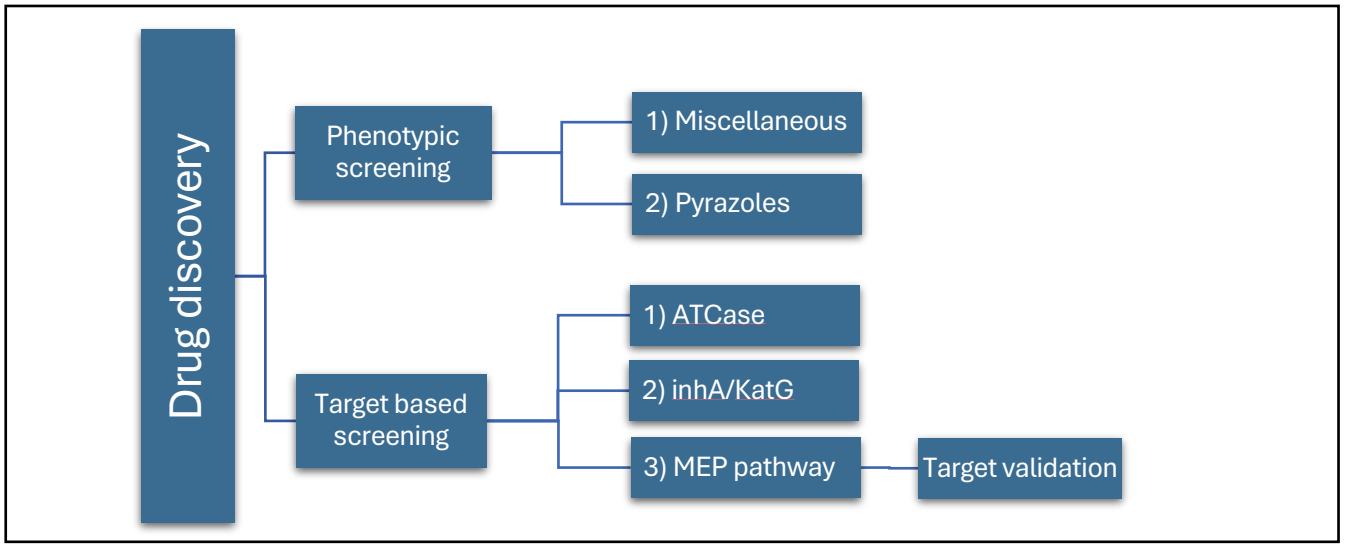

Figure 10: Drug testing approaches and compound classes tested.

Irrespective of the drug discovery approach, all the compounds went through similar phenotypic activity assays against Mtb. An overview of the workflow in a stepwise manner is illustrated in **Figure 11.** This

stepwise workflow was used for testing all novel compounds, with progression to each subsequent step decided based on the activity in the previous step. Compounds were considered to be active in the first step if the MIC90 was 64uM or lower.

All the compounds tested under phenotypic screening and target-based screening are described in detail below.

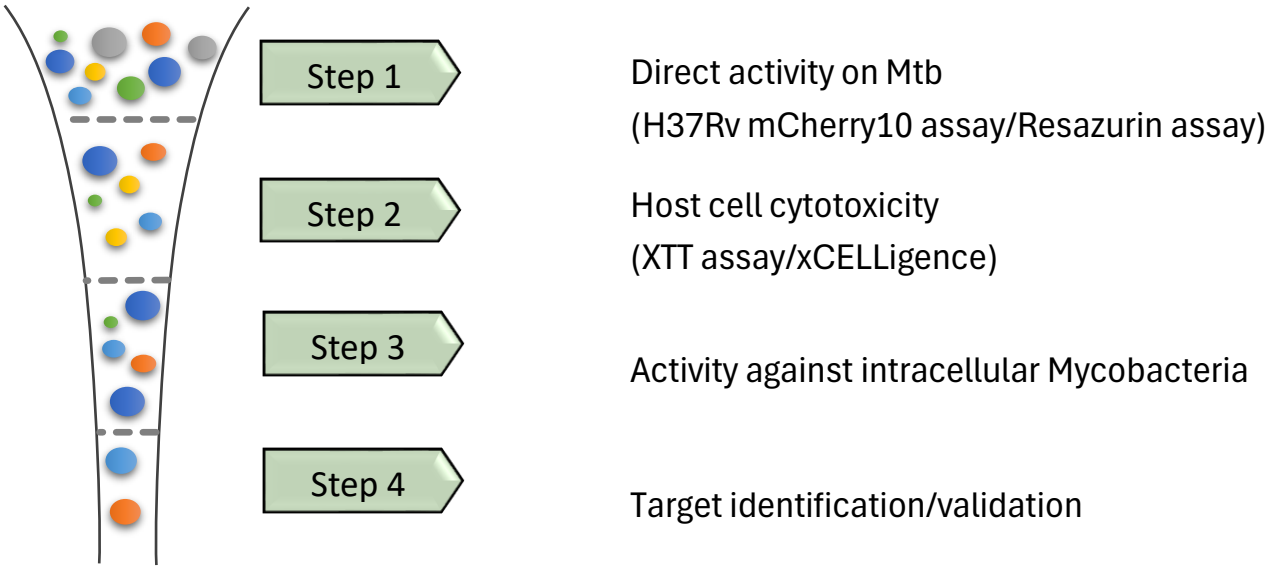

Figure 11: Illustration of workflow to obtain anti-TB compounds: All compounds undergo step 1 where they were tested for growth inhibitory activity against aerobically replicating Mtb H37Rv (strain: mCherry10 or ATCC 27294). Active compounds were then progressed to step 2 where toxicity against human monocyte derived macrophages (HMdM) was tested. Non-toxic compounds progressed to Step 3 where compounds were tested against HMdM infected with Mtb H37Rv ATCC 27294. Once the compounds were found active in this step, target identification or validation assays were carried out.

4.1.1 Phenotypic drug screening

Phenotypic screening is a target-independent method where libraries are screened in whole-cell assays against the organism of interest (Mtb) to find active compounds (140).

4.1.1.1 Batch A compounds

A batch of nineteen miscellaneous compounds collectively labelled as Batch A compounds were obtained from HIPS (Germany) and Specs (The Netherlands) libraries. These compounds were tested in the current study to set up an *in vitro* anti-TB compound testing pipeline. These compounds were previously known for their activity against either *Plasmodium falciparum* (Pf) or Gram-negative bacteria and hence their activity on Mtb was considered interesting to explore. The stepwise screening of Batch A compounds and the results for each step are presented below.

Step 1: Direct activity against Mtb

These compounds were tested against Mtb H37Rv mCherry10 strain at concentrations 16uM and lower. 2×10^5 CFU/well bacteria were cultured in the presence of the compounds in 96-well plates. After 7 days of incubation, the fluorescence of the bacteria was measured and graphs were plotted to determine the compound activity **(Figure 12**). The concentration of drug that caused a 90% inhibition of bacterial growth, relative to a DMSO-treated control, was considered to be the MIC90. The antibiotic rifampicin was used as a positive control at concentrations of 1ug/ml and 0.1ug/ml where 99% of bacterial inhibition was observed. As a bacterial growth control, Mtb alone and Mtb with DMSO were used. Amongst nineteen compounds tested, eight compounds showed an MIC90 of 16uM or lower. Two compounds, AK-105/40694114 and HIPSEx020 had a lower MIC90 of 4uM and 8uM respectively.

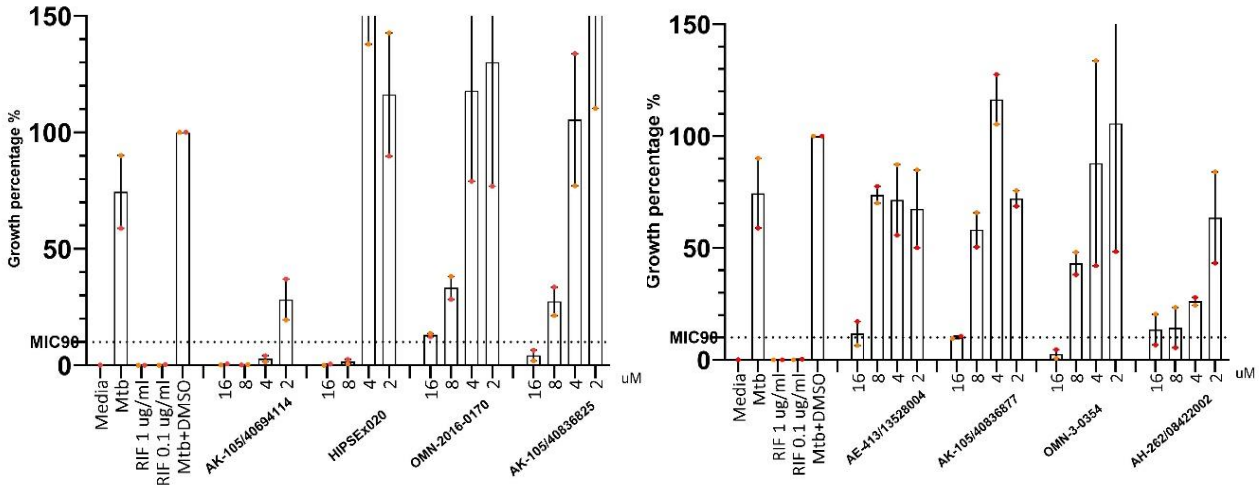

Figure 12: Batch A compounds tested against *Mycobacterium tuberculosis* (Mtb): Compounds diluted in 7H9 + OADC growth media at the respective concentrations, were added to a 96-well plate containing 2×10^5 CFU/well fluorescent Mtb H37Rv mCherry10, followed by a 7-day incubation period. Fluorescence was measured on day 7, and MIC90 values were determined by assessing bacterial growth inhibition. Two independent experiments, each consisting of three technical replicates, were performed and graphs were plotted by normalising the average of experiments to 100 % of Mtb growth with DMSO using GraphPad Prism. 90% or more bacterial growth inhibition was marked as MIC90 concentration for the compounds.

Step 2: Host cell Cytotoxicity assay

The eight compounds active against Mtb were selected to test for their cytotoxicity concentration 90 (CC90) against HMdM. For cytotoxicity determination, one of the assays used was the XTT assay. In this assay, the yellow tetrazolium salt XTT is cleaved to form an orange formazan product by the dehydrogenase activity of the live cells. Hence by measuring the absorbance of the formazan product, live cells can be quantified. Cytotoxicity of the compounds was measured using this assay and graphs were plotted using the absorbance data **(Figure 13A).** 2% and 3% of Tx-100 were used as a positive control where 99% of cell death was observed. As a negative control, Rifampicin at a concentration of 1ug/ml was used. To assess the toxicity of DMSO on HMdM, cells with DMSO alone (at the highest concentration used from the compound stock; approx. <0.1%) were tested. No cell death was observed for the negative control and DMSO control. Six Batch A compounds were tested using this assay with the highest concentration of 64uM **(Figure 13A).** One compound, AH-262/08422002, showed a 90% reduction in cell viability at 16uM making its CC90 16uM. Two other compounds (OMN-3-0354 and OMN-2016-0170) showed a 60% reduction in cell viability at 64uM making their CC90 >64uM. **Table 11** presents the CC90 values for these compounds.

For compounds HIPSEx020 and AK-105/40694114, given their low Mtb MIC90 values, a more sensitive xCELLigence device was used to measure the cytotoxicity. The xCELLigence system uses a micro-electronic biosensor built into the 96-well E-microtiter plates™ to measure electrical impedance. Cells in contact with the sensor alter the impedance, providing real-time data on cell viability. For the assay using xCELLigence, staurosporin was implemented as a positive control and cells with DMSO were used as a negative control

(Figure 13B). A 90% reduction in cell viability was observed for the compound HIPSEx020 at 16uM and for compound AK-105/40694114 at >32uM using xCELLigence.

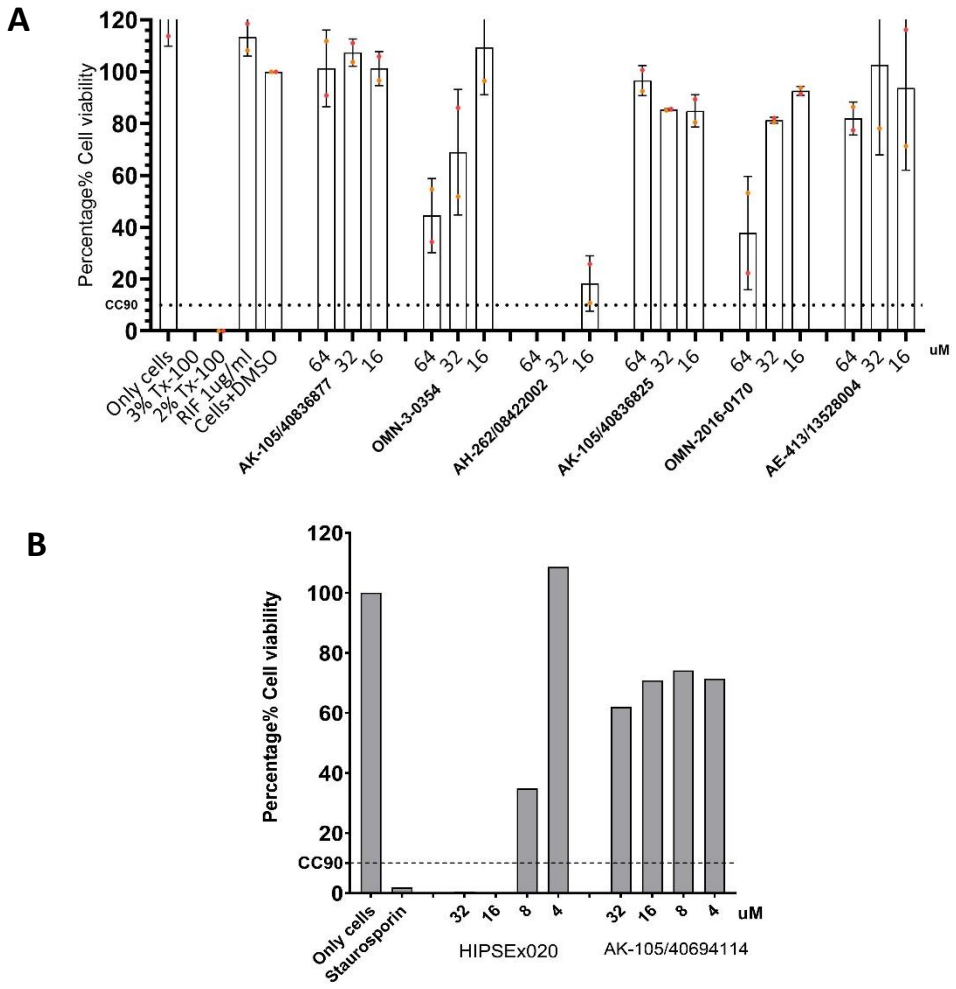

Figure 13: Batch A compounds tested for cytotoxicity. [A] Using XTT assay: Human monocyte-derived macrophages (HMdM) were exposed to compounds and incubated for 24 hours in 96-well plates. XTT dye was subsequently added to the plates, followed by further incubation, and the absorbance of the dye at 450 nm was measured. Untreated cells served as the negative control, while 2% and 3% Tx-100 were employed as the positive control. Two independent experiments, each consisting of three technical replicates were performed and graphs were plotted by normalising the average of experiments to 100 % of viable cells using GraphPad Prism. 90% or more cell death was marked as the cytotoxic concentration (CC90) for the compounds. **[B] Using the xCELLigence system**: Human monocyte-derived macrophages (HMdM) were exposed to the designated compound and incubated for 24 hours in xCELLigence plates and cell death was monitored using the xCELLigence device. Cells with DMSO served as the negative control, while Staurosporin was employed as the positive control. Three technical replicates were used and curves were obtained by the average of the triplicates. Further, the sum of the area under the curve was calculated and presented in bar graphs using GraphPad Prism. 90% or more cell death was marked as Cytotoxic Concentration (CC90) for the compounds.

Selectivity index:

Using both the MIC90 values and CC90 values, the Selectivity Index (SI) of the selected compounds was calculated. SI is the ratio of the toxic concentration of a sample (CC90) against its effective concentration (MIC90) (141). A higher Selectivity Index (SI) indicates the potential for a compound to be more effective and safe *in vivo* for treating a specific infection. An ideal drug would exhibit cytotoxicity only at high concentrations while demonstrating anti-TB activity at very low concentrations, resulting in a high SI value (142). The selectivity index serves as a widely acknowledged parameter for the selection of compounds for further studies.

Selectivity Index (SI)= CC90/MIC90

In this study, an SI value of 8 or higher is considered to be a promising value to consider the compound in the next step of testing. The SI values of Batch A compounds are noted in **Table 11**. The cytotoxicity data for all the Batch A compounds revealed that the SI is below 8 and hence they are not further pursued in the next steps of testing. However, an exception to this was the compound AK-105/40694114 with an SI of 8 which was further tested in Step 3.

Step 3: Activity against intracellular Mycobacteria

The MIC90 of compound AK-105/40694114 against HMdM infected with Mtb H37Rv ATCC 27294 was studied in Step 3. Intracellular MIC90 of compounds are referred to as iMIC90 henceforth. Three independent experiments were conducted where 2×10^5 HMdMs were infected at a multiplicity of infection (MOI) of 0.5; and washed 4 hours postinfection. The number of CFUs were determined by serial dilutions of cellular lysates. Controls used in this assay were the initial inoculum of Mtb, the 4-hour uptake of Mtb by macrophages, and bacteria with DMSO on day 7 **(Figure 14).** Subsequently, the survival of bacteria in the presence of varying compound concentrations (16uM, 8uM, and 4uM) was assessed by CFU plating on day 7. At a compound concentration of 4uM, approximately an 80% decrease in bacterial survival compared to the DMSO control was noted. However, a 90% reduction in bacterial survival was observed at concentrations of 16uM and 8uM compared to the bacterial growth control, defining an iMIC90 of 8uM for this compound.

Collectively, the above experiments from step 1 to step 3 show that test systems to identify novel anti-TB compounds were successfully set up.

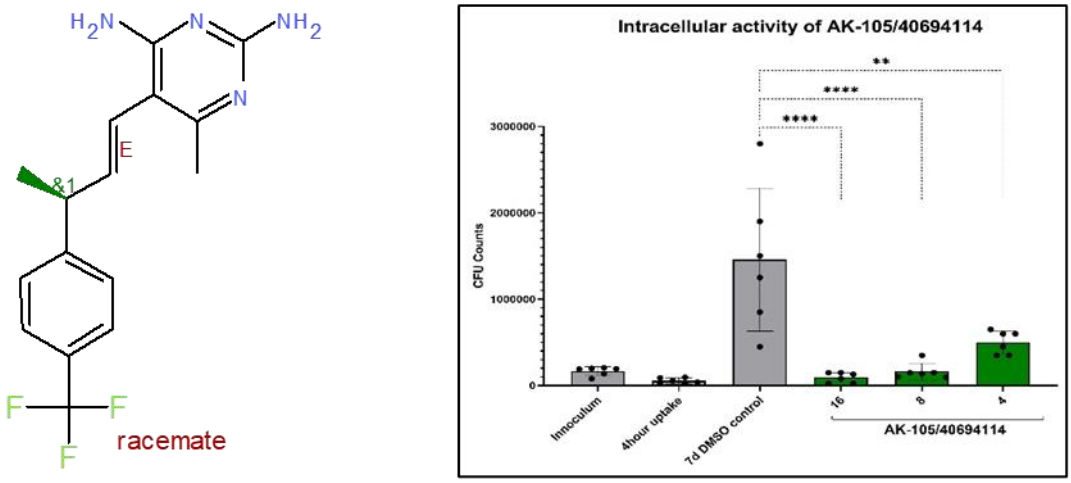

Figure 14: Structure and intracellular activity of compound AK-105/40694114 against *Mycobacterium tuberculosis* (Mtb): [A] Structure of AK-105/40694114 [B] HMdM were infected with Mtb H37Rv at an MOI of 0.5:1 and treated with the compound at respective concentrations, washed at 4h post-infection followed by 7-day incubation. To determine bacterial survival, Colony Forming Units were counted. Three independent experiments, each consisting of two technical replicates, were performed and graphs were plotted using GraphPad Prism. Statistical analysis was performed using one-way ANOVA (n=3) for comparison to the 7d bacterial growth * = p≤0.05; ** = p≤0.01; ***= p≤0.001; ****= p≤0.0001.

Table 11: Summary of the active compounds from Batch A obtained from Helmholtz-Institut für Pharmazeutische Forschung Saarland (HIPS) and Specs library.

Sr. no	Compounds	Minimum Inhibitory Concentration (MIC90) (uM)	Cytotoxic concentration (CC90) (uM)	Selectivity index (SI)	Library	Intracellular Survival assay (iMIC90) (uM)
1	AK-105/40694114	4	32	8	Specs	8
2	HIPSEx020	8	8	1	HIPS	n.d*
3	OMN-2016-0170	16	>64	>3	Specs	n.d
4	AK-105/40836825	16	64	4	Specs	n.d
5	AE-413/13528004	16	64	4	Specs	n.d
6	AK-105/40836877	16	64	4	Specs	n.d
7	OMN-3-0354	16	32	2	Specs	n.d
8	AH-262/08422002	16	16	1	Specs	n.d

n.d: Not determined.

Summary of the results 4.1.1.1:

- 19 compounds selected from HIPS and Specs library and tested for Mtb activity and cytotoxicity.
- 8 compounds were active against Mtb H37Rv mCherry10 with a MIC90 of 16uM or lower.
- AK-105/40694114 compound showed the best activity:
    a. MIC90 against Mtb H37Rv mCherry10: 4uM
    b. Cytotoxicity concentration against Human monocyte derived macrophages (HMdM): 32uM
    c. Intracellular MIC90 (iMIC90) using HMdM: 8uM
-

4.1.1.2 Pyrazoles

At the HIPS institute (Germany) a compound with a core pyrazole moiety was found to be active against Pf and select Gram-negative bacteria; hence a series of pyrazole analogues were synthesized by HIPS and Specs (The Netherlands). Given the anti-malarial and anti-bacterial activity of this compound, it was considered interesting to observe if these pyrazoles also had anti-TB properties. Hence, a total of fifty-one pyrazole compounds were tested against Mtb H37Rv mCherry10 to determine the MIC90.

The overview of the anti-TB activity observed with these compounds is shown in **Figure 15.** Amongst all the pyrazoles tested, twenty-six compounds showed anti-TB activity (MIC90) below 64uM against Mtb. Amongst these, one compound with MIC90 of 4uM and five compounds with MIC90 of 8uM were identified.

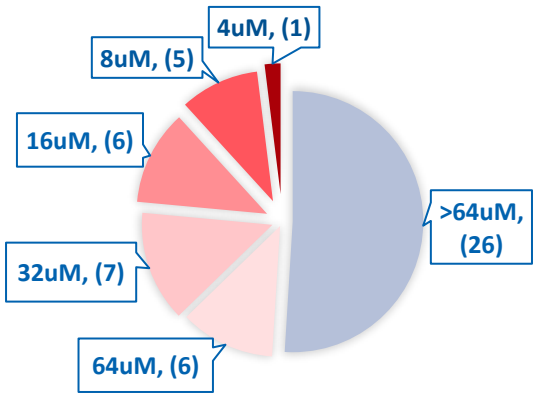

Figure 15: Overview of the pyrazoles tested against Mtb H37Rv mCherry10. The text represents the active **concentration** and the number of compounds active at that concentration.

The core structure of the pyrazole series consists of a pyrazole moiety attached to either amines or guanidines via an amide linkage. The pyrazole derivates containing amines were found to be cytotoxic at their MIC90 concentrations against HepG2 cell lines tested at the HIPS institute (Results in **Supplementary Table 2**). However, the guanidine derivatives showed comparatively better cytotoxicity against HepG2 cell lines, which was further confirmed by testing these compounds against HMdM using the XTT assay. Guanidine derivates also had comparatively better MIC90 activity against Mtb H37Rv mCherry10 (Results **Supplementary Table 2**).

Amongst these active pyrazoles, compound Mepanti0062, which is a guanidine derivative, was found to be the most active against Mtb. The structure of Mepanti0062 is presented in **Figure 16A**. This compound showed an MIC90 of 4uM against Mtb H37Rv mCherry10 **(Figure 16B).**

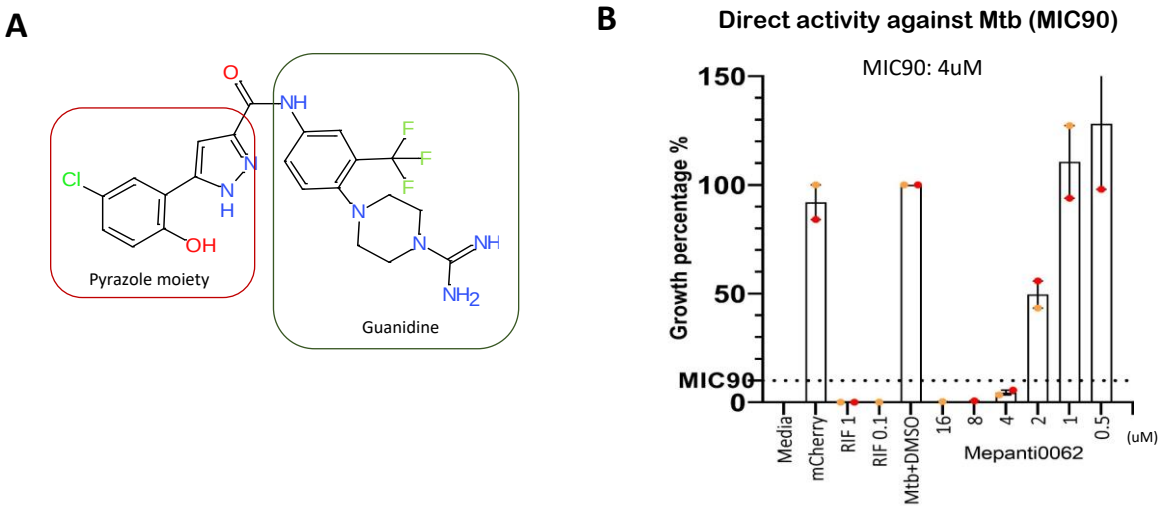

Figure 16*:* Structure and anti-Tb activity of Pyrazole compound Mepanti0062. [A] Structure of Mepanti0062 with a pyrazole moiety and a linked guanidine group. [B] Activity Assay: Compounds diluted in 7H9 + OADC growth media at the respective concentrations, were added to a 96-well plate containing 2×10^5 CFU/well fluorescent Mtb H37Rv mCherry10, followed by a 7-day incubation period. Fluorescence was measured on day 7, and MIC90 values were determined by assessing bacterial growth inhibition. Two independent experiments, each consisting of three technical replicates, were performed and graphs were plotted by normalising the average of experiments to 100 % of Mtb growth with DMSO using GraphPad Prism. 90% or more bacterial growth inhibition was marked as MIC90 concentration for the compounds.

Since Mepanti0062 was active at 4uM, further cytotoxicity analysis of this compound was performed using the xCELLigence assay on HMdM. At 32uM, approx. 20% cell death was observed compared to the healthy cells **(Figure 17A).** Hence**,** this compound was tested for the intracellular survival assay at a concentration of 16uM or lower.

For the intracellular survival assay, three independent assays with two replicates each using HMdM against Mtb H37Rv ATCC 27294 were performed and iMIC90 was determined (**Figure 17B)**. After 7 days, a significant reduction of bacterial CFU development, of approximately 80%, was observed at a concentration of 16uM when compared to the DMSO control. Hence the iMIC90 (90% of growth inhibition) was noted to be >16uM

for Mepanti0062. This data also demonstrates that the iMIC90 of Mepanti0062 intracellularly is > 4-fold higher than the MIC90 in broth (7H9 media).

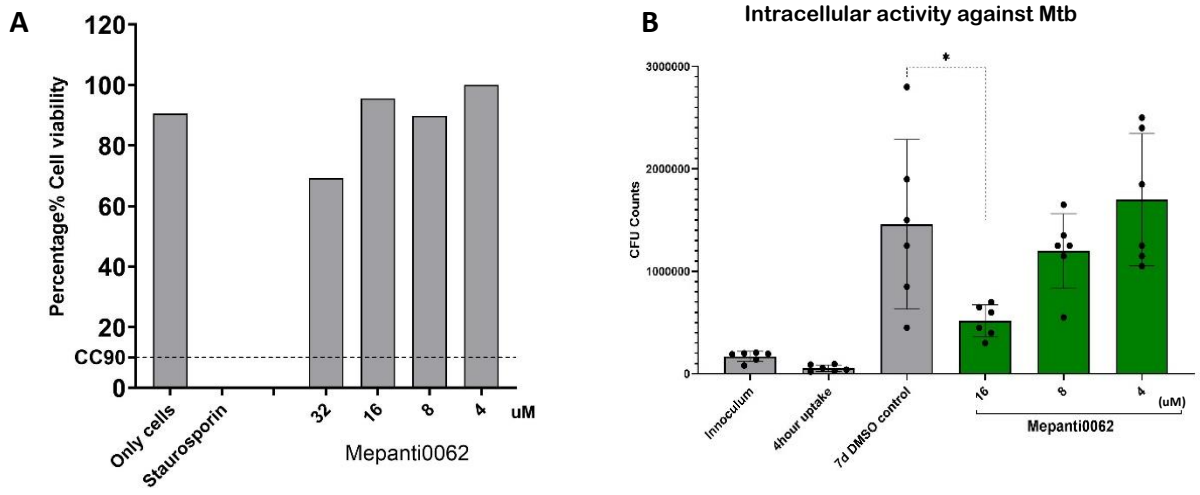

Figure 17: Cytotoxicity Assay and Intracellular survival assay for compound Mepanti0062: [A] Cytotoxicity assay: Human monocyte-derived macrophages (HMdM) were exposed to the compound and incubated for 24 hours using the xCELLigence system and cell impedance was monitored. Cells treated with DMSO (<0.1%) served as the negative control, while Staurosporin was employed as the positive control. The sum of area under curve was calculated and presented in bar graphs using GraphPad Prism. 90 percent or more cell death was marked as Cytotoxic Concentration (CC90) for the compounds. **[B] Intracellular survival assay:** HMdM were infected with Mtb H37Rv at an MOI of 0.5:1 and treated with the compound at respective concentrations washed at 4h post infection followed by 7-day incubation. To determine the bacterial survival, Colony Forming Units were counted. Three independent experiments, each consisting of two technical replicates, were performed and graphs were plotted using GraphPad Prism. Statistical analysis was performed using one-way ANOVA (n=3) for comparison to the 7d bacterial growth * = p≤0.05, (p=0.022)

Summary of the results 4.1.1.2:

- 51 pyrazoles tested, amongst them the compound Mepanti0062, showed the best activity **(Figure 16 and 17).**
- Activity of Mepanti0062:
    a. MIC 90 against Mtb H37Rv mCherry10: 4uM
    b. Cytotoxicity concentration against Human monocyte derived macrophages (HMdM): 32uM
    c. Intracellular iMIC90 using HMdM: >16uM

4.1.2 Target-based drug discovery

One of the approaches for drug discovery for Mtb is target-based drug discovery. In this approach, the target protein is predetermined before the hit discovery phase starts. Consequently, compounds are screened and further modified to interact with the identified target using various virtual and biochemical assays. Therefore, the selected target must ideally be essential for the survival of the organism (140, 143). This study focuses on the following Mtb targets: ATCase (*pyrB*; Rv1380), InhA (*inhA*; Rv1484), and select enzymes within the MEP Pathway in Mtb Dxs (*dxs1*; Rv2682c) and Dxr (*dxr;* Rv2870c).

4.1.2.1 Aspartate carbamoyl transferase (ATCase) inhibitors

In Mtb, *de novo* synthesis of pyrimidine nucleotides is carried out in six enzymatic steps that lead to the formation of Uridine monophosphate (UMP) (23, 67). In the second step of the pathway, Aspartate carbamoyltransferase (ATCase) (*pyrB*; Rv1380) catalyses the condensation of aspartate and carbamoyl phosphate to generate carbamoyl aspartate. ATCase is reported as an essential gene for the *in vitro* growth of Mtb, suggesting it could be an attractive drug target (76).

Based on fragment screening performed on Pf ATCase at the University of Groningen, a series of ten compounds (BDA series) was developed (80). Based on a structural evaluation of the ATCase enzymes of Pf and Mtb similarities were noted (80), prompting the testing of this compound series against Mtb.

Prior to testing the BDA series against Mtb, the solubility of these compounds in Mtb growth media was evaluated using a dynamic light scattering (DLS) assay. In this assay, light is passed through a growth media containing the dissolved compound using a Zetasizer instrument that measures the scattering of light. If aggregates are formed, or if the compound precipitates, more light is scattered leading to a higher derived count rate (DCR). Hence, a high DCR suggests that the compound is insoluble or aggregated in the growth media. The results of the DLS assay for the ten compounds from the BDA series are presented in **Figure 18.** Two compounds (BDA-14 and BDA-69) were soluble at concentration 64uM whereas BDA-67 was soluble at 16uM. For the other compounds, the maximum solubility concentration was 8uM.

Based on the solubility data, these ten compounds were tested further against Mtb H37Rv mCherry10 at the concentration of 8uM **(Figure 19A)**. One compound BDA-06 showed more than a 90% reduction in bacterial burden. This compound was further selected for dose response testing from concentration 8uM to 0.062uM. As shown in **Figure 19B**, a dose-dependent reduction in Mtb was observed and more than 90% reduction in bacterial burden was observed at 4uM making its MIC90 4uM.

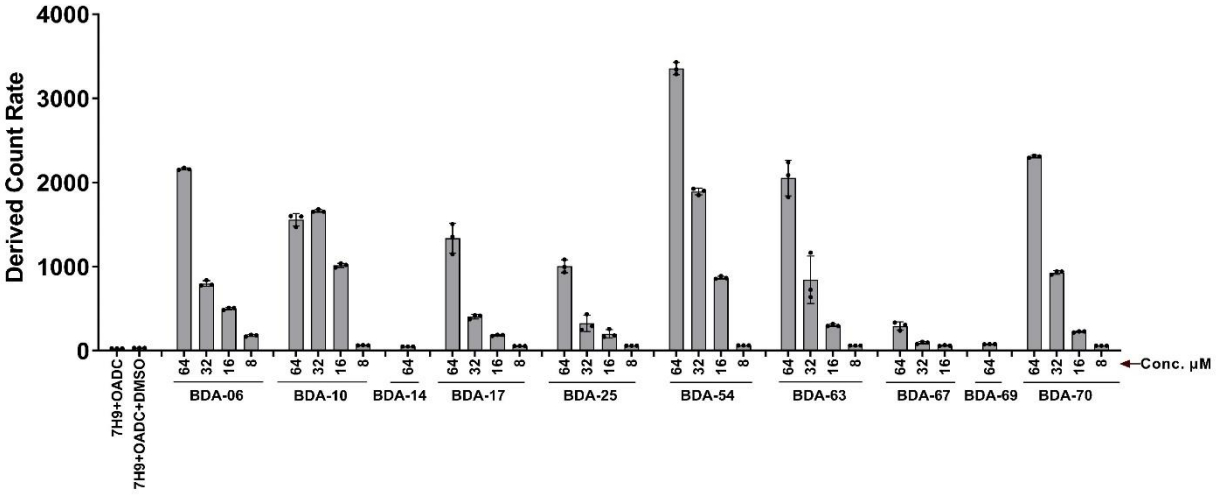

Figure 18: Solubility Assay: Compounds were diluted in 7H9 + OADC growth media at their respective concentrations and subjected to solubility testing using a zetasizer device. This device measures the aggregate formation of the compounds by analysing the light dispersed through the media. The assay was performed using three technical replicates and the graph was plotted using GraphPad prism.

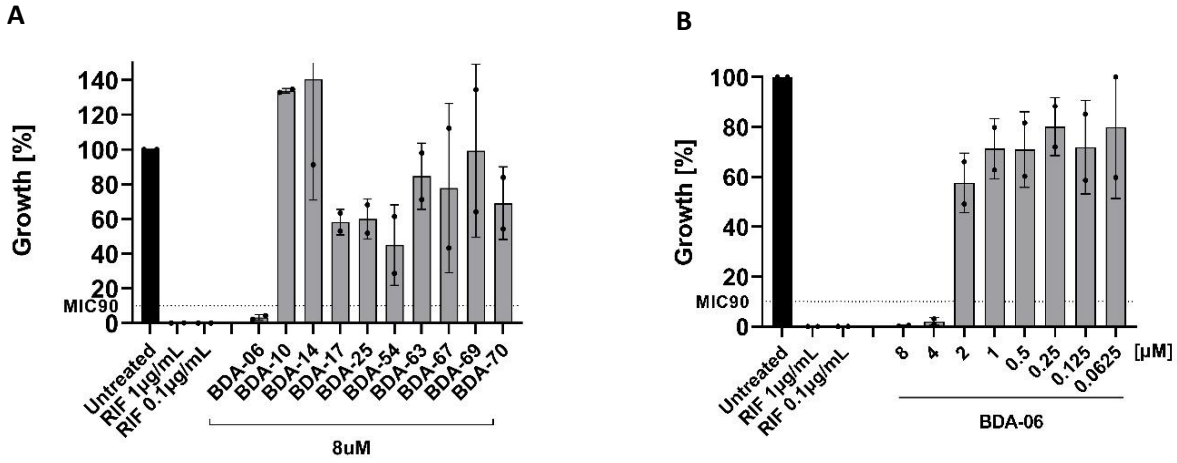

Figure 19: Aspartate carbamoyl transferase (ATCase) inhibitors tested against *Mycobacterium tuberculosis* (Mtb): Compounds diluted in 7H9 + OADC growth media at the respective concentrations, were added to a 96-well plate containing 2×10^5 CFU/well fluorescent Mtb H37Rv mCherry10, followed by a 7-day incubation period. Fluorescence was measured on day 7, and MIC90 values were determined by assessing bacterial growth inhibition. Two independent experiments, each consisting of three technical replicates, were performed and graphs were plotted by normalising the average of experiments to 100 % of Mtb growth with DMSO using GraphPad Prism. 90% or more bacterial growth inhibition was marked as MIC90 concentration for the compounds. [A] Ten compounds tested against Mtb at 8uM concentration. [B] BDA-06 compound tested against Mtb from concentrations 8uM to 0.062uM.

Given the activity of compound BDA-06, it was further tested for cytotoxicity on HMdM using the XTT assay at concentrations from 64uM to 1uM. At 64uM, 90% cell death was observed making the CC90 for BDA-06 64uM **(Figure 20).**

These findings of the ATCase inhibitors are published in a peer-reviewed journal (77). Given the MIC90 and CC90 of the compound BDA-06, the SI is calculated to be 16. This makes the compound an interesting candidate for studying its activity against intracellular Mtb. However, further chemical modifications of BDA-06 are ongoing. Therefore, studying the intracellular activity of BDA-06 after these modifications will be of significant interest.

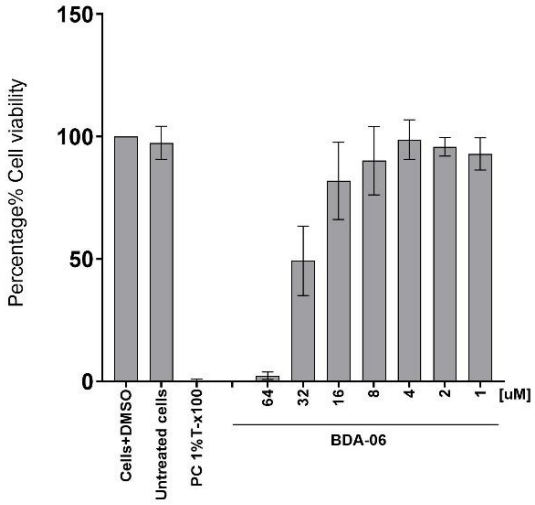

Figure 20: BDA-06 tested for cytotoxicity: Human monocyte-derived macrophages (HMdM) were exposed to a compound and incubated for 24 hours in 96-well plates. XTT dye was subsequently added to the plates, followed by further incubation, and the absorbance of the dye at 450nm was measured. Untreated cells served as the negative control, while 1% Tx-100 was employed as the positive control. Graphs were plotted by normalising the values to viable cells using GraphPad Prism. 90 percent or more cell death was marked as Cytotoxic Concentration (CC90) for the compounds.

Summary of the results 4.1.2.1:

- 10 compounds, designed as potential inhibitors of Mtb Aspartate carbamoyltransferase (ATCase), were tested for growth inhibitory activity against Mtb and one compound (BDA-06) was active (MIC90 <8uM)
- Activity of BDA-06:
    a. MIC 90 against Mtb H37Rv mCherry10: 4uM
    b. Cytotoxicity concentration against Human monocyte derived macrophages (CC90): 64uM

4.1.2.2 Terpenoid derivatives

In TB treatment, INH is known to be one of the most potent anti-TB drugs. Hence in a further attempt to develop new anti-TB inhibitors, structural modifications were made to INH to enhance its efficacy. In this study, 6 derivatives of INH containing terpenoid appendages were synthesized and tested for anti-Tb activity. Terpenoids were chosen due to their potency against pathogenic bacteria and lack of mammalian toxicity (91).

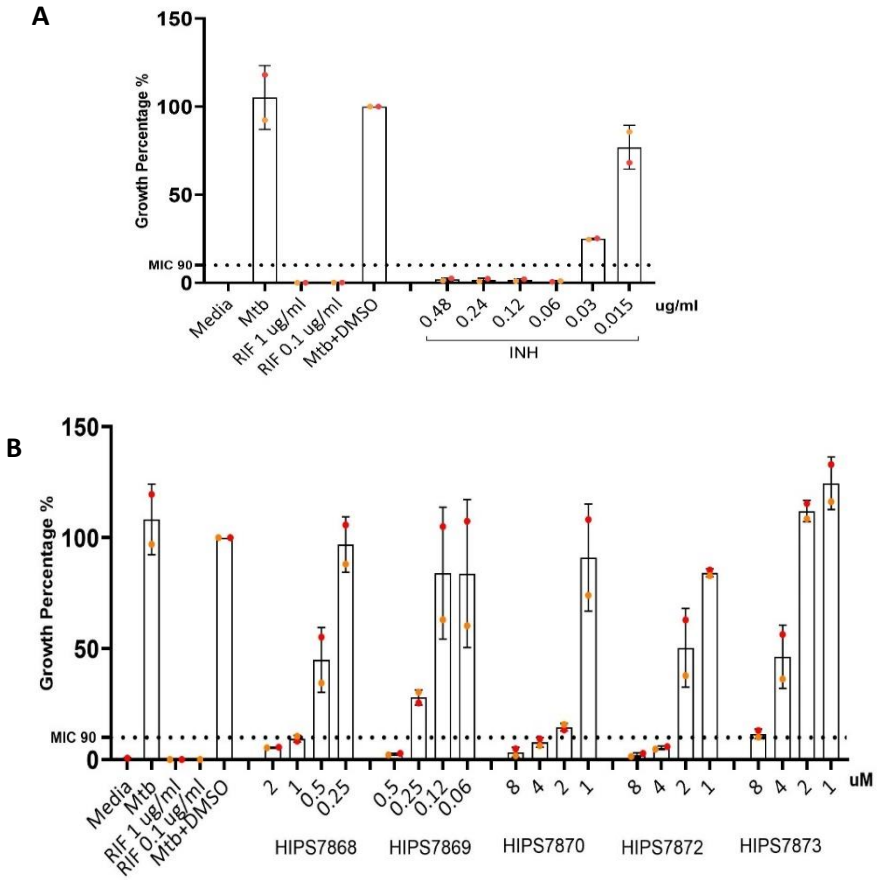

Figure 21: Terpenoid compounds tested against *Mycobacterium tuberculosis* (Mtb): Compounds diluted in 7H9 + OADC growth media at the respective concentrations, were added to a 96-well plate containing 2×10^5 CFU/well fluorescent Mtb H37Rv mCherry10, followed by a 7-day incubation period. Fluorescence was measured on day 7, and MIC90 values were determined by assessing bacterial growth inhibition. Two independent experiments, each consisting of three technical replicates, were performed and graphs were plotted by normalising the average of experiments to 100 % of Mtb growth with DMSO using GraphPad Prism. 90% or more bacterial growth inhibition was marked as MIC90 concentration for the compounds. [A] MIC90 testing of Isoniazid (INH) [B] MIC90 testing of Terpenoid derivatives.

First, INH was tested against Mtb H37Rv mCherry10 at a range of concentrations **(Figure 21A)** and the MIC90 of INH was observed to be 0.06ug/ml (0.44uM) which is in line with the MIC90 reported in published literature (144). Five of the terpenoid inhibitors displayed single-digit MIC90 concentrations **(Figure 21B)**. Amongst these, HIPS7869 was the most active with an MIC90 of 0.5uM, similar to the MIC90 of INH. The MIC90 values of all terpenoid derivatives are listed in **Table 12.**

These five active compounds were further tested for cytotoxicity against HMdM using an XTT assay. Due to the limited availability of the compound, only four compound concentrations depending on the MIC90 of respective compounds, were tested. **Figure 22** shows the XTT assay data for these compounds. At the concentrations tested (approx. 4-fold higher than MIC90) these compounds were found to be nontoxic.

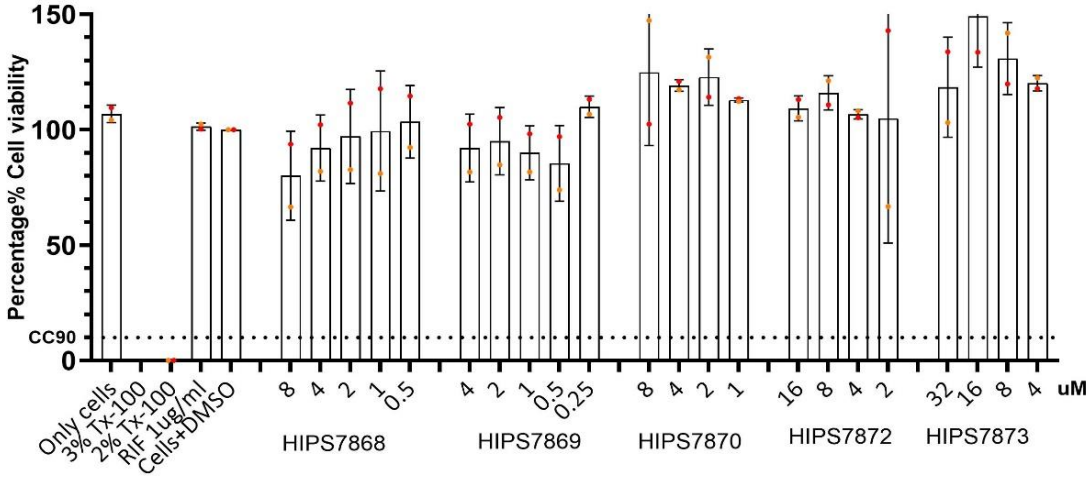

Figure 22: Terpenoid compounds tested for cytotoxicity: Human monocyte-derived macrophages (HMdM) were exposed to compounds and incubated for 24 hours in 96-well plates. XTT dye was subsequently added to the plates, followed by further incubation, and the absorbance of the dye at 450nm was measured. Untreated cells served as the negative control, while 2% and 3% Tx-100 were employed as the positive control. Two independent experiments, each consisting of three technical replicates were performed and graphs were plotted by normalising the average of experiments to 100 % of viable cells using GraphPad Prism. 90% or more cell death was marked as Cytotoxic Concentration (CC90) for the compounds

Given the nontoxic nature of the compounds, they were further tested in an intracellular survival assay using HMdM **(Supplementary Figure 1).** The iMIC90 values of these compounds are presented in **Table 12.** HIPS7869 was the most potent of all terpenoid derivatives, its structure and intracellular assay are shown in **Figure 23A** and **Figure 23B** respectively. INH was used as a positive control in this assay and was found to inhibit 90% of Mtb at 0.3ug/ml (2.18uM) and approx. 60% at 0.03ug/ml (0.22uM). HIPS7869 showed a dose-dependent decrease in the bacterial CFU (from 1uM to 0.125uM) and showed a 90% reduction in bacterial CFU at a concentration of 0.5uM. Hence, the Mtb iMIC90 of HIPS7869 was 0.5uM which is similar to its MIC90 in broth (7H9 media).

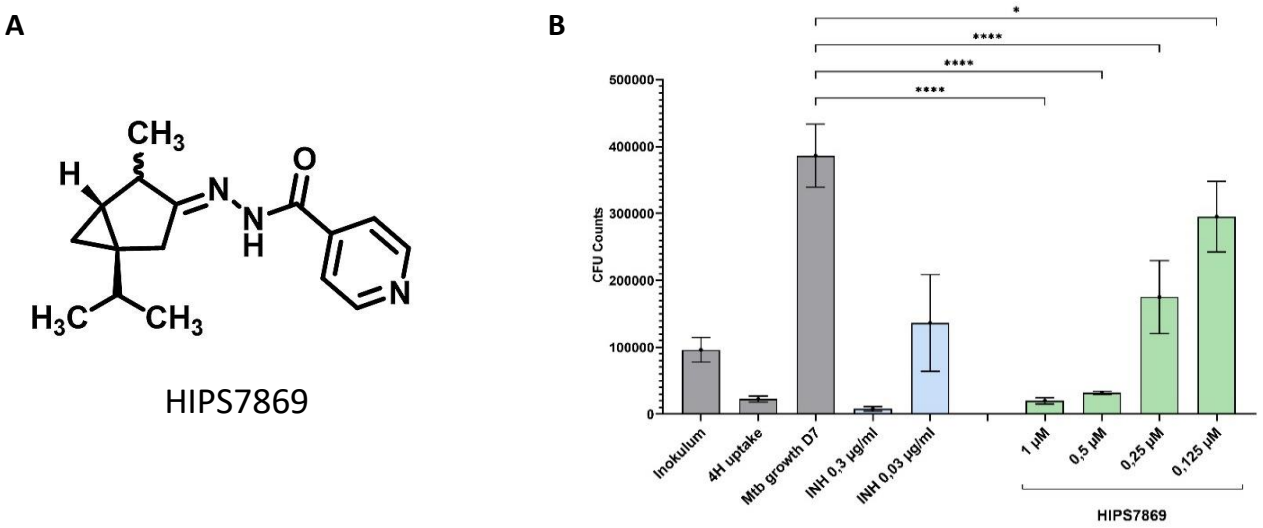

Figure 23: Structure and Intracellular activity of compound HIPS7869 against *Mycobacterium tuberculosis* (Mtb): [A] Structure of HIPS7869 [B] HMdM were infected with Mtb H37Rv at an MOI of 0.5:1 and treated with the compound at respective concentrations washed at 4h post-infection followed by 7-day incubation. To determine bacterial survival, Colony Forming Units were counted. Two independent experiments, each consisting of two technical replicates, were performed and graphs were plotted using GraphPad Prism. Statistical analysis was performed using one-way ANOVA (n=2) for comparison to the 7d bacterial growth * = p≤0.05; ** = p≤0.01; ***= p≤0.001; ****= p≤0.0001.

Since these compounds are modifications of INH, the target of these compounds was hypothesized to be similar to INH. INH is known to be activated by the enzyme KatG and the resulting metabolite targets the InhA protein. To test if terpenoid inhibitors also have a similar mode of action, they were tested against two different clinical isolates of Mtb. These isolates were INH mono-resistant strains harbouring the resistance-determining mutations in either the *katG* (S315T) or *inhA* (c-15t) genes. To assess the MIC90 against these strains, the Alamar blue assay was used. This assay utilizes the dye resazurin, which is blue in colour. In the presence of live bacteria, resazurin undergoes reduction to form resorufin, which is pink and highly fluorescent. All five terpenoid derivatives tested using Alamar blue assay showed an MIC90 of >16uM against both the Mtb clinical isolates. This strongly suggests that they are also activated by KatG and target InhA. These results are presented in the **Supplementary Figure 2 and Figure 3.**

Table 12: Summary of the active Terpenoid inhibitors. n.d: not determined

Sr. no	Compounds	Minimum Inhibitory Concentration (MIC 90) (uM)	Cytotoxic concentration (CC 90) (uM)	Intracellular Survival assay (uM)	MIC 90 against Mtb H37Rv *katG* mutant (uM)	MIC 90 against Mtb H37Rv *inhA* mutant (uM)
1	HIPS7869	0.5	>4	0.5	>16	>16
2	HIPS7868	1	>8	0.5	>16	>16
3	HIPS7870	2	>8	8	>16	>16
4	HIPS7872	4	>16	n.d	>16	>16
5	HIPS7873	8	>32	n.d	>16	>16

Summary of the results 4.1.2.2:

- Five terpenoid inhibitors showed MIC90 activity below 8uM against MtbH37Rv mCherry10.
- All five compounds were non-toxic against HMdM at MIC90 concentrations.
- The five compounds showed iMIC90 below 8uM against intracellular Mtb.
- All five compounds were inactive against *inhA* and *katG* mono-resistant clinical Mtb strain.

4.1.2.3 methyl-D-erythritol phosphate (MEP) pathway inhibitors

The methyl-D-erythritol phosphate (MEP) or non-mevalonate pathway, as discussed previously, is an essential pathway in Mtb and is absent in humans, thus serving as an attractive target for antitubercular drug development. The EU consortium, MepAnti, was formed with the overall goal of exploiting the MEP pathway for anti-infective compound development against a range of human pathogens, using a combination of *in silico*, *in vitro* and whole cell activity assays. In this section, compounds previously assessed by virtual screening or biochemical enzymatic assays against the MEP pathway enzymes Dxs, Dxr and IspD were tested against Mtb.

In total, one hundred and thirty-five compounds were obtained from either HIPS or the Ghent University library. Amongst these compounds tested on Mtb H37Rv mCherry10 for MIC90 activity, twenty-six compounds were active at 64uM or lower. **Figure 24** gives an overview of the number of compounds tested.

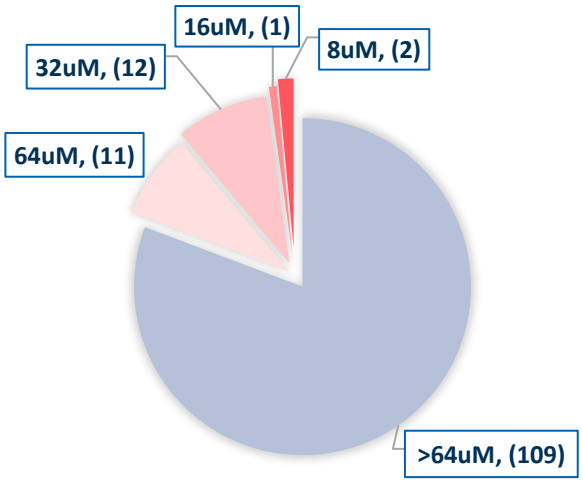

Figure 24*:* Overview of compounds developed against the Methyl-D-erythritol phosphate pathway. The text represents the concentration and number of compounds active at that respective concentration.

Of all the compounds tested, two compounds, HIPS768 and CC143, demonstrated the lowest Mtb MIC90 at 8uM **(Figure 25A).** HIPS768 was tested for its cytotoxicity using XTT assay revealing the CC90 to be 16uM **(Figure 25B).** From the MIC90 and CC90 values, the SI of HIPS768 was calculated to be 2, Since the SI was low, the compound was not further tested for its intracellular activity.

The second active compound was CC143, obtained from Ghent University. This compound was an analogue of fosmidomycin which is known to target the enzyme Dxr of the MEP pathway in Pf. Its published half-maximal inhibitory concentration (IC50) against Mtb H37Ra was determined to be 0.42uM (1). However, despite its potent activity, CC143 showed cytotoxicity against MRC-5 fibroblast cells at a very low concentration of 0.61uM, prompting the cessation of further studies (1). Nonetheless, given its structural similarity to fosmidomycin and therefore the potential of targeting the Dxr enzyme, CC143 was tested and utilized in the target validation of Dxr within this study. For CC143 the MIC90 against Mtb H37Rv mCherry10 was found to be 8uM **(Figure 25A)**.

In summary, amongst all the MEP compounds screened, significant growth inhibitory activity (MIC90) was only observed at concentrations >8uM, and those that were tested further, were also found to be cytotoxic. A list of all compounds tested in this study potentially targeting the MEP pathway is presented in **Supplementary Table 3.** Consequently, the compounds require further modification to enhance their activity while reducing the cytotoxic effects.

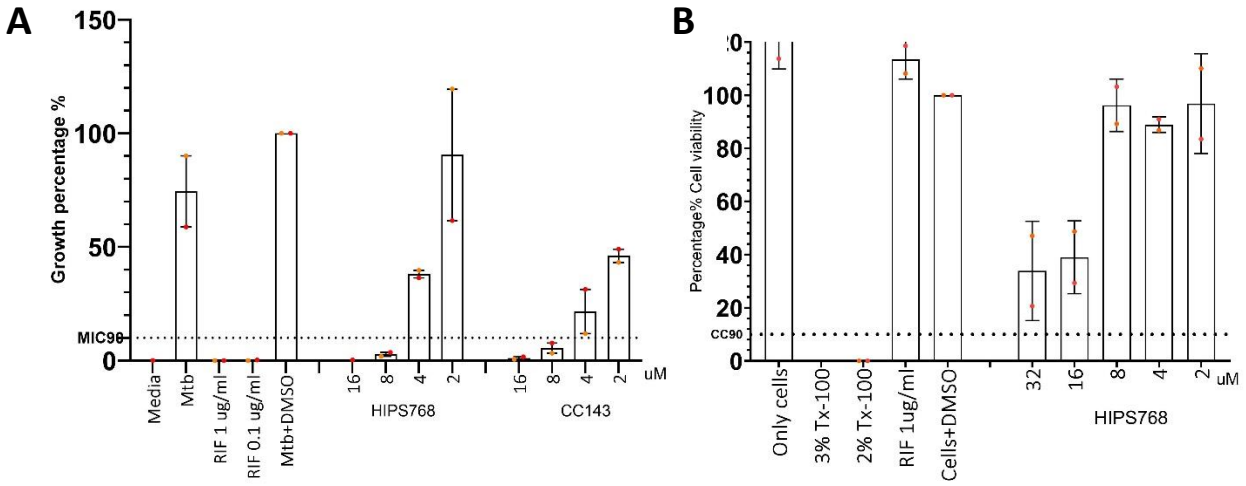

Figure 25: Anti-TB activity and Host cell cytotoxicity of MEP pathway inhibitors: [A] Activity assay: Compounds diluted in 7H9 + OADC growth media at the respective concentrations, were added to a 96-well plate containing 2×10^5 CFU/well fluorescent Mtb H37Rv mCherry10, followed by a 7-day incubation period. Fluorescence was measured on day 7, and MIC90 values were determined by assessing bacterial growth inhibition. Two independent experiments, each consisting of three technical replicates, were performed and graphs were plotted by normalising the average of experiments to 100 % of Mtb growth with DMSO using GraphPad Prism. 90% or more bacterial growth inhibition was marked as MIC90 concentration for the compounds. **[B] Cytotoxicity assay:** Human monocyte-derived macrophages (HMdM) were exposed to compounds and incubated for 24 hours in 96-well plates. XTT dye was subsequently added to the plates, followed by further incubation, and the absorbance of the dye at at 450nm was measured. Untreated cells served as the negative control, while 2% and 3% Tx-100 were employed as the positive control. Two independent experiments, each consisting of three technical replicates were performed and graphs were plotted by normalising the average of experiments to 100 % of viable cells using GraphPad Prism. 90% or more cell death was marked as Cytotoxic Concentration (CC90) for the compounds

Summary of the results 4.1.2.3:

- Amongst 135 compounds tested, 26 displayed Mtb MIC90 values of 64uM or lower.
- The top two active compounds were:
- HIPS768
    a. MIC 90 against Mtb H37Rv mCherry10: 8uM
    b. Cytotoxicity concentration against Human monocyte derived macrophages (CC90): 16uM
- CC143
    a. MIC90 against Mtb H37Rv mCherry10: 8uM
    b. Cytotoxic at 0.61uM against MRC-5 fibroblasts according to literature (1)
    c. Fosmidomycin analogue; with potential target as Dxr enzyme.

4.2 Target validation for Dxs and Dxr

Compounds targeting the MEP pathway exhibited activity at concentrations of 8uM and higher as described previously (section 4.1.2.3). These compounds were initially designed through a combination of structure-based and ligand-based *in silico* drug discovery methodologies (145). Subsequently, selected hits were subjected to *in vitro* assays, beginning with biochemical enzymatic studies to assess their inhibitory activity against specific enzymes. While these assays with purified proteins provide initial evidence of target specificity, further validation within a biological system is necessary. Therefore, to validate the biological targets of these compounds in whole cells, conditional mutants of Mtb were generated, where the expression of the target gene was manipulated, either upregulated or downregulated. This modulation of target gene expression allowed us to evaluate the change in the compound activity further confirming its target specificity.

4.2.1 Promoter replacement (Tet OFF and Tet ON) mutants

4.2.1.1 Strategy and Generation of Promoter Replacement Mutants

To generate conditional mutants, one of the approaches used was a promoter replacement method, where the native gene promoter was replaced with a tetracycline-controlled promoter for inducible gene regulation. Conditional mutants were generated for *dxs1* and *dxr* in Mtb using this method. Prior to mutant generation, *dxs1* and *dxr* genes were assessed bioinformatically for their presence in an operon. If the genes are in an operon, gene modification using these methods might also affect downstream genes within the same operon and the system would not remain specific to the desired target gene. Based on the literature, *dxs1* and *dxr* were not found to be transcribed as parts of operons, based on the position of the transcriptional start sites of the neighbouring genes (146, 147). Therefore, no additional precautions were deemed necessary during mutant construction. To generate conditional mutants a two-step homologous recombination-mediated genetic modification method previously described (123) was employed. In the first step, the native promoter of each gene was replaced with a tet operator-containing strong mycobacterial promoter, pmyc1tetO, using modified versions of the plasmid pSE100. In the second step, to allow for Atc-dependent regulation of the target genes, either TetR or RevTetR protein (for Tet ON and Tet OFF respectively)-encoding plasmids were introduced into the SCO strains.

For generating Tet ON strains (upregulation of target gene expression upon addition of Atc), the L5 integration-based vector pMC1s was utilized. In the absence of Atc, the TetR protein encoded by pMC1s binds to the tetO sequence within the pmyc1tetO promoter and therefore blocks transcription of the target

gene. Upon addition of Atc, TetR binds to the ligand resulting in a conformational change and release of the complex from the promoter, and therefore alleviation of transcriptional repression.

Conversely, for Tet OFF strains, an episomal plasmid, pTEK-4S-OX, expressing a reverse TetR protein (rev TetR) from a strong promoter was employed. Rev TetR proteins, which have poor DNA binding affinities in their native state, effectively block the tet operator region upon binding Atc, resulting in Atc-mediated gene downregulation.

Following the generation of Tet ON and Tet OFF mutants, they were tested for their Atc-dependency by measuring their growth phenotypes and quantifying mRNA (results section 4.2.2.2)

4.2.1.2 Confirmation of generation of promoter replacement mutants

The conditional mutants were generated using promoter replacement by a single homologous recombination method. After the first step of pSE100 plasmid integration, the mutants were cultured in growth media with 25ug/ml hygromycin. Before proceeding to the next transformation step, it was crucial to establish that the plasmid had integrated in the correct location in the Mtb genome. For this validation, two methods were used; 1) southern blotting, 2) Next Generation Sequencing

1) Southern blotting

Southern blotting is a technique that enables the identification of specific DNA sequences within a complex nucleic acid mixture, such as those derived from whole genome DNA (138). Molecular hybridisation is performed during southern blotting using specific nucleic acid probes to highlight the presence and size of the desired target DNA sequence **(Figures 26 and 27).** This was performed on gDNA obtained from two colonies each for SCO Dxs and SCO Dxr mutants. Along with the mutants, WT Mtb H37Rv ATCC 27294 gDNA was used as a control for the experiment.

1A) For the Dxs SCO mutant:

The WT and Dxs SCO mutants were first digested with the restriction enzymes Pvu II and Xba I. **Figure 26A** illustrates the map of expected DNA fragment size and labelling after the restriction digestion. Pvu II cleaves the Mtb DNA at positions flanking the *dxs1* gene, resulting in a 4.9 kb band in the Mtb WT sample after gel electrophoresis. This DNA fragment contains the *dxs1* gene (1.9 kb) along with its up- and downstream adjacent nucleotides. Conversely, Xba I exclusively cleaves the DNA fragment at the tetO (tet op) region of the psmyc1tetO promoter introduced during the homologous recombination step. In the Dxs mutant, where the tet operator region is expected to be integrated, two distinct bands of 4.42 kb and 3.68 kb were observed instead of a single continuous band. **Figure 26B** shows the southern blot membrane with the two distinct bands that are highlighted by molecular hybridisation probes. The presence of these two bands of known lengths confirms the integration of the pmyc1tetO promoter into the genome. The precise sizes of these

bands further confirm the correct location and orientation of the tet operator region, thereby confirming successful single homologous recombination.

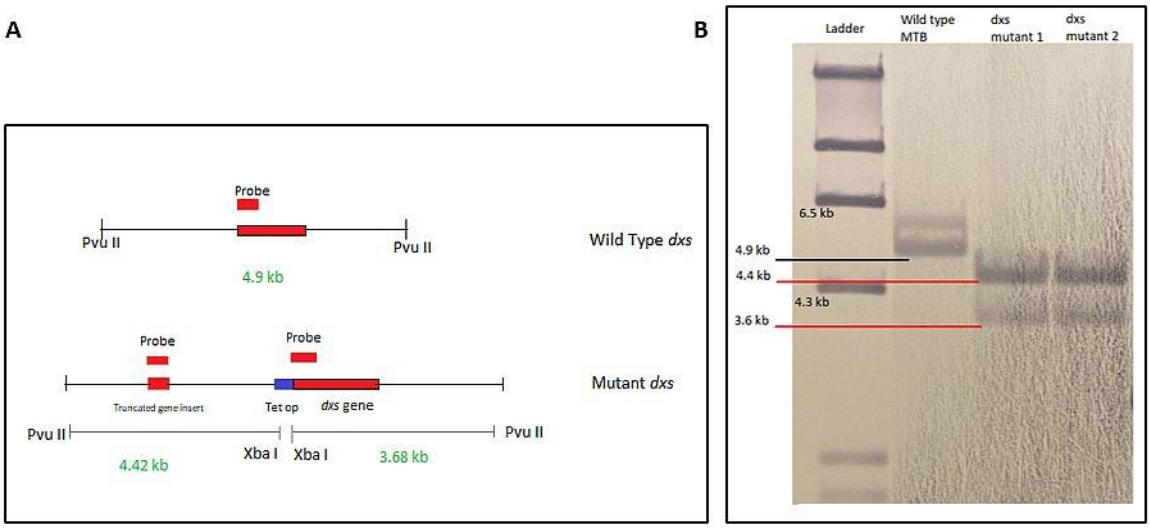

Figure 26: Southern blotting for Single homologous recombinant (SCO) Dxs mutant. The genomic DNA was isolated from Mtb H37Rv Wild type and Mtb Dxs mutants. Restriction digestion was performed using the respective enzymes followed by gel electrophoresis. The gel underwent molecular hybridisation and probe labelling to specific DNA sequences using the DIG-High Prime DNA Labelling and Detection Starter Kit I (Roche). The gel was transferred to the nitrocellulose membrane and bands were visible after incubation of 4-5 hours. [A] Map of the expected labelling and expected DNA length of the bands. [B] The nitrocellulose membrane with the visible bands for SCO Dxs mutant.

1B) For the Dxr SCO mutant:

Similarly, the WT and Dxr mutants were subjected to digestion with the Age I restriction enzyme prior to gel electrophoresis. **Figure 27A** illustrates the map of expected DNA fragment size and labelling. This process yielded a 2.4 kb band on the gel for the WT Mtb sample, which is expected to contain the *dxr* gene (1.24kb) along with its neighbouring nucleotides. The second restriction enzyme, Xba I, specifically cleaved the DNA fragment at the tetO region. Two separate bands of lengths 2.9 kb and 2.6 kb were observed on the gel for the Dxr mutant. **Figure 27B** shows the southern blot membrane with these bands.

However, one of the Dxr mutants failed to exhibit bands of the anticipated lengths and was therefore excluded from further analysis. For the remaining mutant, the observation of two bands of the expected lengths confirms the successful integration of the pmyc1tetO promoter into the genome. Additionally, the specific sizes of these bands validate the accurate integration of the recombinant DNA at the anticipated position and orientation, thus confirming successful single homologous recombination of the Dxr mutant.

Collectively, Southern blotting was successfully conducted for the Dxs and Dxr SCO mutants. Single homologous recombination was achieved in these mutants, and the correct orientation of the integrated plasmid, containing the pmyc1tetO promoter, was confirmed.

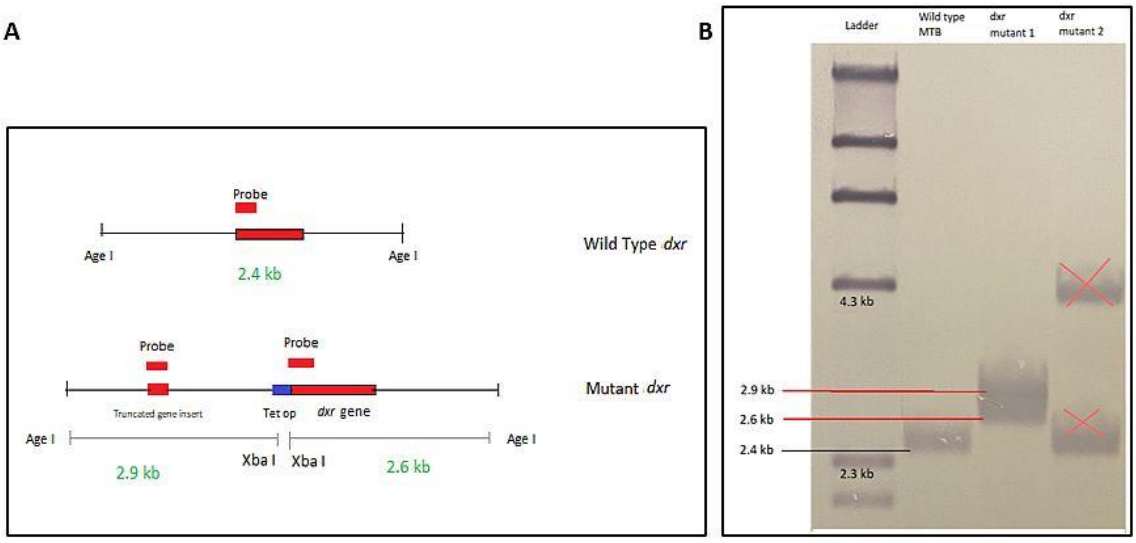

Figure 27: Southern blotting for Single homologous recombinant (SCO) Dxr mutant. The genomic DNA was isolated from Mtb H37Rv Wild type and Mtb Dxs mutant. Restriction digestion was performed using the respective enzymes followed by gel electrophoresis. The gel underwent molecular hybridisation and probe labelling to specific DNA sequences using the DIG-High Prime DNA Labelling and Detection Starter Kit I (Roche). The gel was transferred to the nitrocellulose membrane and bands were visible after incubation of 4-5 hours. [A] Map of the expected labelling and expected DNA length of the bands. [B] The nitrocellulose membrane with the visible bands for SCO Dxr mutant.

2) Next Generation Sequencing (NGS)

After the successful confirmation of the mutants using southern blotting, a second validation technique for the SCO mutants using Next-generation sequencing (NGS) was implemented to find if any Single-nucleotide polymorphisms (SNPs) were located in the mutant sequences. gDNA was isolated from the Mtb SCO Dxs and Mtb SCO Dxr mutant. The DNA concentration of both samples was around 200ng/ml. The pSE100 plasmid obtained from the Addgene supplier was also sequenced because from past experiments the DNA sequence data obtained from the Addgene website was not entirely accurate and resulted in SNPs during alignments. To avoid this and to maintain consistency in sequencing methods the plasmid pSE100 was also sequenced.

NGS sequencing was performed in collaboration with the NGS team of the research group Molecular and Experimental Mycobacteriology at the Research Center Borstel. The de novo assembly of the raw data from the Illumina sequencer resulted in 200 and 206 contiguous sequences (contigs) for Mtb SCO Dxs and Mtb SCO Dxr, respectively. To analyse this data, a construct of the expected outcome of the modified genome area was generated. To generate this construct, the sequences of the genes (*dxs1* and *dxr*) from the National Center for Biotechnology Information (NCBI) website and the newly sequenced data for the pSE100 plasmid were used.

Individual contigs were blasted against this construct to identify contigs that contain the plasmid insertion site. Contig00011 contained the modified region for *dxs1*, while for *dxr*, the modified area was distributed across two contigs (contig00005 and contig00079). The access to all the results for NGS is presented in **Supplementary Table 4**.

When the contigs were aligned against the construct, a 100% match for the Dxs SCO mutant and a near-complete match for the Dxr SCO mutant were observed. For Dxr SCO mutants the borders of the contig breaks (contig00005 and contig00079) resulted in the loss of 309 base pairs. However, since the lost sequence were not proximal to the modified genome region, the sequencing was not repeated and the integrations of the plasmid were considered successful.

Summary of the results 4.2.1.1 and 4.2.1.2:

- The Promoter replacement mutants for
    a. Tet OFF Dxs and Tet OFF Dxr
    b. Tet ON Dxs and Tet ON Dxr

  were successfully generated and confirmed using Southern blotting and Next Generation Sequencing

4.2.1.3 Atc dependency for gene regulation.

After the validation of the successful generation of SCO mutants, in the next step, the transformation of the respective TetR-containing plasmid for either Tet ON (pMC1s) or Tet OFF (pTEK-4S-0X) was carried out using electroporation. The transformed colonies were successfully isolated on kanamycin (kan) and hygromycin (hyg) containing plates and cultured. Additionally, for Tet ON, the plates contained 500ng/ml of Atc.

Post transformation, Tet OFF mutants showed no change in growth phenotype relative to the SCO mutants. For Tet ON mutants, the bacteria were cultured using 500ng/ml Atc concentration, since they theoretically require Atc to express the *in vitro* essential *dxs1/dxr* gene. Normal growth phenotypes (relative to SCO mutant) were observed at this high Atc concentration for both strains (**Supplementary Figure 5**).

1) Tet OFF Dxs and Dxr

For Tet OFF mutants, increasing concentrations of Atc should dose-dependently decrease the target gene expression levels. To experimentally validate this, the mutants were grown in standard growth media containing a single high Atc concentration (500ng/ml) for 7 days and OD600 measurements of the cultures were monitored over time. Wild Type (WT) Mtb H37Rv was also included in the experiment as a negative control. The OD600 values of the Tet OFF Dxs and Dxr mutants were similar to WT Mtb in the presence and absence of Atc **(Figure 28A).** No significant differences were observed in the growth of any of the mutants

compared to WT Mtb. Hence, this phenotype suggests that the Tet OFF Dxs and Dxr mutants did not show phenotypic growth changes when subjected to the Atc supplement.

Upon completion of the growth assay, RNA of these mutants was extracted, in order to directly measure expression levels of the target genes. Real-time quantitative Reverse Transcription PCR (RT-qPCR) was performed for *dxs1* and *dxr* genes as explained in the methods section. For both the Tet OFF Dxs and Dxr mutants, transcript levels of the target genes were quantified from cultures grown with and without (w/wo) 500ng/ml Atc. The data analysis was performed by normalising to the reference gene *sigA*. Wild-type Mtb was used as a control for the experiment. No difference in gene concentration was seen in either the Tet OFF Dxs or Dxr mutants when Atc was present **(Figure 28B).** Moreover, the target gene transcript levels in the mutants were similar to levels observed in the WT Mtb. This suggests that the mRNA levels were not affected in the Tet OFF mutant Dxs and Dxr in the presence of 500ng/ml Atc. Hence, ATC-dependent gene downregulation of the promoter replacement Tet OFF mutants was not observed.

Collectively the data shows that gene downregulation was observed neither phenotypically by measuring the growth of the mutants in the presence of Atc nor by quantifying the mRNA of the target genes. Hence, the gene downregulation of these mutants using Atc was not successful.

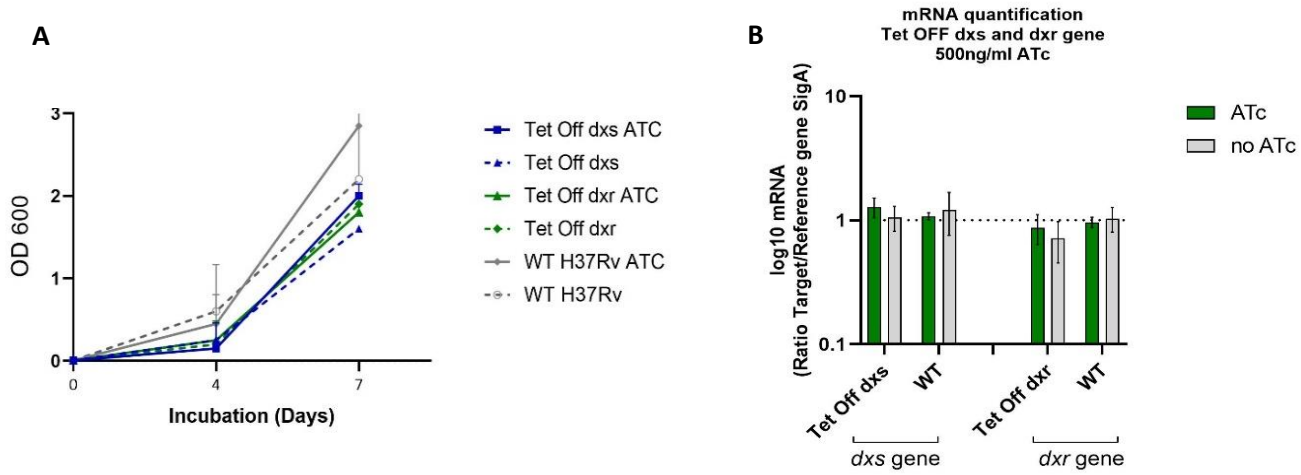

Figure 28*:* Growth characteristics and mRNA quantification of Promoter replacement mutant Tet OFF (A) The Tet OFF mutants were cultured in growth media containing kanamycin and hygromycin, either with Atc (500ng/ml) and without Atc (0ng/ml) for 7 days. OD600 was monitored and the graph was plotted to observe the difference in bacterial growth phenotype in presence and absence of Atc. Wild type Mtb H37Rv was used as a negative control. Two independent experiments were performed and are presented as mean ± SD. (B) Mutants and WT Mtb was grown for 4 days and RNA was extracted. Complementary DNA was synthesized and used to quantify *dxs1* and *dxr* gene expression via qRT-PCR. All mRNA expression levels were normalized against sigA mRNA expression levels. Two independent experiments were performed and are presented as mean ± SD.

2) Tet ON Dxs and Dxr

The Tet ON mutants were analysed separately and in order to maintain target gene expression were routinely cultured in growth media with kan, hyg and 500ng/ml Atc. To observe if increasing concentrations of Atc induce dose-dependent gene upregulation, cultures at the mid-exponential phase were pelleted, washed with growth media without Atc, and finally resuspended in media w/wo (0ng/ml and 500ng/ml) Atc and left to incubate for 7 days. OD600 values of these cultures were monitored over time; Wild-type Mtb was included in the experiment as a negative control. The Tet ON Dxs and Dxr mutants showed no difference in growth when Atc was absent **(Figure 29A)**. Moreover, no significant differences were observed in the growth of any of the mutants compared to the WT Mtb. Hence, this phenotype suggests that in our study the Tet ON Dxs and Dxr mutants did not show phenotypic growth changes when subjected to Atc.

Similar to the Tet OFF mutants, *dxs1* and *dxr* transcript levels were quantified by qPCR for the Tet ON mutants, following growth with or without 500 ng/ml Atc. No difference in the transcript levels of *dxs1* and *dxr* was seen under any condition tested for either of the Tet ON mutants **(Figure 29B)**. Moreover, the mRNA levels were very similar to the WT Mtb *dxs1* and *dxr* levels. This suggests that the mRNA levels were not affected in the Tet ON Dxs and Dxr mutants in the absence of Atc. Hence, the Atc-dependent target gene upregulation of the promoter replacement Tet ON mutants was unsuccessful.

Collectively the data shows that gene upregulation was observed neither phenotypically by measuring the growth of the mutants nor by quantifying the mRNA of the target genes. Hence, the gene upregulation of these mutants using Atc was not successful.

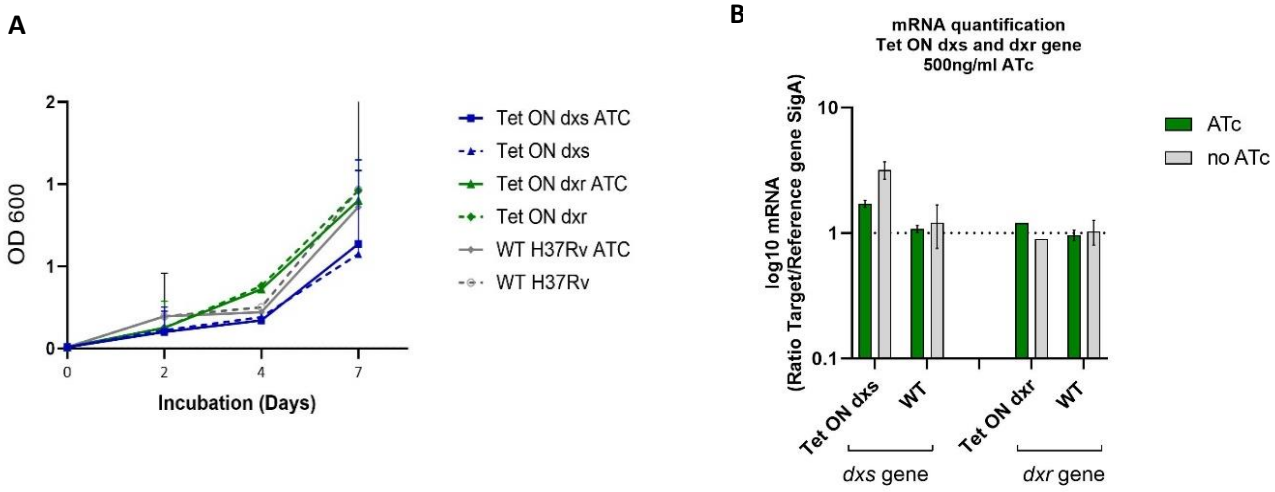

Figure 29: Growth characteristics and mRNA quantification of Promoter replacement mutant Tet ON. (A) The mutants were cultured in growth media with 25ug/ml of kanamycin and hygromycin either with Atc (500ng/ml) or without Atc (0ng/ml) for 7 days. OD600 was monitored and the graph was plotted to observe the difference in bacterial growth phenotype in presence and absence of Atc. Wild type Mtb H37Rv was used as a negative control. Two independent experiments were performed and are presented as mean ± SD. (B) Mutants and WT Mtb was grown for 4 days and RNA was extracted. Complementary DNA was synthesized and used to quantify *dxs1* and *dxr* gene expression via qRT-PCR. All mRNA expression levels were normalized against sigA mRNA expression levels. Two independent experiments were performed and are presented as mean ± SD.

Summary of the results 4.2.1.3

- For all the promoter replacement mutants, no Atc dependency was observed.
- This was validated by growth curves (OD600 measurement) and quantification of *dxs1* and *dxr* gene mRNA levels

4.2.2 CRISPRi Mutants

4.2.2.1 Strategy and generation of CRISPRi mutants

In a further attempt to validate the putative drug targets Dxs and Dxr, a CRISPRi method for generating conditional knockdown mutants was used, following a previously established protocol (7). Unlike promoter replacement mutants, the CRISPRi system utilizes a single plasmid in a one-step cloning process that generates conditional mutants without modifying the native gene. This reduces both the time required to generate mutants and the potential to introduce undesired polar effects on neighbouring genes. Additionally, empirical data using CRISPRi to target every essential gene in the Mtb H37Rv strain is already available (72), significantly increasing the chances of successful mutant generation. Hence, the CRISPRi system was the next feasible approach for target validation.

Utilizing a catalytically inactivated Cas9 (dCas9) protein derived from *Streptococcus thermophilus* (Sth1Cas9), known for its high efficacy in target knockdown and low cytotoxicity, we aimed to achieve precise and controlled modulation of gene expression (7). Specific guide RNAs (sgRNAs) targeting the genes of interest, namely *rpob, dxs1,* and *dxr* were designed.

A positive control CRISPRi mutant was generated by targeting *rpoB*, the gene encoding the RNA polymerase β subunit and the target of the antibiotic Rifampicin (148, 149). For the negative control, mutants harbouring a non-targeting (NT) scrambled sgRNA were generated. This scrambled sgRNA does not bind anywhere in the Mtb genome with more than 7bp continuous sequence homology.

To ensure robust sgRNA binding, we selected protospacer adjacent motifs (PAMs) with strong binding affinities. PAMs are short DNA motifs crucial for Cas9 binding and subsequent sgRNA-guided DNA cleavage (150). For *dxs1* and *dxr*, three sgRNAs each with strong PAM sequences were identified, while for *rpoB*, a single sgRNA with a strong PAM was selected. These sgRNAs were integrated into the CRISPRi backbone plasmid, pLJR965, comprising all essential components necessary for Atc-inducible CRISPRi gene expression knockdown. These include 1) a sgRNA scaffold, 2) a nuclease-inactivated Cas9 (dCas9) allele, 3) a Tet repressor protein-encoding gene, 4) a Mycobacteriophage L5 integrase gene and L5 *attP* site (for genomic integration in Mtb at the L5 mycobacteriophage integration site) and 5) a kanamycin resistance allele (124) **(Figure 30).**

Following plasmid construction, all plasmids were subjected to Sanger sequencing to confirm successful sgRNA integration. Alignment of the sequencing data with the original sgRNA sequences, using online software Clustal Omega (https://www.ebi.ac.uk/jdispatcher/msa/clustalo), revealed 100% alignment coverage for all plasmids, indicating accurate integration. However, one *dxs1* sgRNA showed single nucleotide polymorphisms (SNPs) and was discontinued from further experiments **(Supplementary Figure 6).**

Following sequence confirmation, constructs were electroporated into Mtb H37Rv and resulting clones were picked and cultured in standard growth media without Atc. Under normal growth conditions, no growth defects for any of the mutants relative to WT H37Rv were observed **(Supplementary Figure 7).**

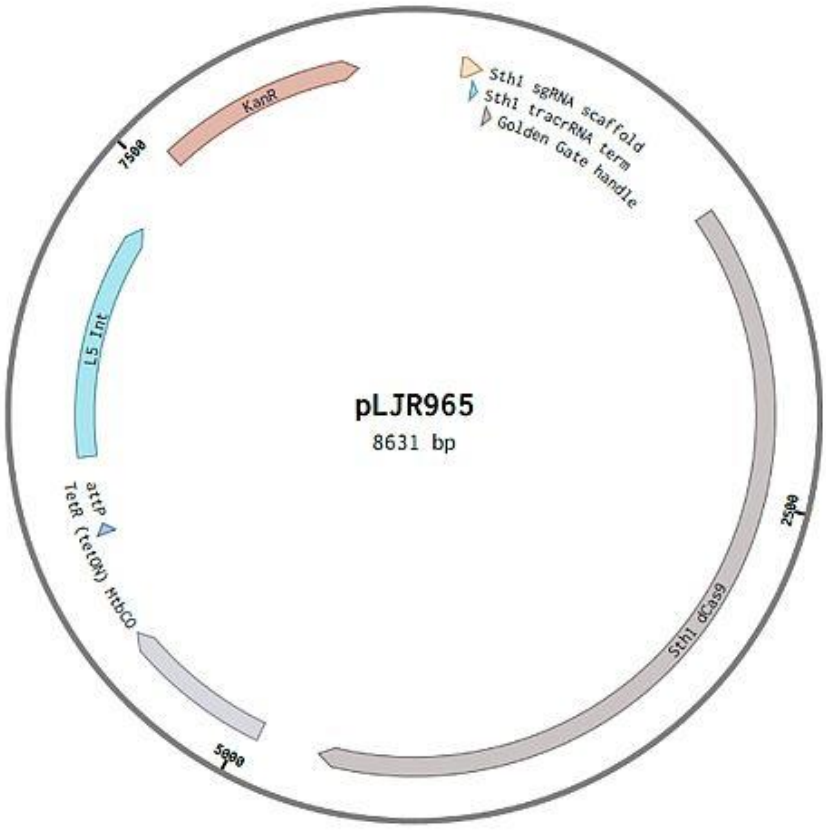

Figure 30*:* CRISPRi Plasmid pLJR965 with dCas9 and sgRNA scaffold

In summary, sequence-confirmed CRISPRi plasmids were successfully generated for *dxs1*, *dxr*, and *rpoB* (as well as a non-targeting negative control) and introduced into Mtb H37Rv. No growth defects were seen for the newly obtained Mtb mutants, relative to wild-type bacteria when cultured in growth media lacking Atc. Hence, the one-step cloning method of generating CRISPRi mutants was successfully achieved.

4.2.2.2 Confirmation for generation of CRSIPRi mutants

Following the successful electroporation and culturing of the CRISPRi mutants, experiments were performed to address the Atc-dependent downregulation of the target genes in these strains. To confirm the gene knockdown in the mutants, several assays were carried out that are presented below.

1) Phenotype:

The first approach was to monitor the phenotypic change or growth impairment of the bacteria following growth in media with or without Atc. *dxs1, dxr* and *rpoB* are essential genes for the *in vitro* survival of Mtb (68). If these genes are knocked down, Mtb cannot compensate for their loss of expression, leading to the cessation of growth of the bacteria. In most cases, the degree of bacterial growth inhibition depends on the magnitude of gene knockdown, an effect that can be efficiently achieved with the CRISPRi system by titrating Atc levels. To test this, the bacteria were grown in growth media containing kanamycin and different concentrations of Atc over a period of 14 days. For Dxs and Dxr mutants, Atc concentrations of 1000, 375, 150, 75, 37.5, and 0 ng/ml were chosen, whereas for Rpob mutant Atc concentrations of 1000, 780, 195 and 0 ng/ml were chosen. OD600 values and CFUs of all bacterial cultures were measured on days 0, 2, 4, 6, 8, 12, and 14. For the RpoB mutant, the OD600 and CFU counts of the mutant with 0ng/ml Atc showed a normal growth phenotype **(Figure 31A left).** In the presence of Atc, at all concentrations tested, the OD600 values of bacteria stayed close to baseline, while the CFU counts decreased dose-dependently with respect to Atc concentration. An approximately, 4 log reduction in CFU was observed on day 6 at 1000ng/ml Atc. **(Figure 31A right).**

Similar observations were made with the Dxs and Dxr CRISPRi mutants. A clear dose dependence of bacterial growth with Atc concentration was observed. Similar to the RpoB CRISPRi mutant, approximately 4 log reductions in CFU for Dxs **(Figure 31B)** and 3 log reductions for Dxr **(Figure 31C)** were observed on day 6 with 1000ng/ml Atc.

For all three mutants, an increase in OD600 values post day 12 and an increase in CFU counts post day 6 was observed. After 14 days the CFU counts were similar to the control bacteria without Atc. This regrowth of bacteria might be due to "escape" mutants that have lost tetracycline-dependent regulation of the CRISPRi elements due to mutations acquired during bacterial growth. To verify if these are escape mutants and not a phenotype observed due to growth media deficiencies (degradation of Atc over time), the culture on day 15 was split into two sets. One set of mutants was left untouched, while the other set was washed with growth media three times and reinoculated into fresh growth media including 250ng/ml of Atc. The growth of the cultures containing Atc was monitored for the next 8 days by measuring the OD600 of all the cultures. Over 8 days, the reinoculated mutants with 250ng/ml Atc showed no growth impairment **(Figure 32)** suggesting that the previously observed regrowth of the mutants could be indeed because these mutants might have ‘escaped’ from the tetracycline-dependent CRISPRi regulation. Further sequencing of

these mutants would help confirm this hypothesis. This phenomenon is in line with previous studies using the CRISPRi system (133) and studies with different tet-regulated promoter systems (73).

Overall, the phenotypic growth curves suggest that the CRISPRi mutants Dxs, Dxr and RpoB show Atc-dependent growth inhibition. The CFU data suggests that in the presence of high Atc concentrations (around 1000ng/ml), the CRISPRi system may induce bacterial killing and not solely bacterial growth inhibition. The observed regrowth of mutants between days 6-12, coupled with findings from prior studies, likely indicates the emergence of escape mutants following prolonged exposure to Atc.

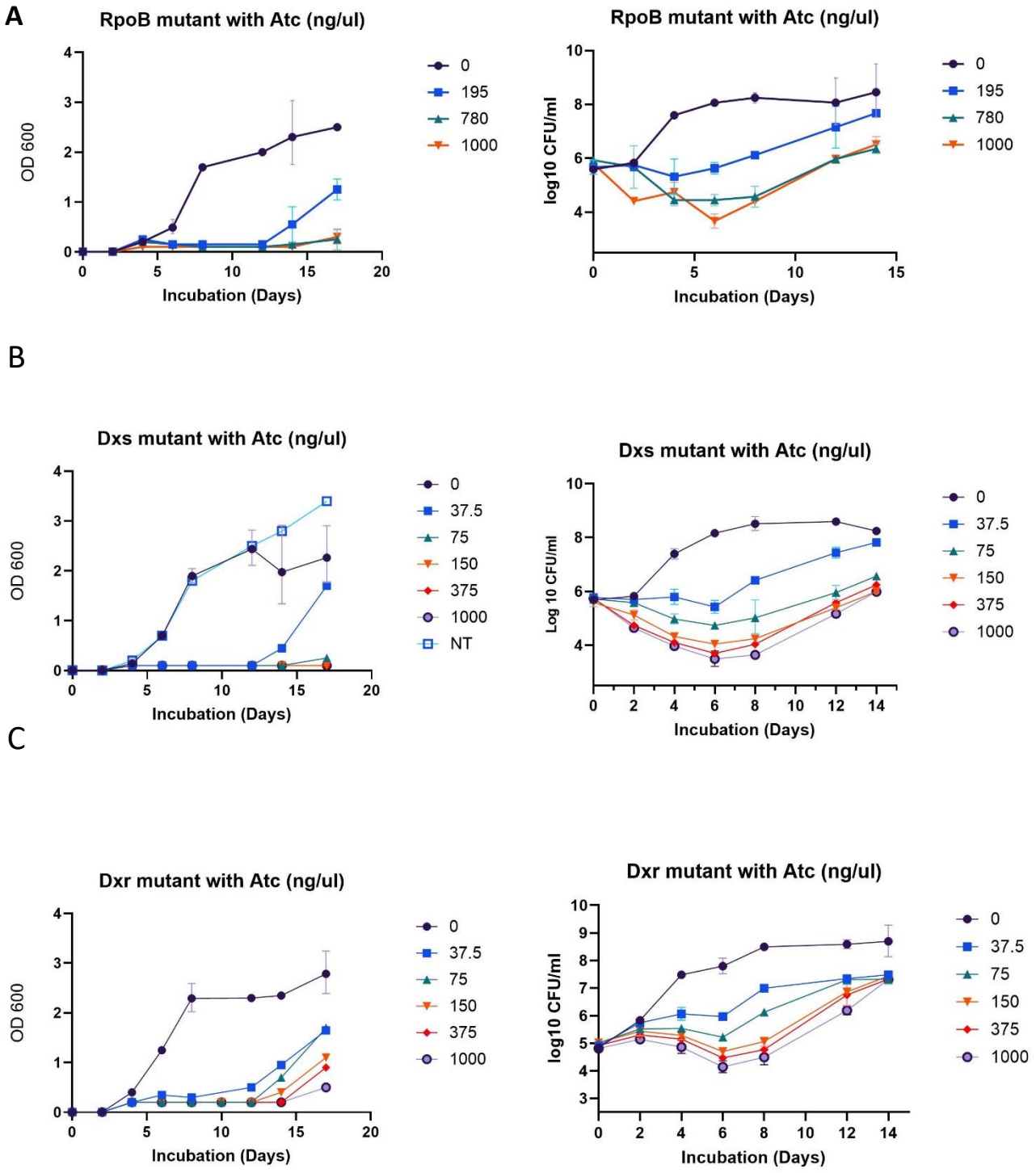

Figure 31: Growth curves of CRISPRi mutants Dxs, Dxr and RpoB measured by OD600 and Colony Forming Units (CFU) counts. Mutants were cultured in growth media including kanamycin and respective concentrations of Anhydrotetracycline (Atc). The OD600 was monitored for 17 days and Colony Forming Units were monitored for 14 days. Two technical replicates were maintained and graphs were plotted using GraphPad Prism. Figures [A], [B] and [C] represent the OD600 measurements (left) and CFU counts (right) for Dxs, Dxr and RpoB CRISPRi mutants respectively.

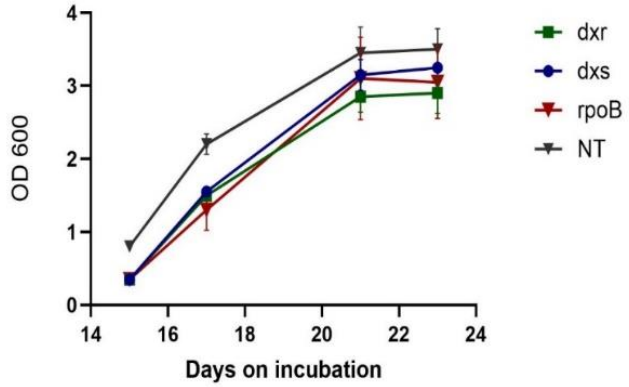

Figure 32: CRISPRi "escape" mutants. Mutants were cultured in growth media including kanamycin with 500ng/ml concentration of Atc. The OD600 was monitored for 15 days. On day 15 the regrowth of bacteria was washed three times with growth media and reinoculated in fresh media with 250ng/ml Atc. These freshly cultured mutants were further monitored for 10 days by measuring the OD600. Two technical replicates were maintained and graphs were plotted using GraphPad Prism.

2) mRNA quantification using RT-qPCR

To further validate the Atc-dependent gene downregulation, the RNA from the mutants was isolated following Atc exposure and mRNA levels of the target genes were quantified. The bacteria were grown w/wo 500ng/ml Atc and the RNA was isolated after three days. RT-qPCR was performed to observe the levels of the *dxs1* and *dxr* gene expression in all the mutants. The data was normalised to the reference gene *sigA*. Both the genes in the CRISPRi NT mutant and RpoB mutant showed similar values w/wo Atc **(Figure 33).**

In the CRISPRi Dxs mutant*, the dxs1* gene was downregulated approximately 2 logs with 500ng/ml Atc when compared to without Atc **(Figure 33A).** Similarly, in the CRISPRi Dxr mutant, 1 log reduction of the *dxr* gene was observed with 500ng/ml Atc when compared to without Atc **(Figure 33B).** This observation in the Dxs and Dxr CRISPRi mutants confirms the Atc-dependent transcription repression on an mRNA level.

Moreover, in the Dxr knockdown mutant, *dxs1* mRNA levels were slightly upregulated (approx. 1 log) Similarly, in the Dxs knockdown mutant, *dxr* mRNA levels were upregulated (approx. 1 log). Hence an interdependency in gene regulation of *dxs1* and *dxr* mRNA levels was observed.

Collectively, the qPCR data suggests that the Atc-mediated transcriptional knockdown was successfully observed for the *dxs1* and *dxr* genes in the respective CRISPRi mutants. Moreover, an interdependency between *dxs1* and *dxr* mRNA levels was also observed, where the *dxs1* gene is slightly upregulated when the *dxr* gene is downregulated and vice versa.

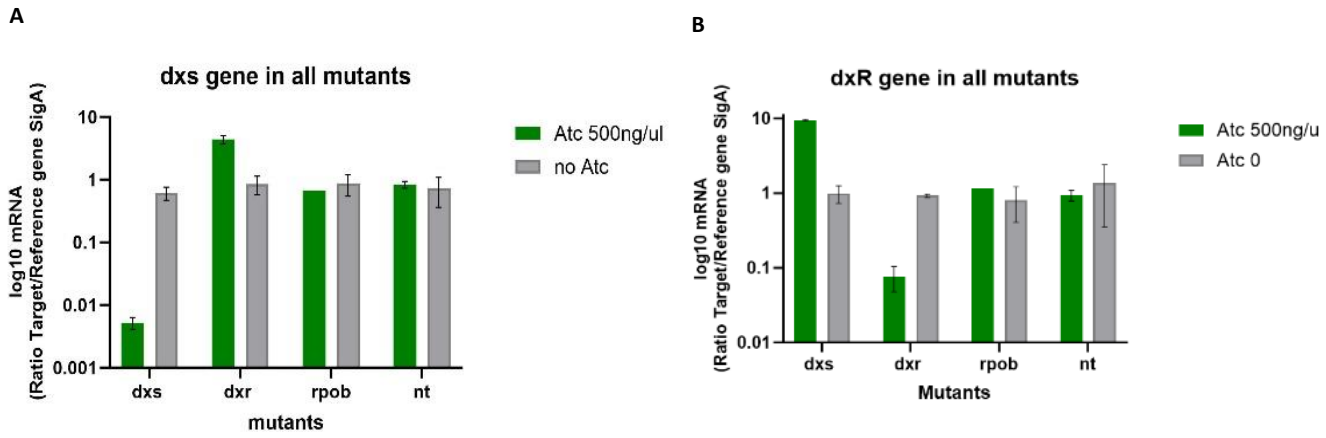

Figure 33: mRNA quantification of *dxs1* and *dxr* gene in the CRISPRi mutants. The mutants were grown for 4 days and RNA was extracted. Complementary DNA was synthesized and used to quantify *dxs1* and *dxr* gene expression via qRT-PCR. All mRNA expression levels were normalized against *sigA* mRNA expression levels. Two independent experiments were performed and are presented as mean ± SD. [A] *dxs1* mRNA levels in all four CRISPRi mutants, [B] *dxr* mRNA levels in all four CRISPRi mutants in the presence and absence of Atc.

3) Protein quantification

After the successful validation of CRISPRi downregulation by growth curves and mRNA quantification, we aimed to validate the presence of *dxs1* and *dxr* regulation also on a protein level.

Dxs and Dxr proteins were quantified from cell extracts using proteomics assays at a collaborative institute (OmicScouts, Freising, Germany). The CRISPRi mutants were grown w/wo Atc (500ng/ml and 1.95ng/ml) for 3 days. Lysates were obtained and sent for further quantification. The abundance of the target proteins was quantified by Mass Spectrometry and graphs were plotted. The NT mutant did not show any changes in the protein levels of RpoB, Dxs or Dxr **(Figure 34).** In contrast, Atc dose-dependent decreases in target protein abundance were observed in all of the other three mutants. With 500 ng/ml Atc, Dxs and Dxr protein levels were decreased by approximately 0.5 to 1 log **(Figure 34B and Figure 34C).** For RpoB, this shift was even more prominent and approximately a 2-log decrease in protein levels was observed in the presence of Atc (500ng/ml) **(Figure 34A).**

Hence, proteomic analysis revealed that the protein abundance of RpoB, Dxs and Dxr is reduced in the presence of 500ng/ml Atc as compared to the absence of Atc, in their respective CRISPRi strains. These observations further confirm the gene downregulation in CRISPRi mutants using Atc.

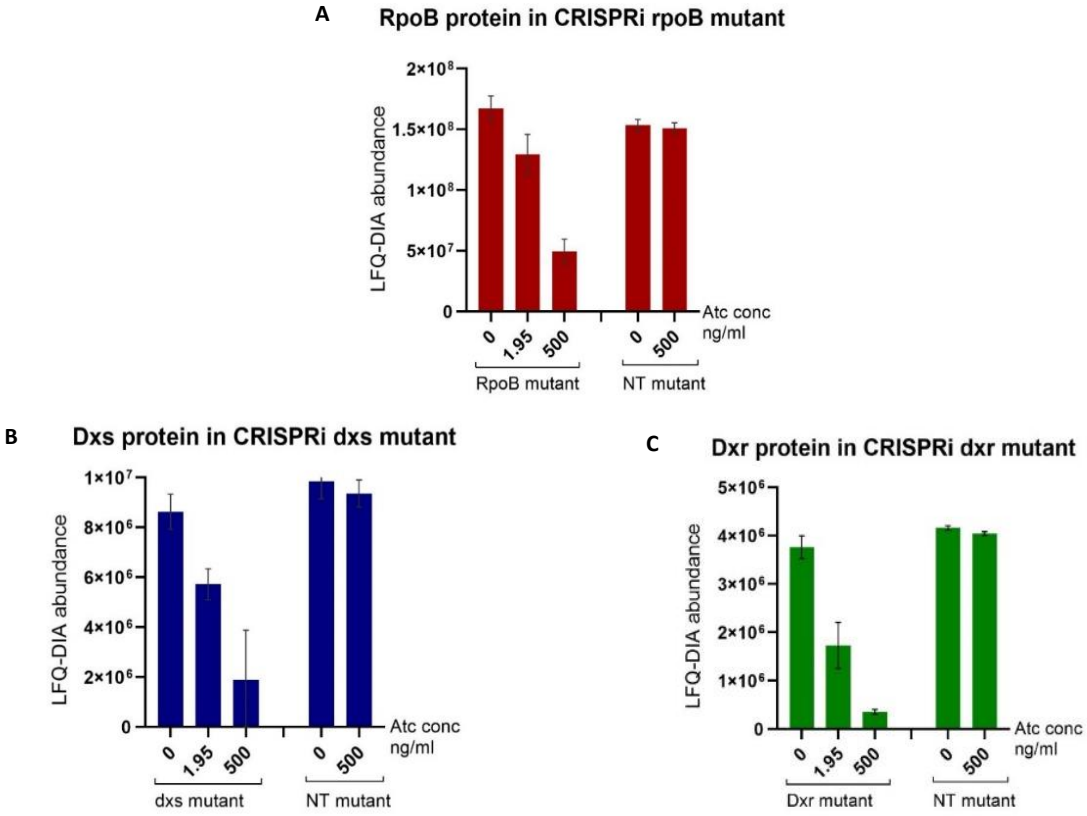

Figure 34*:* Protein quantification of Dxs, Dxr and RpoB in the respective CRISPRi mutants. Mutants were cultured in growth media including 25ug/ml kanamycin with 500ng/ml concentration of Atc for three days and lysates were obtained by bead beating. The lysates were then shipped to a collaborative institute where mass spectrometry-based proteomics was performed to quantify the protein levels. Two independent experiments were performed and are presented as mean ± SD. [A] RpoB protein abundance in RpoB mutant, [B] Dxs protein abundance in Dxs mutant, [C] Dxr protein abundance in Dxr mutant in presence of different Anhydrotetracycline (Atc) concentrations.

Summary of the results 4.2.2.1 and 4.2.2.2

- CRISPRi mutants were successfully generated for Mtb genes *rpoB*, *dxs1*, *dxr*. Mutants for *rpoB* and non-targeting sgRNA served as the positive and negative controls, respectively.
- The Atc dependency of these mutants were validated using:
  1. Growth curves, measured by OD600 and Colony Forming Units counting.
  2. Quantification of mRNA levels.
  3. Quantification of protein levels.
- The CRISPRi mutants showed successful gene downregulation with increasing Atc concentrations supplemented in the growth media.

Mtb can reside and replicate in macrophages despite the onslaught of the immune system (151, 152). Hence, for drug development against Mtb, it is necessary to study the activity of compounds against Mtb residing intracellularly in a macrophage. Moreover, it is important to investigate if the *dxs1* and *dxr* genes continue to be essential and vulnerable intracellularly, making these enzymes much more valuable drug targets.

A recent study published in 2022, showed that Atc was able to cross eukaryotic membranes and activate CRISPRi within Mtb inside macrophages (153). To verify this finding and investigate the intracellular essentiality of the genes, CRISPRi mutants *dxs1, dxr* and *rpoB* were subjected to an intracellular survival assay.

1) Toxicity of Atc:

Prior to the intracellular survival assay, it is crucial to assess the cytotoxicity of Atc against HMdM which was performed using the xCELLigence system. Different concentrations of Atc ranging from 0.24ng/ml to 500ng/ml were tested for cytotoxicity in real time for 120 hours **Figure 35**. The data shows that Atc is not toxic to the HMdM even at a high concentration of 500ng/ml. This finding is in line with previous studies for Atc toxicity (122, 153)

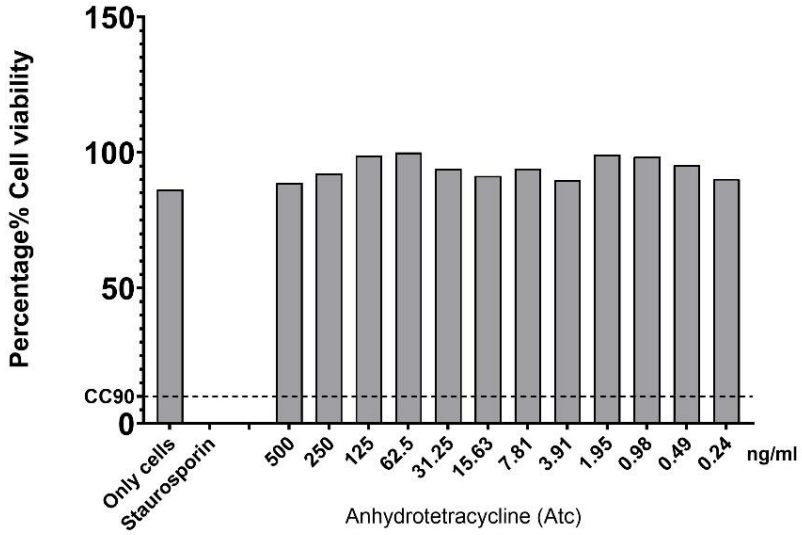

Figure 35: Toxicity analysis of Anhydrotetracycline (Atc) (concentration range from 0.24ng/ml to 500ng/ml): Human monocyte-derived macrophages (HMdM) were exposed to the designated compound and incubated for 24 hours in xCELLigence plates and cell death was monitored using the xCELLigence device. Cells with DMSO served as the negative control, while Staurosporin was employed as the positive control. Three technical replicates were used and curves were obtained by the average of the triplicates. Further, the sum of the area under the curve was calculated and presented in bar graphs using GraphPad Prism. 90% or more cell death was marked as Cytotoxic Concentration (CC90) for the compounds.

2) Intracellular Atc dependency

Since Atc was found to be non-toxic to the cells, HMdM were infected with all four mutants in the presence (500ng/ml) and absence of Atc. The assay was performed similarly to the Intracellular drug testing previously described. CFUs were plated on day 3, day 5 and day 7 for all the conditions. The NT mutant showed no growth defect over 7 days w/wo Atc. For the three other mutants, in the absence of Atc, normal growth phenotypes were observed **(Figure 36).** However, in the presence of 500ng/ml Atc, approx. 2 log decreases in growth were observed on day 5 and approx. 4 log decreases on day 7 for all three mutants. This observation confirms that Atc can cross biological membranes and activate CRISPRi mediated gene downregulation intracellularly in HMdM. Moreover, it strongly suggests that *dxs1* and *dxr* are essential for the growth of the bacterium inside the host macrophage.

Regrowth of the Dxs mutant on day 7 was observed in one replicate suggesting the presence of escape mutants as previously seen *in vitro* assays (section 4.2.2.2). Further sequencing will be needed to confirm the development of these "escape" mutants.

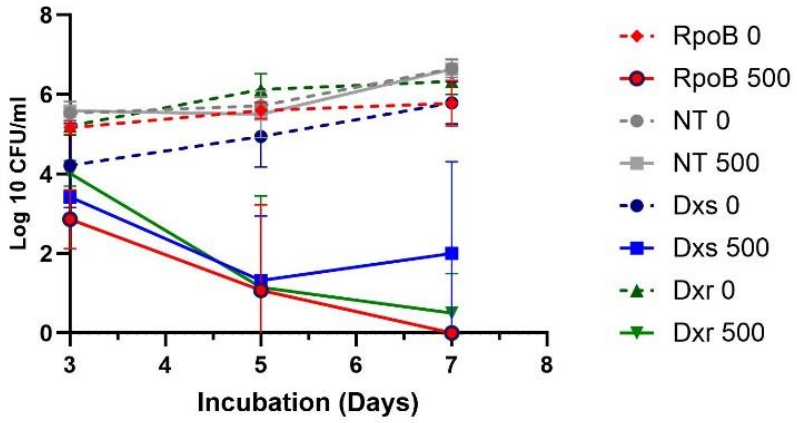

Figure 36: Intracellular growth characteristic of Mtb CRISPRi mutants in the presence and absence of Atc HMdM were infected with Mtb H37Rv at an MOI of 0.5:1 and treated with Atc at 500ng/ml, washed at 4h post-infection followed by 7-day incubation. To determine the bacterial survival, Colony Forming Units were counted on days 3, 5 and 7. Two independent experiments, each consisting of two technical replicates, were performed and graphs were plotted using GraphPad Prism.

Summary of the results 4.2.2.3

- Atc was shown to be non-toxic against Human monocyte derived macrophages (HMdM) even at 500ng/ml concentration.
- In the presence of 500ng/ml Atc approx. 4log decrease in bacterial CFU were observed in all three CRISPRi mutants

4.2.2.4 Target Validation of compounds

As described above, CRISPRi gene downregulation was successfully set up for the MEP pathway genes *dxs1* and *dxr* in Mtb H37Rv ATCC 27294. Following the identification of phenotypically active compounds designed against Mtb Dxs and Dxr (section 4.1.2.3) some of the actives were selected for their target validation against Dxs and Dxr CRISPRi mutants.

Prior to testing the novel compounds, rifampicin was evaluated against the RpoB mutant. The rationale behind this is that rifampicin is a crucial first-line antibiotic employed in Mtb treatment (11, 12). It functions by interacting with the beta subunit of RNA polymerase, inhibiting the DNA-directed RNA synthesis of Mtb. This beta subunit is encoded by the gene *rpoB* in Mtb (12, 13). *rpoB* is a highly essential gene for Mtb survival, with a vulnerability index of -9.56, indicating its significant potential as a drug target (14, 15). Therefore, *rpoB* was selected as a positive control to confirm the target of Rifampicin.

1) Target validation of Rifampicin:

The validation of the rifampicin target was conducted using various concentrations of Atc (31.25, 62.50, and 125 ng/ml) over 7 days followed by Alamar blue assay by measuring the resazurin fluorescence as detailed in the methods section.

When rifampicin was tested without Atc (0 ng/ml) against the NT mutant and the RpoB mutant, a comparable IC50 of 0.02 +/- 0.01 ug/ml was observed **(Figure 37A).** The addition of 31.25, 62.50, and 125 ng/ml Atc demonstrated a dose-dependent decrease in the IC50 values of rifampicin, i.e., 0.019, 0.009, and 0.0037 ug/ml, respectively for the CRISPRi RpoB mutant. This dose dependency was not observed in the NT mutant. In the RpoB mutant, a fold shift in IC50 for RIF of 2.27 and 5.64 was observed at the two higher concentrations of Atc. The >5-fold shift indicates that the increased susceptibility of Rifampicin is specific to *rpoB* knockdown **(Table 13).**

2) Target validation of CC143:

Following the successful validation of RIF, compound CC143 was tested against the Dxr and NT mutants. The analogues of this compound have been studied previously for its activity against purified Dxr using biochemical assays (1). CC143 is a fosmidomycin prodrug synthesized at Ghent University. When tested against Mtb H37Ra (at Ghent University), CC143 showed an IC50 value of 0.42uM (1), whereas a higher MIC90 of 16uM was observed when tested against Mtb H37Rv (section 4.1.1.3). However, as the target binding studies showed good affinity against the Dxr enzyme and hence this compound was selected to be tested against the Dxr CRISPRi mutant.

When CC143 was tested against the CRISPRi NT and Dxr mutants in the absence of Atc, comparable IC50 values of 36.4uM and 28.7uM were observed **(Figure 37B).** For the Dxr CRISPRi mutant, with increasing concentrations of Atc from 31.25, 62.50 and 125ng/ml Atc a dose-dependent reduction of IC50 was

observed i.e. 19.9, 9.5 and 4.7uM respectively. Similar to the positive control RIF, a > 5-fold decrease in IC50 was observed with 125ng/ml Atc concentration **(Table 13).** This strongly suggests that the compound targets Dxr in Mtb.

3) Target validation of HIPS759:

Another compound HIPS759, showed MIC90 against Mtb H37Rv mCherry10 of 64uM. When tested against NT mutant and Dxs mutant with 0ng/ml Atc, comparable IC50s of 27.8uM and 34.4uM were observed **(Figure 37C).** With increasing concentrations of Atc from 31.25, 62.50 and 125ng/ml no significant shifts in the IC50 were noted. The fold change with the highest Atc concentration used (125ng/ml) was 1.81. Since the fold change was not significant relative to the positive control, the compound HIPS759 may not target Dxs in Mtb.

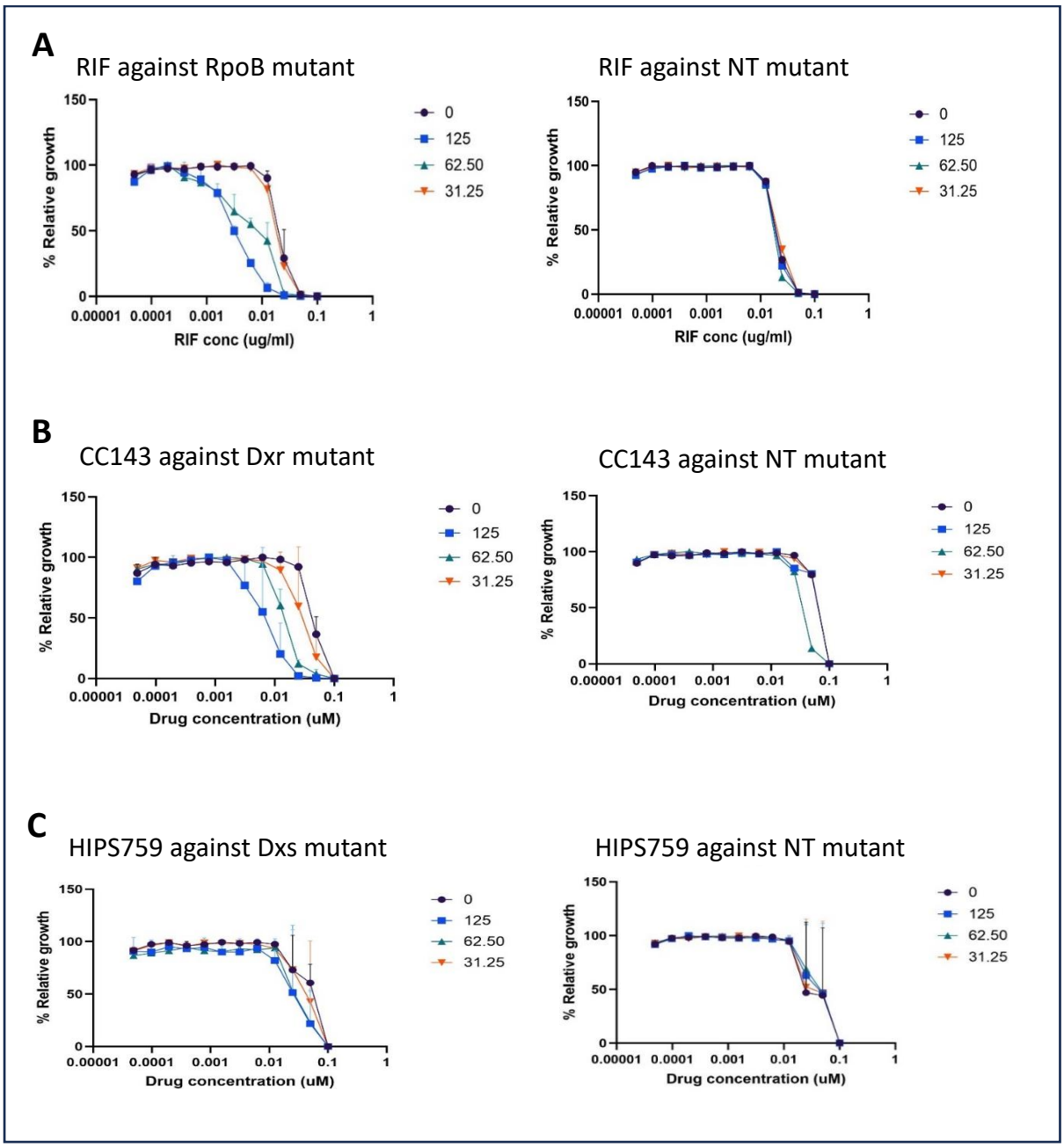

Figure 37: Target validation of Rifampicin and novel compounds using CRISPRi mutants. Mutants were cultured in growth media including 25ug/ml kanamycin with 3 different concentrations of Atc as represented for 7 days in 96 well plates followed by the addition of novel compounds at different concentrations (as represented on the X-axis). The plates were incubated for 7 days and resazurin was added followed by 24-hour incubation and fluorescence measurement. Two independent experiments were performed and are presented as mean ± SD. [A] Rifampicin tested against RpoB mutant (left) and Non-targeting (NT) mutant (right), [B] CC143 tested against Dxr mutant (left) and NT mutant (right), [C] HIPS759 against Dxs mutant (left) and NT mutant (right) in presence of different Anhydrotetracycline (Atc) concentrations.

Table 13: IC50 values and shift of IC50 values of rifampicin, CC143 and HIPS759 against respective mutants in the presence of different Atc concentrations. IC50 values and IC50 fold shift were calculated using GraphPad prism. *ng/ml for RIF.

		IC50 values (uM) (*ng/ml)				Shift in IC50 log10		
		Atc concentrations (ng/ml)				Atc concentrations (ng/ml)		
Compounds	**Mutants**	**0**	**125**	**62.50**	**31.25**	**125**	**62.50**	**31.25**
RIF*	Rpob	0.021	0.003	0.009	0.019	**5.641**	**2.279**	1.095
	NT	0.029	0.020	0.018	0.022	1.045	1.122	0.948
CC143	Dxr	28.73	4.79	9.58	19.93	**6.00**	**3.00**	1.44
	NT	40.34	41.32	23.22	40.81	0.98	1.74	0.99
HIPS759	Dxs	34.42	18.98	20.24	28.61	1.81	1.70	1.20
	NT	25.84	28.54	29.42	27.46	0.91	0.88	0.94

Summary of the results 4.2.2.4

- In the presence of Atc, a greater than 5-fold shift in the susceptibility towards RIF was observed for the RpoB CRISPRi mutant (relative to without Atc).
- In the presence of Atc, a greater than 5-fold shift in the susceptibility towards CC143 was observed for the Dxr CRISPRi mutant.
- HIPS759 showed a limited fold shift (approx. 2-fold) in susceptibility in the presence of Atc for the Dxs CRISPRi mutant

Chapter 5

Discussion

This doctoral thesis focused on discovering novel compounds for TB treatment through phenotypic and target-based *in vitro* drug screening. Conditional Mtb mutants were generated for the MEP pathway genes *dxs1* and *dxr* using both promoter replacement and CRISPRi methods to validate the targets of the novel compounds. While promoter replacement mutants failed to exhibit Atc-dependent gene regulation, the CRISPRi system successfully knocked down *dxs1* and *dxr*, enabling the validation of whole-cell target engagement for novel test compounds. In this context, the challenges, reasoning, and achievements of this doctoral thesis are discussed below.

5.1 Target-based versus phenotypic-based drug discovery

For drug testing against Mtb, two approaches (Phenotypic Drug Screening and Target-Based Drug Development) have been used in this doctoral study. Compounds from both these approaches were found active below 8uM MIC90 against Mtb H37Rv. However, both these approaches have their pros and cons in drug discovery. Phenotypic screening can identify compounds with novel mechanisms of action; however, subsequent target identification is often a tedious and lengthy process. On the other hand, target-based drug discovery has the advantage of focusing on pre-selected promising cellular targets but has a poor success rate in translating to whole-cell active compounds. A brief comparison of these approaches has been presented in **Table 14** (154, 155).

This certainly raises the question of what is the best method of drug development, in our case, for Mtb. Drugs discovered through phenotypic drug discovery are far more likely to result in clinical leads than those discovered through target-based approaches for TB treatment (156). This certainly could be because target-based drug systems focus on one target, while biological systems are much more complex and the action of compounds could be more complex than just targeting one gene/enzyme. Does this mean target-based drug discovery is futile? Certainly not. The methods used in target-based approaches provide invaluable insights into the molecular targets which can also be helpful in phenotypic screening (26, 157). For instance, the understanding gained from CRISPRi studies of genes can enhance our knowledge of gene function and

regulation, thereby informing and improving both target-based and phenotypic drug discovery efforts (158). Moreover, even though the use of target-based screening has increased over the years, it is still not as widely used compared to phenotypic screening (156).

Table 14: Comparison between the drug testing approaches: Phenotypic Drug Screening and Target-Based Drug Development.

	Phenotypic Drug Screening	Target-Based Drug Development
Pros	• No need for prior knowledge of the target. • Can identify novel mechanisms of action. • Higher potential for finding broad-spectrum therapies. • Can potentially discover compounds that overcome resistance.	• Focused approach using known targets. • Can be more time-efficient through targeted screening assays. • Facilitates understanding of drug mechanism of action. • Allows for the design of drugs to avoid known resistance mechanisms.
Cons	• Complex screening process and resource intensive due to live culture handling. • Additional work is required to identify the mechanism and target. • Hit validation can be lengthy and complicated.	• Requires detailed understanding of target and disease pathology. • May miss out on novel targets and mechanisms. • Potential development of drug resistance if the target mutates.

In conclusion, the most effective approach for drug development could be to combine both methods, finding a balance that maximizes their strengths. For example, performing phenotypic screening of a compound library and then discovering the targets using bioinformatics tools, followed by target-based testing and validation (154, 159). Ultimately, the success of either approach depends on the quality of the drug target, including its essentiality and vulnerability (124).

5.2 Fate of the compounds

In both approaches used for drug testing in this study, a total of 234 compounds were tested, among which 24 compounds showed activity with MIC90 values equal to or below 8uM. Each class of these active compounds needs further evaluation to determine their potential for advancing to the next stages of TB drug discovery. The other compounds tested in this study exhibited limited or no activity against Mtb.

Compounds screened phenotypically

Batch A compounds were tested against Mtb H37Rv mCherry10, and one compound, AK-105/40694114, with a moderate SI of 8, was found to be active intracellularly against Mtb H37Rv with an MIC90 of 8uM

(section 4.1.1.1). Identifying the target of this compound was the next step. To achieve this, a literature review of the compound's structure was conducted, and compounds with similar structures were identified using bioinformatic tools: PubChem (https://pubchem.ncbi.nlm.nih.gov/) and CAS SciFinder (https://www.cas.org/solutions/cas-scifinder-discovery-platform/cas-scifinder-n). A thorough structure similarity search was performed for AK-105/40694114 and was found that the compound might be a novel Dihydrofolate Reductase (DHFR) inhibitor. This compound is an analogue of the drug Methotrexate which is used in certain cancer chemotherapies (160). In this way, the target DHFR is not unique to Mtb but is also present in humans, which could result in a drug with significant undesired side effects. Consequently, this may limit the compound's therapeutic window. Nevertheless, DHFR inhibitors have been successful to inhibit other pathogens and for Mtb (161, 162) and still remains an interesting target in drug discovery. The likelihood of obtaining a patent for AK-105/40694114 compound was low due to its similarity with drug methotrexate, leading to a retraction of further interest in its development. Nonetheless, AK-105/40694114 remains valuable for research purposes and for validating DHFR as a potential target.

Another compound, Mepanti0062, was found to be active with an MIC90 of 8uM against Mtb. However, its intracellular activity was >16uM (section 4.1.1.1, Figure 15), and therefore, further target identification studies were not pursued for this compound. However, chemical modification of these compounds to improve potency can always be an option. Further work will be needed to develop these compounds.

Compounds from Target-based drug discovery

The compounds tested in this study predominantly originated from target-based drug discovery approaches, having been developed for pre-selected ideal targets present in Mtb. Notably, compounds targeting *inhA* (INH-Terpenoid conjugates) (section 4.1.2.2) demonstrated significant activity at single-digit uM concentrations (MIC90) in broth and intracellular assays. These were the most potent compounds identified in this doctoral study.

The targets of these compounds were validated by testing them against INH-monoresistant clinical isolates (harbouring resistance-determining SNPs in either the *katG* or *inhA* genes) where they exhibited a cross-resistance pattern similar to INH. Additionally, these compounds were assessed for their anti-inflammatory activity by measuring cytokine levels of Tumor necrosis factor alpha (TNF-α) and Interleukin 6 (IL-6) at HIPS, Saarbrücken (**Supplementary Figure 4**). TNF-α and IL-6 are cytokines known to recruit immune cells and maintain the granuloma structure to suppress TB dissemination (163, 164). However, this can also result in excessive inflammatory immune responses and lung tissue damage (165). Controlling this excessive inflammation with antibiotics can help reduce lung damage. Furthermore, studies have shown that anti-inflammatory activities during TB infection can increase susceptibility to first-line Mtb drugs in mouse and rabbit models (166-168). Hence, the INH-terpenoid conjugates used in this study were tested and found to be anti-inflammatory, reducing the levels of TNF-α and IL-6 *in vitro*. The combination of antimicrobial and anti-inflammatory properties makes these compounds promising candidates for further testing in mouse models for their activity against *in vivo* TB infection.

The MEP pathway compounds explored in this study were active against Mtb *in vitro* at atleast 8uM (section 4.1.2.3). However, they were found to be cytotoxic against HMdM. These compounds were synthesized to target the Dxs and Dxr enzymes of the MEP pathway in Mtb. Although these compounds are not sufficiently potent (MIC90 higher than 8uM) to be pursued further for Mtb drug development, they represent the first compounds ever synthesized against the MEP pathway enzymes in Mtb. Further medicinal chemistry approaches and testing are required to enhance their activity and reduce cytotoxicity. Despite their high MIC90 (>8uM), these compounds can be valuable for target validation studies and can serve as positive controls for further research. Thus, while these compounds are currently cytotoxic, they serve as an initial scaffold for future drug development studies against the MEP pathway in Mtb.

In summary, this doctoral thesis explored multiple pathways for target-based drug discovery. INH-terpenoid derivatives were found to be active intracellularly without cytotoxicity and demonstrated anti-inflammatory properties. These compounds have been selected for further testing in animal models. Additionally, MEP pathway compounds demonstrated MIC90 values >8uM against Mtb in broth and require further modifications to improve their activity and reduce cytotoxicity.

5.3 Challenges in drug testing against Mtb

Compounds tested in this study were found to have MIC90s >8uM against Mtb in broth. These compounds need further chemical modifications to improve their activity and cytotoxicity. However, these compounds have to face multiple challenges to target Mtb and inhibit the bacteria efficiently which are the plausible reasons why these compounds fail to show activity. Some of these challenges are discussed below.

Challenges by Mtb

Mtb, unlike other bacteria, has a very thick and complex cell wall (169) **(Figure 38).** This consists of an initial peptidoglycan layer covalently attached to an overlaying branched polysaccharide structure known as arabinogalactan. The arabinogalactan layer is further covalently attached to a network of long-chain hydrophobic mycolic acids, which limits the entry of hydrophilic compounds (169). Studies have shown that deletion of genes or operons contributing to cell wall formation in Mtb can lead to increased sensitivity to anti-Tb drugs including RIF and INH (170, 171). This proves that the cell wall of Mtb is a significant obstacle to intracellular drug accumulation. Therefore, if the molecular target of a compound resides in the cell cytoplasm, the compound has to cross the entire cell wall barrier to reach the target. In the case of the compounds tested in the current study, in particular the ATCase inhibitors (section 4.1.2.1) and MEP pathway inhibitors (section 4.1.2.3), the relevant target enzymes are present in the cytoplasm of the bacteria. This means the compounds have to cross the thick cell wall barrier of Mtb to reach the target. This challenge can be one plausible explanation for the low phenotypic activity of these compounds. Even if the compounds are chemically equipped to cross the cell wall, Mtb has efflux pumps that can extrude them back into the extracellular environment (172-174). Compared to other bacteria, Mtb has a larger

contingency of efflux pumps (175) at its disposal, complicating drug discovery efforts further. A combination of these novel compounds with anti-TB drugs known to target the cell wall of Mtb, such as EMB or INH (176), maybe a good strategy to proceed further with these compounds. Further studies to evaluate the potential synergy between these compounds and existing anti-TB drugs may facilitate their development and enhance their efficacy.

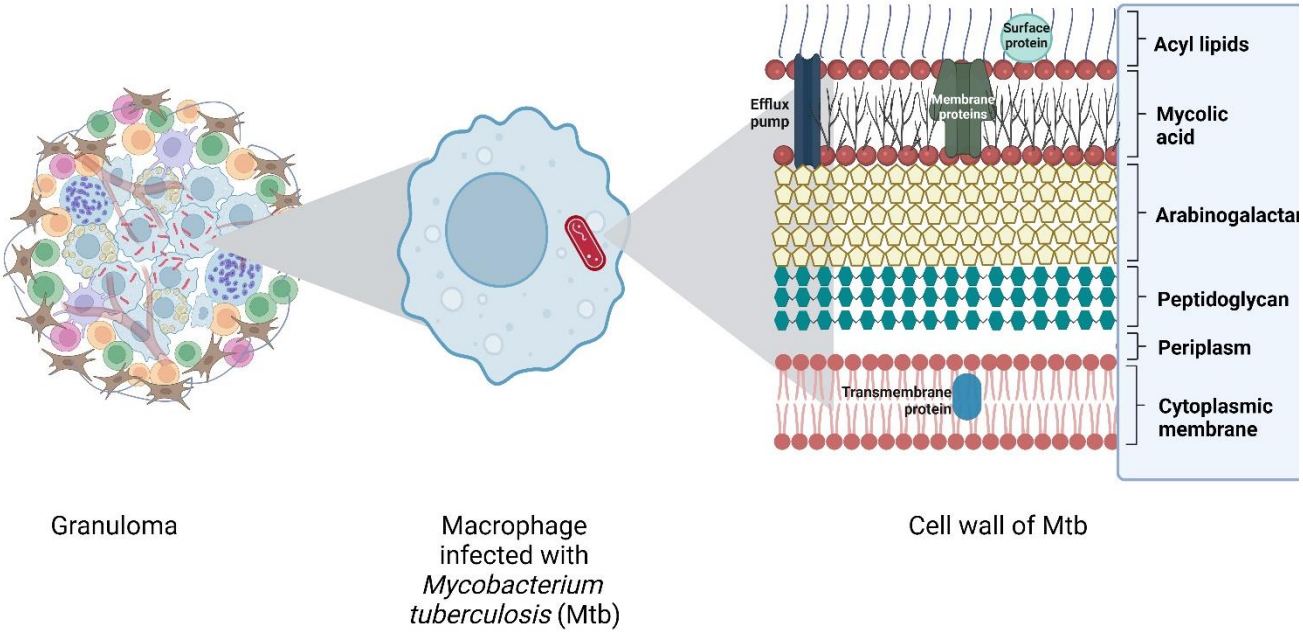

Figure 38: Illustration of multiple challenges faced by a compound to inhibit *Mycobacterium tuberculosis*. The granuloma in the lungs (detailed in Figure 1) is the first challenge, where immune cells aggregate around infected macrophages. The compound must then cross the macrophage membrane to reach Mtb. Once inside, it must overcome the complex cell wall of Mtb, which contains efflux pumps and long-chain hydrophobic mycolic acids.

Some of the compounds used in this study, such as the BDA-06 inhibitor targeting the Mtb ATCase enzyme (section 4.1.2.1) and the INH-terpenoid compounds (section 4.1.2.2), showed low single-digit MIC90 activities against Mtb, meaning they were able to circumvent the cell wall challenges of Mtb. As the terpenoid compounds are derivates of INH itself, the mechanism of uptake of terpenoids could be similar to INH which has been described as passive diffusion through the cell membrane (81), however further studies are needed to confirm this. Another mechanism studied for compounds to render success in transporting inside Mtb is the presence of proline-glutamate/proline-proline-glutamate (PE/PPE) proteins (177). The PE/PPE protein class have been shown to act as solute transporters through the outer cell membrane, in particular, to allow molecules to pass the highly hydrophobic outer lipid layer (177).

If the compounds are successfully transported inside the cell, the next challenge they have to face is the physiological conditions inside the bacteria before inhibiting its target protein. The bacterial cell is complex and physiological conditions such as pH and oxygen concentration are not always taken into consideration when synthesizing these compounds (178). These conditions can change depending on whether the bacteria are replicating (aerobic conditions) or non-replicating (such as under anaerobic conditions). Hence sustaining these harsh environments and still targeting and inhibiting the target protein is the next challenge

for these compounds. This can make the compound lose its activity and not inhibit the target at a lower concentration (178).

Challenges in macrophages

The inhibitors that overcome the challenges proposed by Mtb itself, and can access and inhibit their target protein, are then selected to test their activity against Mtb residing within macrophages. As macrophages are the primary niche of Mtb, it is crucial to understand if these compounds can cross the macrophage barrier and still inhibit the Mtb residing inside it (179). In this process, it is very important to test if these inhibitors are not toxic for the macrophages themselves. Hence multiple compounds tested in this study, especially against the MEP pathway, need further modifications to improve this balance between activity and cytotoxicity. Once a compound successfully achieves the balance of activity and safety and can penetrate macrophages, it must then contend with the physiological environment within the macrophages themselves (180, 181). Macrophages are complex cells that expose Mtb to multiple stress factors such as low pH, nitrosative stress, oxidative stress, osmotic changes, carbohydrate limitation, and cell envelope damage (182-186). Additionally, the environment within granulomas contributes to this stress, presenting challenges such as hypoxia (187) and host factors that sequester iron (184) or contain enzymes producing reactive oxygen species (ROS) (188). Despite these harsh conditions, Mtb survives by making significant transcriptional, proteomic, and metabolic changes. These changes, along with the host environmental conditions, may cause the iMIC90 of drugs to shift compared to testing against Mtb in broth. An illustration of plausible challenges faced by the compound in TB drug discovery is presented in Figure 38.

One of the compounds tested in this study, Mepanti0062 (section 4.1.1.2), showed a MIC90 of 4uM against Mtb in broth. However, the iMIC90 of this compound shifted more than 4-fold (from 4uM to >16uM). This suggests that while the compound can overcome challenges within the bacterium, it struggles with the additional complexities presented by the macrophage environment. Another possible reason could be that the drug's target is not as vulnerable in the host environment as it is in broth.

In contrast, the terpenoid derivatives showed consistent MIC90 values in both broth and intracellular environments (section 4.1.2.2), indicating their ability to effectively function within macrophages. Studies have correlated the similarity of MIC90 values in broth and macrophage models to the tissue penetration capacity of anti-TB drugs. For instance, drugs that effectively penetrate tissues, such as clarithromycin, display similar MIC90 values in both these settings (179, 189, 190). In line with this finding, terpenoid derivatives were evaluated for their human tissue penetration capacity using Franz cell permeability assay using Caco cells at HIPS, and they were found to be effective at penetrating human skin (with a high value of P_{app} 20 × 10^{-6} cm/s). Consequently, in addition to their anti-TB and anti-inflammatory activities, terpenoid derivatives demonstrate successful tissue penetration, making them promising candidates also for treating TB skin lesions.

Technical challenges

In addition to the biological challenges faced in drug discovery against Mtb, technical challenges also play a significant role in the development of these compounds. To test these compounds against Mtb, the lab strain Mtb H37Rv mCherry10 was used. This strain contains a plasmid encoding a constitutively expressed fluorescent protein that facilitates bacterial quantification by measuring fluorescence. This assay provides a rapid and non-invasive detection method of MICs, with a robust signal-to-noise ratio. However, Mtb's tendency to clump in growth media often results in large standard deviations or shifts in MIC90 values (section 4.1). Additionally, dead bacteria in the culture may retain active fluorescent proteins, which may impact MIC90 determination.

One way employed in this study to improve experimental confidence and independently validate MIC values of a given compound was the use of the Alamar blue assay for the assessment of bacterial growth. This is a resazurin dye-based assay where the substrate, added to the cells at a specific end time point, changes its colour from blue (non-fluorescent) to pink (fluorescent) in the presence of live bacteria by undergoing a Redox reaction. (191) Consequently, measuring the fluorescence of this dye also allows for quantification of bacterial viability in the presence of test compounds. However, using the Alamar blue assay also has limitations that can affect the results. Factors such as inoculum size, temperature variations, evaporation, compound precipitation, and a poor signal-to-noise ratio have been studied to influence the assay's accuracy and reliability (27). Moreover, Resazurin is dependent on the activity of cellular dehydrogenases and oxidoreductases. It has been shown that compounds that inhibit the cytochrome bc1 complex in Mtb can inhibit resazurin reduction at lower concentrations as compared to growth inhibition leading to incorrect MIC90 (192). Nevertheless, in the present study, the Alamar blue assay was found to produce reliable results.

Consequently, for the compounds addressed in this study, the different testing methods may result in slight differences in the MIC90 of the compounds. Since the shift observed was minor (approx. one dilution) this was not considered to be a major issue.

Compounds that were active against Mtb and non-cytotoxic to HMdM were tested against infected HMdM to assess their ability to cross the macrophage membrane and inhibit intracellular bacteria. Compounds detailed in the results section of the study (e.g., Mepanti0062 and AK-105/40694114) were tested in three independent assays. High standard deviations were observed in these assays, particularly for the bacterial growth control over seven days. A plausible reason for the high standard deviation could be the high donor variability in HMdM, as macrophages used in these studies are obtained from human donors to replicate the actual *in vivo* system. This donor variability suggests that macrophages respond differently to Mtb infection, adding another layer of technical challenge.

Collectively, this doctoral study successfully established a compound testing system for *in vitro* drug development against Mtb. Challenges such as variation in Mtb strains, testing methods, and donor variability in macrophages were addressed and considered as variables worth investigating and optimizing when setting up a robust pipeline.

5.4 Strategies and challenges of Conditional mutants

In an attempt to discover new drugs for TB treatment, a biological target validation of novel compounds with anti-TB activity in Mtb is crucial. For this, conditional mutants of the essential genes were generated. The conditional mutant system is based on the well-characterized phenomenon that a reduction in the expression of an essential gene should increase the sensitivity of a compound that acts on the target. In this way, the genetic knockdown of the protein is used as a surrogate for chemical inhibition of the protein. However, it is crucial to note that genetic inhibition and chemical inhibition can have significantly different effects (193). For example, the kinetics of chemical inhibition are significantly faster than gene silencing (194). Moreover, genetic modifications may impact the fitness of Mtb which may not reflect the actual effects of chemical inhibition of the same target. Hence, even specific regulated gene repression using genetic methods may not always mimic the phenotypic consequences of chemical inhibition of the same target enzyme. However, multiple studies have proven that this limitation is not always a hindrance in the successful validation of drug targets of novel compounds (128, 129, 195).

In this doctoral study, we aimed to generate conditional knockdown mutants of MEP pathway enzymes Dxs and Dxr in an attempt to validate the targets of newly synthesized novel compounds. Dxs and Dxr were chosen since these enzymes have previously been well characterised and the research for synthesizing novel compounds against these two enzymes was ahead of other enzymes of the pathway. Before generating any conditional mutants, we checked if these genes were in a functional operon. If they were in an operon then the gene manipulation would possibly also affect the downstream genes in the operon. This was checked using multiple online genetic databases, namely: TB Genome Annotation Portal, BioCyc and Mycobrowser. *dxs1* was notably not in an operon. However, in the case of *dxr*, two other genes were seen to be immediately downstream, which made *dxr* appear to be in an operon. A study from 2011 (112) concluded the presence of *dxr* in an operon with the neighbouring genes (*rip* and *gcpE*) however they failed to find the transcriptional start site which was located at the end of *dxr* gene and the beginning of the *rip* gene (ripp, ripp2) **(Figure 39)**. This transcriptional start site was found by a study in 2015 (147) which suggests that the transcription of the neighbouring genes does not depend on the *dxr* promoter**.** Hence *dxr* was assumed to not be present in a functional operon and the modifications happening to the *dxr* promoter should likely not affect the transcription of the neighbouring genes.

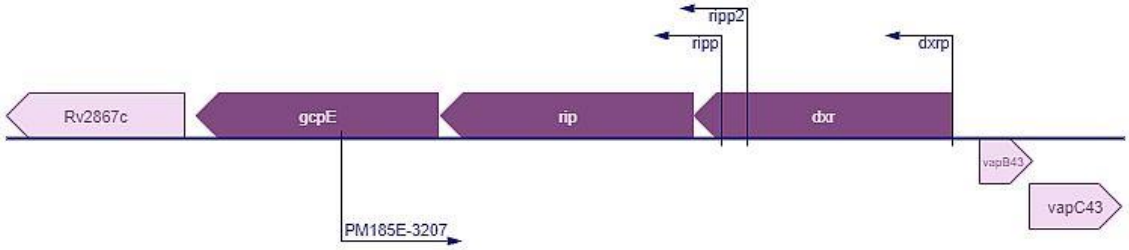

Figure 39 The location of the *dxr* gene in the Mtb genome. Based on S. Shell et. al 2015 (147). *dxr* appears to be in an operon with the neighbouring genes *rip* and *gcpE*. However, the transcriptional start site ripp2 and rip regulates the transcription of *rip* and *gcpE* genes. This suggests that *dxr* is not in a functional operon. Picture source: BioCyc (https://biocyc.org/)

5.4.1 Promoter Replacement Mutants

In this doctoral thesis, the initial approach to generating conditional mutants was through promoter replacement. This method has been successfully utilized for various genes in Mtb (129, 196, 197). The Tet ON and Tet OFF systems have been established both *in vitro* and within macrophages (195, 197), and the Tet OFF system has been effectively employed in animal models (198).

Given that *dxs1* and *dxr* are known to be essential (112), we chose to construct both Tet ON and Tet OFF mutants for these genes (section 4.2.1.1). Before introducing the regulatory proteins (TetR and revTetR), SCO strains were generated by replacing the native gene promoter with a tetO-containing pmyc1tetO promoter via single homologous recombination. Successfully achieving this recombination is a significant challenge in generating SCO mutants. To assess the success of recombination and ensure proper alignment and orientation of the plasmid, Southern blotting and NGS using the Illumina sequencer were performed (section 4.2.1.2) on isolated mutants. For the SCO Dxs mutant, NGS sequencing showed 100% alignment. However, this was not the case for the SCO Dxr mutant. One limitation of using Illumina sequencing is that, although it produces long genomic reads, these are not continuous and contain breaks in the sequencing data. Unfortunately, a part of the Dxr mutant sequence was lost in these breaks between the two contigs (**Supplementary Table 4**). Nonetheless, the region of interest, including tetO and the *dxr* gene sequence was intact, and successful alignment of this region was observed, concluding the success of NGS.

After successfully constructing and confirming these mutants, they were exposed to Atc, and no phenotypic changes were observed in either Tet OFF or Tet ON mutants for both genes. This suggests that the *dxs1* and *dxr* genes may not be essential for the growth of Mtb in the experimental setup used. However, this contradicts previous studies that identified *dxs1* and *dxr* as *in vitro* essential (112) and highly vulnerable (VI scores -11.29 and -7.04 respectively) (72). The reason for the failure of this approach remains unknown. Since no dependency on Atc was observed, it is likely that the regulatory proteins (TetR and revTetR) are not

binding to the tetO region. This could be due to the instability of these regulatory proteins in the bacterial environment or the loss of the plasmids producing them. Another plausible reason could be that the tetO-containing promoter region is inactive and the native promoter is still functioning to transcribe these genes. When constructing the plasmid (pSE100), a ribosomal binding site of 14 and 19 bp for *dxs1* and *dxr* genes, respectively, was maintained before the start of the genes. According to previous studies, this was sufficient for the binding of Atc and regulatory proteins (123). However, this requirement is highly gene-dependent and may not be suitable for the *dxs1* and *dxr* genes rendering the tetO to be inactive (199). Nonetheless, these are plausible explanations for the system's failure, and other technical reasons may also contribute to the ineffectiveness of these systems.

However, it is known that this approach may not uniformly affect all essential genes, and its efficacy is difficult to predict beforehand (73). This variability depends on multiple factors, a significant one being the difference in vulnerability of the target gene to genetic modification.

In conclusion, the promoter replacement mutants were generated for *dxs1* and *dxr* using both Tet ON and Tet OFF systems, however, the Atc-dependent gene regulation was not observed in these mutants.

5.4.2 CRISPRi mutants for target validation of novel compounds

Only recently has the technology of CRISPRi been developed for generating conditional mutants in Mtb. Thus, to overcome the limitations of promoter replacement mutants and generate conditional mutants of *dxs1* and *dxr*, the CRISPRi system was utilized. This system does not modify the gene at its native site, and its one-step cloning process makes it both easier and more time-efficient. Using this technique, gene knockdown mutants for *dxs1* and *dxr* were successfully generated and subjected to various Atc concentrations. Gene knockdown was confirmed through phenotypic assessment (OD600 and CFU), mRNA quantification, and protein quantification (section 4.2.2.2). These multiple experimental methods validated the successful gene repression with increasing Atc concentrations.

The product of the first reaction in the MEP pathway, catalysed by Dxs, is DXP, which is also a substrate in the thiamine production pathway in Mtb. The thiamine pathway is essential and recognized as a promising drug target (200, 201). This implies that CRISPRi knockdown of *dxs1* may impact thiamine biosynthesis similarly to its effect on isoprenoid synthesis. Consequently, the bacterial growth inhibition observed from *dxs1* knockdown could be attributed to the depletion of both isoprenoids and thiamine. However, further studies are necessary to confirm this.

Escape mutants:

During extended growth of Mtb CRISPRi mutants in the presence of Atc in broth (*in vitro*) (section 4.2.2.2, Figure 29) and within macrophages (4.2.2.3, Figure 33), regrowth of mutants was observed for all studied genes. When this regrowth was re-cultured in growth media, a loss of Atc dependency was observed

phenotypically (Figure 30). This regrowth was suspected to be due to mutations occurring in the bacteria making them escape from the CRISPRi regulation. These “escape” mutants have been previously observed with CRSIPRi and promoter replacement methods (73, 125, 133). Studies found that these mutants emerge mainly due to the loss of the integrated plasmid but also due to mutations in the region coding for the regulatory proteins as a consequence of the pressure Mtb is under due to the knockdown of its essential genes. Further sequencing of these escape mutants will confirm the accurate reasoning behind its loss of CRISPRi regulation.

Gene interdependency:

mRNA quantification of the *dxs1* and *dxr* genes successfully validated the gene knockdown in the CRISPRi mutants. During qPCR, an interdependency between the *dxs1* and *dxr* genes was observed. When the *dxs1* gene was downregulated, the *dxr* gene in the same mutant was slightly upregulated, and vice versa. This interdependency has not been observed before in literature but is suspected to be due to a feedback loop present between the two enzymes. Further work is necessary to confirm this interdependency and its consequences on the MEP pathway.

Target validation of novel compounds:

After successfully generating the CRISPRi mutants, targeting of the regulated proteins by the investigational compounds was assessed by testing them against the CRISPRi mutants in the presence of Atc (Section 4.2.2.4). Three different concentrations of Atc were used, which helped to accurately observe and quantify the fold shift in the susceptibility of the compounds relative to the Atc concentrations. The CRISPRi RpoB mutants showed a fold shift of >5 in the presence of Atc compared to no Atc. This shift is in line with previous studies whose targets were validated with CRISPRi (133), confirming the effectiveness of the positive control and the success of the CRISPRi system in target validation.

When the novel compound CC143 was then tested on the CRISPRi Dxr mutant, a similar >5-fold shift in the MIC90 was observed, suggesting Dxr as its target (Section 4.2.2.4). This compound is an analogue of fosmidomycin, which is a well-known drug targeting the Dxr enzyme in *Plasmodium falciparum*. While CC143 was found to be toxic to fibroblast cells, raising concerns that its activity against Mtb could be due to the release of reactive species or fragments rather than targeting Dxr, the >5-fold shift in MIC90 observed in our biological target validation system supports the idea that CC143 indeed targets the Dxr enzyme in Mtb.

Furthermore, whether Dxr is the sole target of this compound remains unknown. Further studies, comparing the metabolic profiles of the knockdown strain and the chemical inhibition of the Dxr enzyme, can help determine if Dxr is the sole target of the compound.

In conclusion, the results obtained in this doctoral study using CRISPRi support the notion that Dxr is the target of CC143. Despite the toxicity of CC143, this compound can be a useful tool for further research in drug discovery against enzymes of the Mtb MEP pathway and could potentially be used as a positive control in future target validation systems.

Another compound tested against the CRISPRi Dxs mutants was HIPS768, which did not show any substantial fold shift in the MIC90 in the presence or absence of Atc (Section 4.2.2.4). This compound was developed as part of a target-based drug discovery effort using virtual screening against the Dxs enzyme of Mtb. The lack of an MIC shift suggests that the compound may not target the Dxs enzyme of Mtb. However, there might be other reasons why a shift in susceptibility was not observed. Firstly, the compound could have multiple targets, with Dxs being only one of them, thus resulting in no change in the MIC90. Secondly, the chemical inhibition of some compounds can be more efficient than the genetic inhibition of the target gene. Hence, the compound might act faster than the CRISPRi knockdown can be initiated in Mtb (193). For example, in the target validation of trimethoprim as an inhibitor of DHFR, upregulation of DHFR validated trimethoprim as its drug target in *M. smegmatis* (193). However, the downregulation of DHFR did not show increased susceptibility. A comparison of the metabolomic profiles of the genetic knockdown and chemical inhibition of DHFR revealed similar results, confirming that trimethoprim was the sole target of DHFR. Therefore, the inability to observe a shift in the MIC90 using knockdown strains was discussed to be due to the drug clearing the protein more efficiently than the genetic modification would (193). However, compound HIPS768 is active against Mtb at a high MIC90 of 64uM, hence the chances of the compound to have more efficient chemical inhibition than genetic inhibition is low. Nonetheless, further testing of the compound against an overexpressing Dxs mutant will help confirm if Dxs is the target of the compound.

Intracellular essentiality of the genes:

After successfully generating the CRISPRi mutants and validating the targets of novel compounds, the next step was to employ the CRISPRi tool intracellularly using HMdM. In the presence of Atc, the CRISPRi system was activated inside the macrophages, repressing gene transcription and leading to bacterial growth inhibition (section 4.2.2.4). This suggests that Atc can cross eukaryotic membranes and still activate the system in Mtb. This finding is consistent with published data where CRISPRi was activated in macrophages (133). Moreover, it suggests that the genes *dxs1* and *dxr* are essential even inside macrophages. While the essentiality of Mtb genes *dxs1* and *dxr* has been studied *in vitro*, their role in the intracellular macrophage environment has not been previously explored. Previous studies have indicated that genes that are essential in broth cultures may not always be vulnerable in the host environment as they might circumvent their essentiality by utilizing host metabolites (202). Thus, the finding in the present study suggests that Mtb cannot compensate for the loss of the MEP pathway even intracellularly. Further work to determine the essentiality of these genes in animal models would be necessary to evaluate their essentiality in living host conditions.

Limitations of CRISPRi:

CRISPRi is a promising tool for gene regulation and compound target validation studies. However, it has a few limitations. One of the limitations of the CRISPR system is the bad-seed effect. For the CRISPR system to work, the sgRNA of minimum 12bp is needed (131, 203) However, the first 7 nucleotides are crucial in the binding to the target DNA hence referred to as a 'seed' region. Any mutations in the first 7 nucleotides will likely result in lower efficiency of the CRISPR system irrespective of the rest of the sgRNA sequence. This effect is referred to as a bad-seed effect and is one of the limitations of the CRISPR system. Another limitation of the CRISPR system is that the Cas9 protein has been shown to have off-target effects, meaning it can bind to other unrelated genes and stop the transcription of these genes. These off-target effects are mostly seen to be sgRNA dependent (204-206) where the seed sequence of as little as 7 nucleotides can bind to off-target genes. However, some studies have also shown that these off-target effects can also be sgRNA independent (207, 208) and further research to understand this is needed. In the present study, the CRISPRi mutants were not checked for off-target effects however, further *in silico* studies can be used to study this effect for the mutants generated (209).

In summary, this doctoral study successfully established the CRISPRi system for the first two essential genes of the MEP pathway in Mtb (*dxs1*, *dxr*). Furthermore, this system was effectively able to validate the target of a novel compound CC143 as the Dxr enzyme. Hence, the system is successfully set up and applied for target validation within the context of this study. This system can be further used to test more compounds and is a strong tool for the target validation of compounds in Mtb drug development.

5.5 Conclusion

This doctoral thesis focuses on the *in vitro* drug development of Mtb, establishing a robust testing process and evaluating novel compounds for their activity and toxicity against Mtb. Several compounds demonstrated promising single-digit MIC90 values, though many were either cytotoxic or inactive intracellularly. Hence this indicates the need for further optimization of these compounds. Notably, compounds from the INH-terpenoid class showed potent intracellular activity and are candidates for subsequent animal model testing.

A significant achievement of this study was the successful implementation of a system to validate the targets of MEP pathway compounds, specifically the *dxs1* and *dxr* genes, using CRISPRi mutants. These mutants were successfully confirmed for their Atc-dependent gene knockdown. Consequently, the target of RIF as *rpoB* was validated using a CRISPRi RpoB mutant. Using the CRISPRi Dxr mutant, the target of the novel compound CC143 was successfully validated as the Dxr enzyme of the MEP pathway. Furthermore, the essentiality of the genes *dxs1* and *dxr* was confirmed intracellularly using HMdM, underscoring the effectiveness of the CRISPRi system to function both in broth and intracellularly.

Hence, this study highlights the potential of CRISPRi as a powerful tool for TB drug discovery, enabling rapid validation of compound targets and essential gene studies. This system can be expanded to identify targets for other MEP pathway compounds and to generate more CRISPRi mutants against essential Mtb genes, thereby accelerating the drug discovery process.

In summary, this doctoral thesis has established a solid base for *in vitro* drug testing and target validation of compounds targeting the MEP pathway in Mtb, providing valuable insights and tools for future research and development in TB drug discovery.

Summary

Tuberculosis (TB), caused by *Mycobacterium tuberculosis* (Mtb), remains a significant global health threat. Despite being a curable disease, the rise of drug-resistant strains has rendered many current antibiotics ineffective, necessitating the urgent development of new drugs that can shorten the TB treatment regimen and produce fewer unwanted side effects. This doctoral study aimed to discover novel anti-tubercular compounds through either phenotypic or target-based screening. A panel of *in vitro* assays for testing novel compounds was established, including phenotypic activity tests against Mtb in broth media (MIC90), cytotoxicity tests against human monocyte-derived macrophages (HMdM), growth inhibition assays against Mtb residing intracellularly within HMdM, and whole cell drug target/validation assays using specialized genetically modified strains of Mtb. A total of 234 compounds were tested using this workflow, 24 of which demonstrated MIC90 values of 8uM or lower against broth-grown Mtb H37Rv. Among these, compounds AK-105/40694114, Mepanti0062, and BDA-06 (MIC90s of 4uM, 4uM, and 8uM, respectively), were progressed further for testing against intracellular Mtb. Amongst these, AK-105/40694114 was found active intracellularly with the lowest MIC90 (iMIC90) of 8uM. Of particular interest was a class of INH-terpenoid conjugates, which showed potent activity against Mtb at MIC90 values below 1uM, similar to the MIC90 of INH (0.44uM). These compounds were also active intracellularly, with the most potent one displaying an iMIC90 value of 0.5uM. Their mode of action was shown to most likely be the same as INH, as they were inactive against INH-monoresistant Mtb clinical isolates (harbouring resistance-determining SNPs in either the *inhA* or *katG* gene). Three compounds amongst the one hundred thirty-five compounds, potentially targeting the MEP pathway, demonstrated MIC90 values lower than 16uM. Despite promising anti-tubercular activity, all of these compounds require further chemical modifications to improve potency and reduce cytotoxicity. To validate the targets of these compounds, the study aimed to generate conditional transcriptional-knockdown mutants of essential *M. tuberculosis* genes, since chemically inducible control of gene expression is a well-established and powerful tool for identifying and studying gene functions and cellular processes. In the context of drug discovery, a reduction in the expression of an essential target gene should be linked to an increase in sensitivity to a compound that acts on that particular target. CRISPR interference (CRISPRi), as a recently developed genetic method for highly specific silencing of target gene transcription in prokaryotic cells, has been successfully used in this study to generate *M. tuberculosis rpoB, dxs1* and *dxr* knockdown mutants. These mutants successfully demonstrated target gene downregulation in response to anhydrotetracycline (Atc; chemical inducer of expression of the CRISPRi components) media supplementation, as confirmed by growth curve (OD600, CFU), mRNA abundance, and protein abundance analyses. For target validation studies, an initial proof-of-concept experiment was undertaken using the CRISPRi RpoB mutant. When tested against Rifampicin, a bona fide molecular inhibitor of RpoB, a >5-fold shift in MIC90 in the presence of Atc compared to without Atc was observed, thereby successfully validating the CRISPRi system for drug target identification. Using the same approach, the target of the compound CC143 was validated as Dxr by observing a >5-fold shift in MIC90 when tested against the CRISPRi Dxr

mutant in the presence of Atc. Additionally, it was demonstrated that the CRISPRi system could be activated in Mtb residing intracellularly within HMdM, proving that Atc can cross eukaryotic membranes to activate CRISPRi and that the *dxs1* and *dxr* genes are essential for Mtb survival both *in vitro* and intracellularly. In summary, this doctoral study successfully established an *in vitro* compound testing system to rapidly identify novel compounds active against Mtb, along with establishing a CRISPRi-based system for whole-cell target validation of test compounds. Together, the results presented within have the potential to rapidly accelerate TB drug discovery.

Zusammenfassung

Die durch Mycobacterium tuberculosis (Mtb) verursachte Tuberkulose (TB) stellt nach wie vor eine erhebliche globale Gesundheitsbedrohung dar. Obwohl es sich um eine heilbare Krankheit handelt, hat die Zunahme arzneimittelresistenter Stämme viele der derzeitigen Antibiotika unwirksam gemacht, so dass dringend neue Medikamente entwickelt werden müssen, die die TB-Behandlung verkürzen und weniger unerwünschte Nebenwirkungen haben. Ziel dieser Doktorandenstudie war die Entdeckung neuartiger antituberkulöser Wirkstoffe durch phänotypisches oder zielgerichtetes Screening. Es wurde eine Reihe von In-vitro-Tests für neuartige Verbindungen entwickelt, darunter phänotypische Aktivitätstests gegen Mtb in Brühe (MIC90), Zytotoxizitätstests gegen aus menschlichen Monozyten gewonnene Makrophagen (HMdM), Wachstumshemmungstests gegen Mtb, die sich intrazellulär in HMdM befinden, und Ganzzell-Target-/Validierungstests unter Verwendung spezieller genetisch veränderter Mtb-Stämme. Mit diesem Arbeitsablauf wurden insgesamt 234 Verbindungen getestet, von denen 24 iMIC90-Werte von 8uM oder weniger gegen in Brühe gezüchtete Mtb H37Rv aufwiesen. Von diesen wurden die Verbindungen AK-105/40694114, Mepanti0062 und BDA-06 (MIC90-Werte von 4uM, 4uM bzw. 8uM) für weitere Tests gegen intrazelluläre Mtb ausgewählt. Von diesen erwies sich AK-105/40694114 als intrazellulär aktiv mit einer niedrigsten MHK90 von 8uM. Von besonderem Interesse war eine Klasse von INH-Terpenoid-Konjugaten, die eine starke Aktivität gegen Mtb bei MIC90-Werten unter 1uM zeigten, ähnlich der MIC90 von INH (0,44uM). Diese Verbindungen waren auch intrazellulär aktiv, wobei die stärkste Verbindung einen iMIC90-Wert von 0,5uM aufwies. Ihre Wirkungsweise ist höchstwahrscheinlich die gleiche wie die von INH, da sie gegen INH-monoresistente klinische Mtb-Isolate (mit resistenzbestimmenden SNPs im inhA- oder katG-Gen) inaktiv sind. Drei der einhundertfünfunddreißig Verbindungen, die möglicherweise auf den MEP-Stoffwechselweg abzielen, wiesen MIC90-Werte von weniger als 16uM auf. Trotz ihrer vielversprechenden antituberkulären Aktivität erfordern alle diese Verbindungen weitere chemische Modifikationen, um die Wirksamkeit zu verbessern und die Zytotoxizität zu verringern. Um die Angriffspunkte dieser Verbindungen zu validieren, zielte die Studie auf die Erzeugung von Mutanten mit bedingtem Transkriptions-Knockdown wesentlicher M. tuberculosis-Gene ab, da die chemisch induzierbare Kontrolle der Genexpression ein bewährtes und leistungsfähiges Instrument zur Identifizierung und Untersuchung von Genfunktionen und zellulären Prozessen ist. Im Zusammenhang mit der Entdeckung von Arzneimitteln sollte eine Verringerung der Expression eines wesentlichen Zielgens mit einer erhöhten Empfindlichkeit gegenüber einem Wirkstoff verbunden sein, der auf dieses spezielle Ziel wirkt. Die CRISPR-Interferenz (CRISPRi), eine kürzlich entwickelte genetische Methode zur hochspezifischen Unterdrückung der Transkription von Zielgenen in

prokaryontischen Zellen, wurde in dieser Studie erfolgreich eingesetzt, um M. tuberculosis *rpoB*-, *dxs1*- und *dxr*-Knockdown-Mutanten zu erzeugen. Diese Mutanten zeigten erfolgreich eine Herunterregulierung der Zielgene als Reaktion auf die Zugabe von Anhydrotetracyclin (Atc; chemischer Auslöser für die Expression der CRISPRi-Komponenten) in das Medium, was durch Wachstumskurven (OD600, KBE), Analysen der mRNA-Häufigkeit und der Proteinhäufigkeit bestätigt wurde. Für Studien zur Validierung des Targets wurde ein erstes Proof-of-Concept-Experiment mit der CRISPRi-RpoB-Mutante durchgeführt. Bei Tests mit Rifampicin, einem echten molekularen Inhibitor von RpoB, wurde eine >5-fache Verschiebung der MIC90 in Anwesenheit von Atc im Vergleich zu ohne Atc beobachtet, wodurch das CRISPRi-System erfolgreich für die Identifizierung von Arzneimittelzielen validiert wurde. Mit dem gleichen Ansatz wurde das Ziel der Verbindung CC143 als Dxr validiert, indem eine >5-fache Verschiebung der MIC90 beobachtet wurde, als sie gegen die CRISPRi-Dxr-Mutante in Anwesenheit von Atc getestet wurde. Darüber hinaus konnte gezeigt werden, dass das CRISPRi-System in Mtb aktiviert werden kann, die sich intrazellulär in HMdM aufhalten. Dies beweist, dass Atc eukaryotische Membranen überwinden kann, um CRISPRi zu aktivieren, und dass die *dxs1*- und *dxr*-Gene für das Überleben von Mtb sowohl *in vitro* als auch intrazellulär wesentlich sind. Zusammenfassend lässt sich sagen, dass im Rahmen dieser Doktorandenstudie erfolgreich ein In-vitro-Substanztestsystem zur raschen Identifizierung neuartiger, gegen Mtb wirksamer Substanzen sowie ein CRISPRi-basiertes System zur Validierung der Zielstrukturen von Testsubstanzen in ganzen Zellen entwickelt wurde. Zusammen haben die hier vorgestellten Ergebnisse das Potenzial, die Entdeckung von TB-Medikamenten zu beschleunigen.

Supplementary Data

Supplementary Table 1: List of Bacteria/Mtb mutants and plasmids used in this study.

Strains	Description
Mtb H37Rv (ATCC 27294)	Wild type Mtb
Mtb H37Rv mCherry10 (ATCC 27294)	Containing mCherry expressing pCherry10 plasmid
Mtb SCO-Dxs	H37Rv derivative in which expression of *dxs* is controlled by Pmyc1tetO
Mtb SCO-Dxr	H37Rv derivative in which expression of *dxr* is controlled by Pmyc1tetO
Mtb Tet OFF Dxs	SCO-Dxs containing pMC1s integrated at the L5 *attB* site
Mtb Tet OFF Dxr	SCO-Dxr containing pMC1s integrated at the L5 *attB* site
Mtb Tet ON Dxs	SCO-Dxs containing pTEK-4SOX integrated at the Tweety *attB* site
Mtb Tet ON Dxr	SCO-Dxr containing pTEK-4SOX integrated at the Tweety *attB* site
Mtb pLJR965:dxs1_sgRNA1	Knockdown of *dxs1* expression. KanR; single copy, L5-integrated
Mtb pLJR965:rpoB_sgRNA	CRISPRi positive control Mtb strain. KanR; single copy, L5-integrated
Mtb pLJR965:neg_sgRNA	CRISPRi negative control Mtb strain. KanR; single copy, L5-integrated
Mtb pLJR965:dxr_sgRNA2	Knockdown of *dxr* expression. KanR; single copy, L5-integrated

plasmid	Description	Reference
pCherry10	fluorescent protein containing plasmid, High copy	Lo et al., 2021 (210)
pDRIVE	*E.coli* shuttle vector containing MCS. Kan r	Qiagen plasmids
pSE100	*E.coli* -Mycobacterium shuttle vector carrying Pmyc1tetO; Hyg^r	(129) (Guo et al., 2007)

pTEK-4S-OX	*E.coli* -Mycobacterium shuttle vector harbouring psmyc-tetR r1.7; Kan^r	(129) (Guo et al., 2007)
pMC1s	L5-based integration vector harboring Psmyc-tetR; Kan^r	(129) (Guo et al., 2007)
pJR965	Sth1 dCas9 L5-Integration, attP for *Mtb* TetR and $Kan^{r,}$ multicopy, episomal plasmid	(124) (Rock et al., 2017)

Supplementary Table 2: List of Pyrazoles with activity against *Mycobacterium tuberculosis*.

Compounds	Minimum Inhibitory Concentration (MIC 90) (uM)	HepG2 Cytotoxicity Concentration (CC 50) (uM)	XTT assay Cytotoxic concentration (CC 90) (uM)	Pyrazole derivative	Activity against Mtb infected macrophages (iMIC90) (uM)
Mepanti0062	4	30.3	32	Guanadine	>16
Mepanti0065	8	>25	>32	Guanadine	n.d
Mepanti0057	8	>50	>32	Guanadine	n.d
Mepanti0058	8	>25	>32	Guanadine	n.d
Mepanti0070	32	>50	n.d	Guanadine	n.d
Mepanti0054	64	>50	n.d	Guanadine	n.d
Mepanti0067	64	>50	n.d	Guanadine	n.d
Mepanti0075	64	>50	n.d	Guanadine	n.d
Mepanti0056	8	n.d	n.d	Amines	n.d
Mepanti0069	16	n.d	n.d	Amines	n.d
Mepanti0071	16	>50	n.d	Amines	n.d
Mepanti0073	16	n.d	n.d	Amines	n.d
Mepanti0074	16	>50	n.d	Amines	n.d
Mepanti0027	16	5.9	n.d	Amines	n.d
Mepanti0029	32	9.2	n.d	Amines	n.d
Mepanti0028	32	8.4	n.d	Amines	n.d
Mepanti0079	32	7.2	n.d	Amines	n.d
Mepanti0068	32	>50	n.d	Amines	n.d
Mepanti0008	64	8.5	n.d	Amines	n.d
Mepanti0066	64	n.d	n.d	Amines	n.d
Mepanti0030	64	13	n.d	Amines	n.d
Mepanti0009	64	13	n.d	Amines	n.d

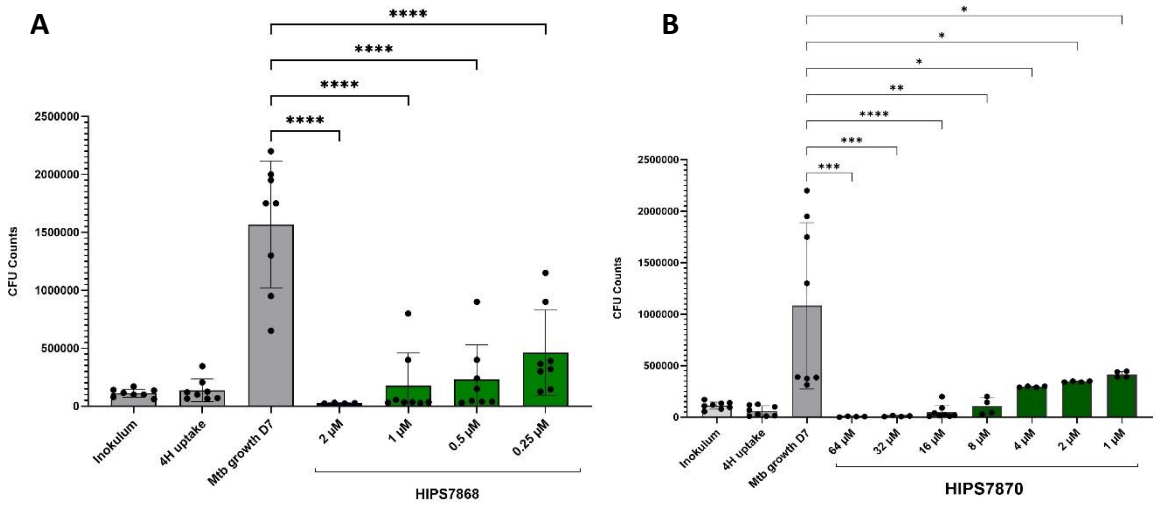

Supplementary Figure 1: Activity of Terpenoid derivatives against Mtb-infected macrophages. HMdM were infected with Mtb H37Rv at an MOI of 0.5:1 and treated with the compound at respective concentrations, washed at 4h post-infection followed by 7-day incubation. To determine bacterial survival, Colony Forming Units were counted. Three independent experiments, each consisting of two technical replicates, were performed and graphs were plotted using GraphPad Prism. Statistical analysis was performed using one-way ANOVA (n=3) for comparison to the 7d bacterial growth * = p≤0.05; ** = p≤0.01; ***= p≤0.001; ****= p≤0.0001. [A] Compound HIPS7868. [B] Compound HIPS7870

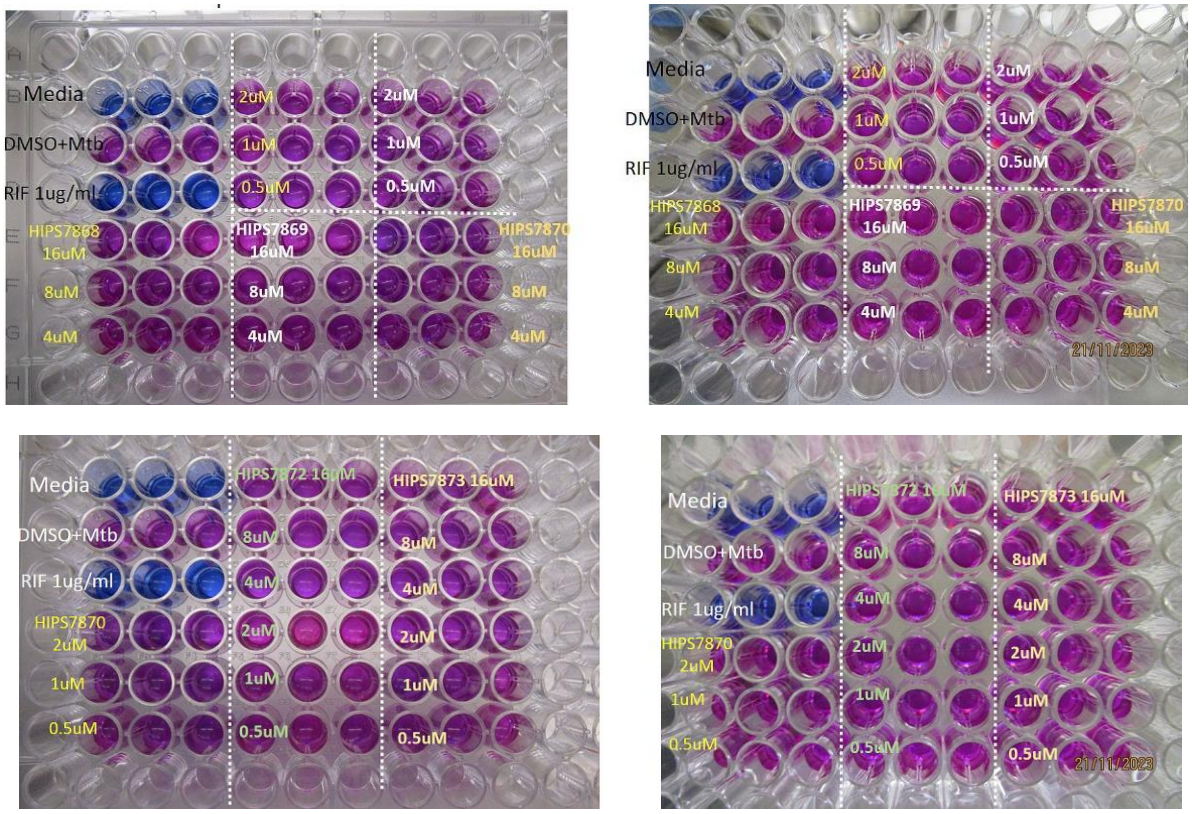

Supplementary Figure 2: Two independent Alamar blue assays for terpenoid derivates against KatG-resistant mutants. Compounds diluted in 7H9 + OADC growth media at the respective concentrations were added to a 96-well plate containing 2×10^5 CFU/ml *katG*-resistant clinical isolate of Mtb, followed by a 7-day incubation period. Resazurin was added on day 7 and incubated for a further 24 hours. Pictures were taken following incubation. The change in the colour of the resazurin dye from blue to pink indicates viable bacteria. Two independent experiments, each consisting of three technical replicates, were performed. The top two images show two independent experiments for compounds HIPS7868, HIPS7869, and HIPS7870 in dose-response concentrations. The bottom two images show two independent experiments for compounds HIPS7870, HIPS7872, and HIPS7873 in dose-response concentrations.

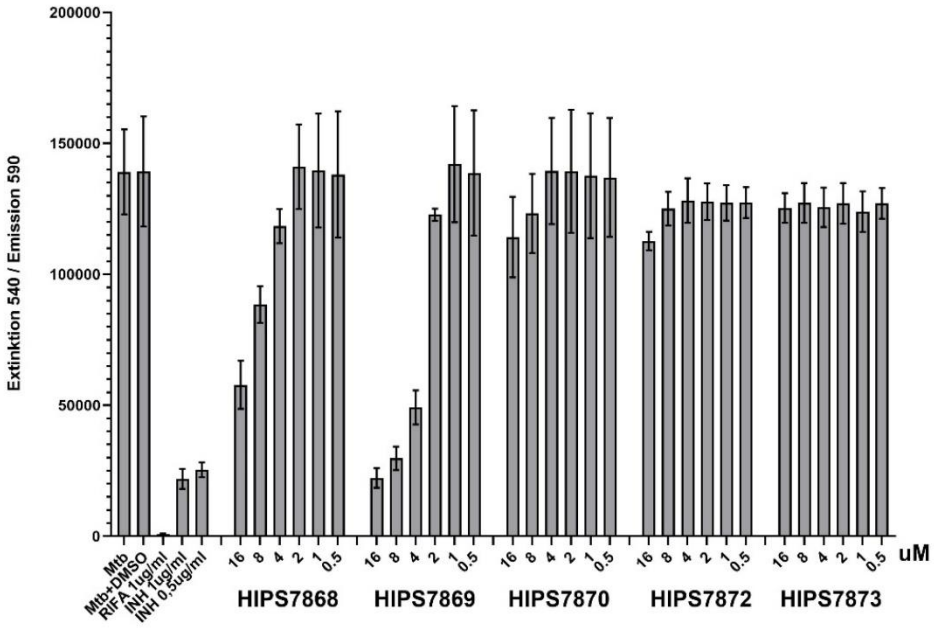

Supplementary Figure 3: Two independent Alamar blue assays for terpenoid derivates against *inhA*-resistant mutants. Compounds diluted in 7H9 + OADC growth media at the respective concentrations were added to a 96-well plate containing 2×10^5 CFU/ml *inhA* resistant clinical isolate of Mtb, followed by a 7-day incubation period. Resazurin was added on day 7 and incubated for a further 24 hours. Fluorescence was measured followed by incubation at Excitation 540 and emission 590. Two independent experiments, each consisting of three technical replicates, were performed and graphs were plotted using GraphPad Prism. 90% or more bacterial growth inhibition was marked as MIC90 concentration for the compounds.

Supplementary Table 3: List of all the compounds potentially targeting the MEP pathway.

Sr. no	Compounds	Solubility concentration in 7H9 media (uM)	Minimum Inhibitory Concentration (MIC 90) (uM)
1	HIPS768	n.d*	8
2	CC143	n.d	8
3	HIPS759	64	16
4	HIPS851	32	32
5	HIPS834	64	32
6	HIPS717	64	32
7	HIPS828	64	32
8	HIPS825	64	32
9	HIPS6344	64	32
10	HIPS7066	64	32
11	HIPS1329	64	32
12	ISPD_6642	64	32
13	ISPD_7450	64	32
14	ISPD_6843	32	32
15	HIPS5345	n.d	32

16	HIPS6074	64	64
17	HIPS7055	64	64
18	HIPS7065	64	64
19	HIPS7067	64	64
20	HIPS778	8	64
21	HIPS920	64	64
22	ISPD_6009	64	64
23	ISPD_6386	64	64
24	ISPD_7479	64	64
25	CC199	n.d	64
26	CC225	n.d	64
27	HIPS813	64	>64
28	HIPS827	8	>8
29	HIPS829	8	>8
30	HIPS824	8	>8
31	HIPS5240	16	>8
32	HIPS826	8	>8
33	HIPS830	64	>64
34	HIPS986	64	>64
35	HIPS588	64	>64
36	HIPS5059	8	>64
37	THQ02115	64	>64
38	HIPS861	8	>64
39	THQ02111	64	>64
40	THQ02113	64	>64
41	THQ02134	64	>64
42	HIPS701	64	>64
43	HIPS712	64	>64
44	THQ02120	64	>64
45	THQ02081	64	>64
46	THQ02123	64	>64
47	HIPS1346	32	>64
48	HIPS709	64	>64
49	HIPS5056	64	>64
50	HIPS70	64	>64
51	HIPS264	64	>64
52	HIPS17	16	>64
53	HIPS2258	64	>64
54	HIPS1532	16	>64
55	HIPS466	64	>64
56	HIPS5589	64	>64

57	HIPS5945	64	>64
58	HIPS5418	64	>64
59	HIPS5050	64	>64
60	THQ02146	64	>64
61	THQ02114	64	>64
62	THQ02108	64	>64
63	THQ02110	64	>64
64	THQ02099	64	>64
65	THQ02130	64	>64
66	THQ02069	64	>64
67	HIPS6560	64	>64
68	HIPS6978	64	>64
69	HIPS6897	64	>64
70	HIPS7116	64	>64
71	HIPS6920	64	>64
72	HIPS5846	64	>64
73	HIPS7058	64	>64
74	HIPS696	64	>64
75	HIPS697	64	>64
76	HIPS702	32	>64
77	HIPS700	64	>64
78	HIPS701	64	>64
79	HIPS706	16	>64
80	HIPS5934	64	>64
81	HIPS6888	64	>64
82	HIPS7293	64	>64
83	HIPS7295	64	>64
84	HIPS7449	64	>32
85	HIPS7451	16	>16
86	HIPS7453	32	>64
87	HIPS7480	64	>64
88	HIPS7481	32	>32
89	HIPS6074	n.d	>16
90	HIPS7067	n.d	>16
91	HIPS6888	n.d	>16
92	HIPS7481	n.d	>16
93	HIPS 6009	n.d	>16
94	HIPS6704	n.d	>16
95	HIPS7690	n.d	>16
96	HIPS7700	n.d	>16

97	HIPS709	n.d	>16
98	HIPS7482	n.d	>16
99	THQ03033	n.d	>16
100	THQ02114	n.d	>16
101	THQ02123	n.d	>16
102	THQ02099	n.d	>16
103	THQ02110	n.d	>16
104	THQ02111	n.d	>16
105	THQ02120	n.d	>16
106	THQ02113	n.d	>16
107	THQ03041	n.d	>16
108	THQ03046	n.d	>16
109	THQ02115	n.d	>16
110	THQ03044	n.d	>16
111	THQ03052	n.d	>16
112	THQ03058	n.d	>64
113	THQ03064	n.d	>64
114	THQ03065	n.d	>64
115	THQ03072	n.d	>64
116	THQ03073	n.d	>64
117	THQ04011	n.d	>64
118	THQ04014	n.d	>64
119	THQ04023	n.d	>64
120	CC319	n.d	>64
121	CC320	n.d	>64
122	THQ04057	n.d	>128
123	THQ04061	n.d	>128
124	THQ4023	n.d	>128
125	THQ4064	n.d	>128
126	HIPS5333	n.d	>64
127	HIPS5325	n.d	>64
128	HIPS5392	n.d	>64
129	HIPS5324	n.d	>64
130	HIPS821	n.d	Solubility issues
131	HIPS1952	n.d	Solubility issues
132	HIPS7078	n.d	Solubility issues
133	HIPS698	n.d	Solubility issues
134	HIPS708	n.d	Solubility issues
135	HIPS824	n.d	Solubility issues

*n.d: Not determined

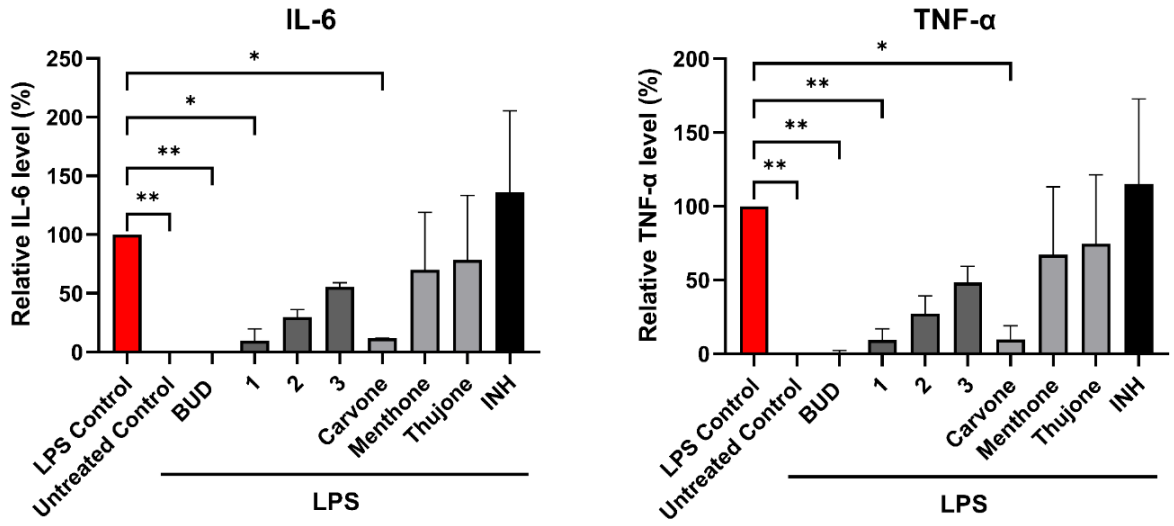

Supplementary Figure 4: Expression of pro-inflammatory cytokines TNF-α and IL-6 in LPS-induced THP-1-derived macrophages treated with 320uM of compounds 1–3, carvone, menthone and thujone for 24 hours. BUD – budesonide (1 μM), positive control. Data shown are mean ± SD. * $p < 0.05$; ** $p < 0.01$; n = 3. [Data obtained from HIPS institute]

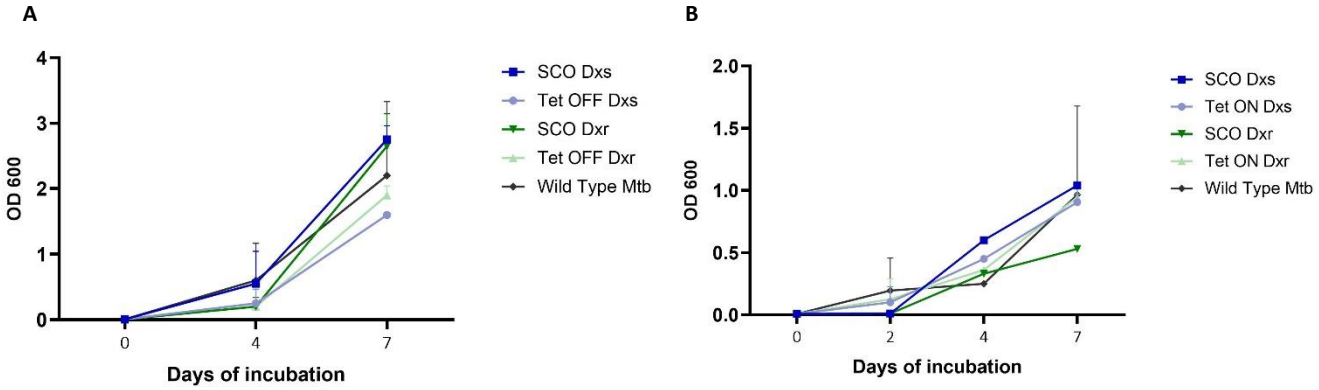

Supplementary Figure 5: Normal growth phenotype of Promoter replacement mutants with respect to Wild Type Mtb. SCO mutants were successfully generated by homologous recombination cultured in growth media with 25ug/ml of hygromycin. Further the Tet OFF and Tet ON mutants were generated by electroporating the plasmid containing the regulatory proteins rev TetR and TetR respectively. These mutants were grown in growth media containing hygromycin and kanamycin (25ug/ml). The growth of all the strains along with Mtb H37Rv ATCC 27294 was monitored by measuring the OD600 over 7 days. Two independent experiments were performed and graphs were plotted using GraphPad. [A] Growth of SCO, TetOFF (for Dxs and Dxr) and Wild type Mtb under normal growth conditions. [B] Growth of SCO, TetON (for Dxs and Dxr) and Wild type Mtb under normal growth conditions. (SCO: Singly crossover mutants)

Supplementary Figure 6: sgRNA sequence alignment. The selected sgRNA (template)was aligned with the results from Sanger sequencing for two replicates (sgRNA_A and sgRNA_B) for each mutant. From top to bottom: sgRNA alignment for Dxs, Dxr, RpoB and Non-Targeting. Alignment performed using Clustal Omega (https://www.ebi.ac.uk/jdispatcher/msa/clustalo)

Supplementary Table 4: Next-generation sequencing alignment of Single Crossover mutants with the expected construct. Dxs is alignment with the contig00011 obtained from NGS sequencing. Dxr is aligned with both contig00005 and contig00079.

The links provided below can be used to access the data from the software Geneious v2023.1.1 (https://www.geneious.com):

https://fzb-cloud.fz-borstel.de/s/EeAWcoWxS24GHfN
Password: NGSDXSDXR

Dxs:

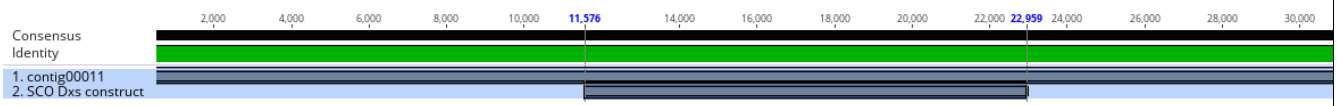

Dxr:

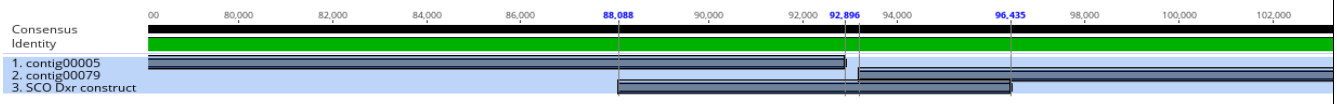

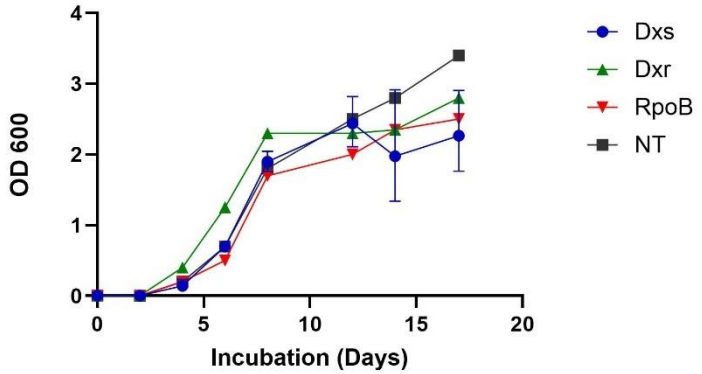

Supplementary Figure 7: Normal growth phenotype of CRISPRi mutants. After the successful transformation of CRISPRi plasmid in *Mycobacterium tuberculosis*, colonies were picked and cultures in growth media containing 25ug/ml kanamycin. The growth of all the mutants was monitored by OD600 measurement over 17 days and normal growth phenotype was observed in all mutants. Two technical replicates were used for the experiment and graphs were plotted using GraphPad Prism.

Bibliography

1. Courtens C, Risseeuw M, Caljon G, Cos P, Van Calenbergh S. Acyloxybenzyl and Alkoxyalkyl Prodrugs of a Fosmidomycin Surrogate as Antimalarial and Antitubercular Agents. ACS Med Chem Lett. 2018;9(10):986-9.
2. Kaufmann SHE, Schaible UE. 100th anniversary of Robert Koch's Nobel Prize for the discovery of the tubercle bacillus. Trends in Microbiology. 2005;13(10):469-75.
3. Bagcchi S. WHO's Global Tuberculosis Report 2022. Lancet Microbe. 2023;4(1):e20.
4. Flynn JL, Chan J. Tuberculosis: latency and reactivation. Infect Immun. 2001;69(7):4195-201.
5. Acharya B, Acharya A, Gautam S, Ghimire SP, Mishra G, Parajuli N, Sapkota B. Advances in diagnosis of Tuberculosis: an update into molecular diagnosis of Mycobacterium tuberculosis. Mol Biol Rep. 2020;47(5):4065-75.
6. Leung AN. Pulmonary tuberculosis: the essentials. Radiology. 1999;210(2):307-22.
7. Luies L, du Preez I. The Echo of Pulmonary Tuberculosis: Mechanisms of Clinical Symptoms and Other Disease-Induced Systemic Complications. Clin Microbiol Rev. 2020;33(4).
8. Schluger NW. The pathogenesis of tuberculosis: the first one hundred (and twenty-three) years. Am J Respir Cell Mol Biol. 2005;32(4):251-6.
9. Russell DG, Cardona PJ, Kim MJ, Allain S, Altare F. Foamy macrophages and the progression of the human tuberculosis granuloma. Nat Immunol. 2009;10(9):943-8.
10. Huszar S, Chibale K, Singh V. The quest for the holy grail: new antitubercular chemical entities, targets and strategies. Drug Discov Today. 2020;25(4):772-80.
11. Chai Q, Zhang Y, Liu CH. Mycobacterium tuberculosis: An Adaptable Pathogen Associated With Multiple Human Diseases. Front Cell Infect Microbiol. 2018;8:158.
12. Marrakchi H, Laneelle MA, Daffe M. Mycolic acids: structures, biosynthesis, and beyond. Chem Biol. 2014;21(1):67-85.
13. Peyron P, Vaubourgeix J, Poquet Y, Levillain F, Botanch C, Bardou F, et al. Foamy macrophages from tuberculous patients' granulomas constitute a nutrient-rich reservoir for M. tuberculosis persistence. PLoS Pathog. 2008;4(11):e1000204.
14. Grosset J. Mycobacterium tuberculosis in the extracellular compartment: an underestimated adversary. Antimicrob Agents Chemother. 2003;47(3):833-6.
15. REPORT of the Committee on Therapy [American Trudeau Society]. Am Rev Tuberc. 1946;54(4-5):439-43.
16. Bi K, Cao D, Ding C, Lu S, Lu H, Zhang G, et al. The past, present and future of tuberculosis treatment. Zhejiang Da Xue Xue Bao Yi Xue Ban. 2022;51(6):657-68.
17. Wulandari DA, Hartati YW, Ibrahim AU, Pitaloka DAE, Irkham. Multidrug-resistant tuberculosis. Clin Chim Acta. 2024;559:119701.
18. WHO. Meeting Report of the WHO Expert Consultation on Drug-Resistant Tuberculosis Treatment Outcome Definitions. World Health Organization2021.
19. Gu P, Lu P, Ding H, Liu Q, Ding X, Chen Y, Zhu L. Effectiveness, cost, and safety of four regimens recommended by WHO for RR/MDR-TB treatment: a cohort study in Eastern China. Ann Med. 2024;56(1):2344821.
20. Ramachandran G, Swaminathan S. Safety and tolerability profile of second-line anti-tuberculosis medications. Drug Saf. 2015;38(3):253-69.
21. Furin J, Cox H, Pai M. Tuberculosis. Lancet. 2019;393(10181):1642-56.
22. Ehrt S, Schnappinger D, Rhee KY. Metabolic principles of persistence and pathogenicity in Mycobacterium tuberculosis. Nat Rev Microbiol. 2018;16(8):496-507.
23. Cole ST, Brosch R, Parkhill J, Garnier T, Churcher C, Harris D, et al. Deciphering the biology of Mycobacterium tuberculosis from the complete genome sequence. Nature. 1998;393(6685):537-44.
24. Hughes JP, Rees S, Kalindjian SB, Philpott KL. Principles of early drug discovery. Br J Pharmacol. 2011;162(6):1239-49.

25. Grzelak EM, Choules MP, Gao W, Cai G, Wan B, Wang Y, et al. Strategies in anti-Mycobacterium tuberculosis drug discovery based on phenotypic screening. J Antibiot (Tokyo). 2019;72(10):719-28.
26. Kana BD, Karakousis PC, Parish T, Dick T. Future target-based drug discovery for tuberculosis? Tuberculosis (Edinb). 2014;94(6):551-6.
27. Franzblau SG, DeGroote MA, Cho SH, Andries K, Nuermberger E, Orme IM, et al. Comprehensive analysis of methods used for the evaluation of compounds against Mycobacterium tuberculosis. Tuberculosis (Edinb). 2012;92(6):453-88.
28. Manjunatha UH, Smith PW. Perspective: Challenges and opportunities in TB drug discovery from phenotypic screening. Bioorg Med Chem. 2015;23(16):5087-97.
29. Zheng W, Thorne N, McKew JC. Phenotypic screens as a renewed approach for drug discovery. Drug Discov Today. 2013;18(21-22):1067-73.
30. Vincent F, Nueda A, Lee J, Schenone M, Prunotto M, Mercola M. Phenotypic drug discovery: recent successes, lessons learned and new directions. Nat Rev Drug Discov. 2022;21(12):899-914.
31. Gilbert-Girard S, Savijoki K, Yli-Kauhaluoma J, Fallarero A. Optimization of a High-Throughput 384-Well Plate-Based Screening Platform with Staphylococcus aureus ATCC 25923 and Pseudomonas aeruginosa ATCC 15442 Biofilms. Int J Mol Sci. 2020;21(9).
32. Katsuno K, Burrows JN, Duncan K, Hooft van Huijsduijnen R, Kaneko T, Kita K, et al. Hit and lead criteria in drug discovery for infectious diseases of the developing world. Nat Rev Drug Discov. 2015;14(11):751-8.
33. McKenna L. Treatment Action group, Pipeline Report 2023 Tuberculosis treatment. December 2023.
34. Palomino JC, Martin A. TMC207 becomes bedaquiline, a new anti-TB drug. Future Microbiol. 2013;8(9):1071-80.
35. Diacon AH, Dawson R, Von Groote-Bidlingmaier F, Symons G, Venter A, Donald PR, et al. Randomized dose-ranging study of the 14-day early bactericidal activity of bedaquiline (TMC207) in patients with sputum microscopy smear-positive pulmonary tuberculosis. Antimicrob Agents Chemother. 2013;57(5):2199-203.
36. Diacon AH, Pym A, Grobusch M, Patientia R, Rustomjee R, Page-Shipp L, et al. The diarylquinoline TMC207 for multidrug-resistant tuberculosis. N Engl J Med. 2009;360(23):2397-405.
37. Alsayed SSR, Gunosewoyo H. Tuberculosis: Pathogenesis, Current Treatment Regimens and New Drug Targets. Int J Mol Sci. 2023;24(6).
38. Stover CK, Warrener P, VanDevanter DR, Sherman DR, Arain TM, Langhorne MH, et al. A small-molecule nitroimidazopyran drug candidate for the treatment of tuberculosis. Nature. 2000;405(6789):962-6.
39. Keam SJ. Pretomanid: First Approval. Drugs. 2019;79(16):1797-803.
40. Manjunatha U, Boshoff HI, Barry CE. The mechanism of action of PA-824: Novel insights from transcriptional profiling. Commun Integr Biol. 2009;2(3):215-8.
41. Singh R, Manjunatha U, Boshoff HI, Ha YH, Niyomrattanakit P, Ledwidge R, et al. PA-824 kills nonreplicating Mycobacterium tuberculosis by intracellular NO release. Science. 2008;322(5906):1392-5.
42. Manjunatha UH, Boshoff H, Dowd CS, Zhang L, Albert TJ, Norton JE, et al. Identification of a nitroimidazo-oxazine-specific protein involved in PA-824 resistance in Mycobacterium tuberculosis. Proc Natl Acad Sci U S A. 2006;103(2):431-6.
43. Matsumoto M, Hashizume H, Tomishige T, Kawasaki M, Tsubouchi H, Sasaki H, et al. OPC-67683, a nitro-dihydro-imidazooxazole derivative with promising action against tuberculosis in vitro and in mice. PLoS Med. 2006;3(11):e466.
44. Diacon AH, Dawson R, Hanekom M, Narunsky K, Venter A, Hittel N, et al. Early bactericidal activity of delamanid (OPC-67683) in smear-positive pulmonary tuberculosis patients. Int J Tuberc Lung Dis. 2011;15(7):949-54.
45. Gler MT, Skripconoka V, Sanchez-Garavito E, Xiao H, Cabrera-Rivero JL, Vargas-Vasquez DE, et al. Delamanid for multidrug-resistant pulmonary tuberculosis. N Engl J Med. 2012;366(23):2151-60.

46. Nasiri MJ, Zangiabadian M, Arabpour E, Amini S, Khalili F, Centis R, et al. Delamanid-containing regimens and multidrug-resistant tuberculosis: A systematic review and meta-analysis. Int J Infect Dis. 2022;124 Suppl 1(Suppl 1):S90-S103.
47. Tadolini M, Lingtsang RD, Tiberi S, Enwerem M, D'Ambrosio L, Sadutshang TD, et al. First case of extensively drug-resistant tuberculosis treated with both delamanid and bedaquiline. Eur Respir J. 2016;48(3):935-8.
48. Trefzer C, Rengifo-Gonzalez M, Hinner MJ, Schneider P, Makarov V, Cole ST, Johnsson K. Benzothiazinones: prodrugs that covalently modify the decaprenylphosphoryl-beta-D-ribose 2'-epimerase DprE1 of Mycobacterium tuberculosis. J Am Chem Soc. 2010;132(39):13663-5.
49. Manina G, Pasca MR, Buroni S, De Rossi E, Riccardi G. Decaprenylphosphoryl-beta-D-ribose 2'-epimerase from Mycobacterium tuberculosis is a magic drug target. Curr Med Chem. 2010;17(27):3099-108.
50. Imran M, Khan SA, Asdaq SMB, Almehmadi M, Abdulaziz O, Kamal M, et al. An insight into the discovery, clinical studies, compositions, and patents of macozinone: A drug targeting the DprE1 enzyme of Mycobacterium tuberculosis. J Infect Public Health. 2022;15(10):1097-107.
51. Pethe K, Bifani P, Jang J, Kang S, Park S, Ahn S, et al. Discovery of Q203, a potent clinical candidate for the treatment of tuberculosis. Nat Med. 2013;19(9):1157-60.
52. Malik I, Cizmarik J, Kovac G, Pechacova M, Hudecova L. Telacebec (Q203): Is there a novel effective and safe anti-tuberculosis drug on the horizon? Ceska Slov Farm. 2021;70(5):164-71.
53. Sacksteder KA, Protopopova M, Barry CE, 3rd, Andries K, Nacy CA. Discovery and development of SQ109: a new antitubercular drug with a novel mechanism of action. Future Microbiol. 2012;7(7):823-37.
54. Protopopova M, Hanrahan C, Nikonenko B, Samala R, Chen P, Gearhart J, et al. Identification of a new antitubercular drug candidate, SQ109, from a combinatorial library of 1,2-ethylenediamines. J Antimicrob Chemother. 2005;56(5):968-74.
55. Song T, Lee M, Jeon HS, Park Y, Dodd LE, Dartois V, et al. Linezolid Trough Concentrations Correlate with Mitochondrial Toxicity-Related Adverse Events in the Treatment of Chronic Extensively Drug-Resistant Tuberculosis. EBioMedicine. 2015;2(11):1627-33.
56. Yano T, Kassovska-Bratinova S, Teh JS, Winkler J, Sullivan K, Isaacs A, et al. Reduction of clofazimine by mycobacterial type 2 NADH:quinone oxidoreductase: a pathway for the generation of bactericidal levels of reactive oxygen species. J Biol Chem. 2011;286(12):10276-87.
57. Lechartier B, Cole ST. Mode of Action of Clofazimine and Combination Therapy with Benzothiazinones against Mycobacterium tuberculosis. Antimicrob Agents Chemother. 2015;59(8):4457-63.
58. Zhang D, Lu Y, Liu K, Liu B, Wang J, Zhang G, et al. Identification of less lipophilic riminophenazine derivatives for the treatment of drug-resistant tuberculosis. J Med Chem. 2012;55(19):8409-17.
59. Miyazaki E, Miyazaki M, Chen JM, Chaisson RE, Bishai WR. Moxifloxacin (BAY12-8039), a new 8-methoxyquinolone, is active in a mouse model of tuberculosis. Antimicrob Agents Chemother. 1999;43(1):85-9.
60. Ji B, Lounis N, Maslo C, Truffot-Pernot C, Bonnafous P, Grosset J. In vitro and in vivo activities of moxifloxacin and clinafloxacin against Mycobacterium tuberculosis. Antimicrob Agents Chemother. 1998;42(8):2066-9.
61. Shee S, Singh S, Tripathi A, Thakur C, Kumar TA, Das M, et al. Moxifloxacin-Mediated Killing of Mycobacterium tuberculosis Involves Respiratory Downshift, Reductive Stress, and Accumulation of Reactive Oxygen Species. Antimicrob Agents Chemother. 2022;66(9):e0059222.
62. Nunn AJ, Rusen ID, Van Deun A, Torrea G, Phillips PP, Chiang CY, et al. Evaluation of a standardized treatment regimen of anti-tuberculosis drugs for patients with multi-drug-resistant tuberculosis (STREAM): study protocol for a randomized controlled trial. Trials. 2014;15:353.
63. Tweed CD, Wills GH, Crook AM, Amukoye E, Balanag V, Ban AYL, et al. A partially randomised trial of pretomanid, moxifloxacin and pyrazinamide for pulmonary TB. Int J Tuberc Lung Dis. 2021;25(4):305-14.
64. WHO consolidated guidelines on tuberculosis: Module 4: treatment - drug-resistant tuberculosis treatment, 2022 update. WHO Guidelines Approved by the Guidelines Review Committee. Geneva2022.

65. Verma S, Prabhakar YS. Target based drug design - a reality in virtual sphere. Curr Med Chem. 2015;22(13):1603-30.
66. Sassetti CM, Boyd DH, Rubin EJ. Comprehensive identification of conditionally essential genes in mycobacteria. Proc Natl Acad Sci U S A. 2001;98(22):12712-7.
67. Sassetti CM, Boyd DH, Rubin EJ. Genes required for mycobacterial growth defined by high density mutagenesis. Mol Microbiol. 2003;48(1):77-84.
68. DeJesus MA, Gerrick ER, Xu W, Park SW, Long JE, Boutte CC, et al. Comprehensive Essentiality Analysis of the Mycobacterium tuberculosis Genome via Saturating Transposon Mutagenesis. mBio. 2017;8(1).
69. Rengarajan J, Bloom BR, Rubin EJ. Genome-wide requirements for Mycobacterium tuberculosis adaptation and survival in macrophages. Proc Natl Acad Sci U S A. 2005;102(23):8327-32.
70. Smith CM, Baker RE, Proulx MK, Mishra BB, Long JE, Park SW, et al. Host-pathogen genetic interactions underlie tuberculosis susceptibility in genetically diverse mice. Elife. 2022;11.
71. Hingley-Wilson SM, Sambandamurthy VK, Jacobs WR, Jr. Survival perspectives from the world's most successful pathogen, Mycobacterium tuberculosis. Nat Immunol. 2003;4(10):949-55.
72. Bosch B, DeJesus MA, Poulton NC, Zhang W, Engelhart CA, Zaveri A, et al. Genome-wide gene expression tuning reveals diverse vulnerabilities of M. tuberculosis. Cell. 2021;184(17):4579-92 e24.
73. Evans JC, Mizrahi V. The application of tetracyclineregulated gene expression systems in the validation of novel drug targets in Mycobacterium tuberculosis. Front Microbiol. 2015;6:812.
74. Singh V, Mizrahi V. Identification and validation of novel drug targets in Mycobacterium tuberculosis. Drug Discov Today. 2017;22(3):503-9.
75. Yuan T, Sampson NS. Hit Generation in TB Drug Discovery: From Genome to Granuloma. Chem Rev. 2018;118(4):1887-916.
76. Warner DF, Evans JC, Mizrahi V. Nucleotide Metabolism and DNA Replication. Microbiol Spectr. 2014;2(5).
77. Du X, Sonawane V, Zhang B, Wang C, de Ruijter B, Domling ASS, et al. Inhibitors of Aspartate Transcarbamoylase Inhibit Mycobacterium tuberculosis Growth. ChemMedChem. 2023;18(17):e202300279.
78. Sun W, Tanaka TQ, Magle CT, Huang W, Southall N, Huang R, et al. Chemical signatures and new drug targets for gametocytocidal drug development. Sci Rep. 2014;4:3743.
79. Lunev S, Bosch SS, Batista Fde A, Wrenger C, Groves MR. Crystal structure of truncated aspartate transcarbamoylase from Plasmodium falciparum. Acta Crystallogr F Struct Biol Commun. 2016;72(Pt 7):523-33.
80. Wang C, Zhang B, Kruger A, Du X, Visser L, Domling ASS, et al. Discovery of Small-Molecule Allosteric Inhibitors of PfATC as Antimalarials. J Am Chem Soc. 2022;144(41):19070-7.
81. Bardou F, Raynaud C, Ramos C, Laneelle MA, Lanrelle G. Mechanism of isoniazid uptake in Mycobacterium tuberculosis. Microbiology (Reading). 1998;144 (Pt 9):2539-44.
82. Zhang Y, Heym B, Allen B, Young D, Cole S. The catalase-peroxidase gene and isoniazid resistance of Mycobacterium tuberculosis. Nature. 1992;358(6387):591-3.
83. Wengenack NL, Jensen MP, Rusnak F, Stern MK. Mycobacterium tuberculosis KatG is a peroxynitritase. Biochem Biophys Res Commun. 1999;256(3):485-7.
84. Singh R, Wiseman B, Deemagarn T, Donald LJ, Duckworth HW, Carpena X, et al. Catalase-peroxidases (KatG) exhibit NADH oxidase activity. J Biol Chem. 2004;279(41):43098-106.
85. Ghiladi RA, Medzihradszky KF, Rusnak FM, Ortiz de Montellano PR. Correlation between isoniazid resistance and superoxide reactivity in mycobacterium tuberculosis KatG. J Am Chem Soc. 2005;127(38):13428-42.
86. Zhao X, Yu H, Yu S, Wang F, Sacchettini JC, Magliozzo RS. Hydrogen peroxide-mediated isoniazid activation catalyzed by Mycobacterium tuberculosis catalase-peroxidase (KatG) and its S315T mutant. Biochemistry. 2006;45(13):4131-40.
87. Wengenack NL, Rusnak F. Evidence for isoniazid-dependent free radical generation catalyzed by Mycobacterium tuberculosis KatG and the isoniazid-resistant mutant KatG(S315T). Biochemistry. 2001;40(30):8990-6.

88. Rozwarski DA, Grant GA, Barton DH, Jacobs WR, Jr., Sacchettini JC. Modification of the NADH of the isoniazid target (InhA) from Mycobacterium tuberculosis. Science. 1998;279(5347):98-102.
89. Banerjee A, Dubnau E, Quemard A, Balasubramanian V, Um KS, Wilson T, et al. inhA, a gene encoding a target for isoniazid and ethionamide in Mycobacterium tuberculosis. Science. 1994;263(5144):227-30.
90. Christianson DW. Structural and Chemical Biology of Terpenoid Cyclases. Chem Rev. 2017;117(17):11570-648.
91. Mahizan NA, Yang SK, Moo CL, Song AA, Chong CM, Chong CW, et al. Terpene Derivatives as a Potential Agent against Antimicrobial Resistance (AMR) Pathogens. Molecules. 2019;24(14).
92. Ludwiczuk A, Skalicka-Woźniak K, Georgiev MI. Chapter 11 - Terpenoids. In: Badal S, Delgoda R, editors. Pharmacognosy. Boston: Academic Press; 2017. p. 233-66.
93. Holstein SA. Chapter 12 - The Isoprenoid Biosynthetic Pathway and Statins. In: Hrycyna CA, Bergo MO, Tamanoi F, editors. The Enzymes. 30: Academic Press; 2011. p. 279-99.
94. Gershenzon J, Dudareva N. The function of terpene natural products in the natural world. Nat Chem Biol. 2007;3(7):408-14.
95. Obiol-Pardo C, Rubio-Martinez J, Imperial S. The methylerythritol phosphate (MEP) pathway for isoprenoid biosynthesis as a target for the development of new drugs against tuberculosis. Curr Med Chem. 2011;18(9):1325-38.
96. Masini T, Hirsch AK. Development of inhibitors of the 2C-methyl-D-erythritol 4-phosphate (MEP) pathway enzymes as potential anti-infective agents. J Med Chem. 2014;57(23):9740-63.
97. Lynen F. Biosynthetic pathways from acetate to natural products. Pure Appl Chem. 1967;14(1):137-67.
98. Katsuki H, Bloch K. Studies on the biosynthesis of ergosterol in yeast. Formation of methylated intermediates. J Biol Chem. 1967;242(2):222-7.
99. Rohmer M. The discovery of a mevalonate-independent pathway for isoprenoid biosynthesis in bacteria, algae and higher plants. Nat Prod Rep. 1999;16(5):565-74.
100. Arigoni D, Sagner S, Latzel C, Eisenreich W, Bacher A, Zenk MH. Terpenoid biosynthesis from 1-deoxy-D-xylulose in higher plants by intramolecular skeletal rearrangement. Proc Natl Acad Sci U S A. 1997;94(20):10600-5.
101. Zhao L, Chang WC, Xiao Y, Liu HW, Liu P. Methylerythritol phosphate pathway of isoprenoid biosynthesis. Annu Rev Biochem. 2013;82:497-530.
102. Wang X, Dowd CS. The Methylerythritol Phosphate Pathway: Promising Drug Targets in the Fight against Tuberculosis. ACS Infect Dis. 2018;4(3):278-90.
103. Cordoba E, Salmi M, Leon P. Unravelling the regulatory mechanisms that modulate the MEP pathway in higher plants. J Exp Bot. 2009;60(10):2933-43.
104. Hoqani UA, Leon R, Purton S. Over-expression of a cyanobacterial gene for 1-deoxy-d-xylulose-5-phosphate synthase in the chloroplast of Chlamydomonas reinhardtii perturbs chlorophyll: carotenoid ratios. J King Saud Univ Sci. 2022;34(6):None.
105. Henkel S, Frohnecke N, Maus D, McConville MJ, Laue M, Blume M, Seeber F. Toxoplasma gondii apicoplast-resident ferredoxin is an essential electron transfer protein for the MEP isoprenoid-biosynthetic pathway. J Biol Chem. 2022;298(1):101468.
106. He L, He P, Luo X, Li M, Yu L, Guo J, et al. The MEP pathway in Babesia orientalis apicoplast, a potential target for anti-babesiosis drug development. Parasit Vectors. 2018;11(1):452.
107. Guggisberg AM, Park J, Edwards RL, Kelly ML, Hodge DM, Tolia NH, Odom AR. A sugar phosphatase regulates the methylerythritol phosphate (MEP) pathway in malaria parasites. Nat Commun. 2014;5:4467.
108. Eoh H, Brennan PJ, Crick DC. The Mycobacterium tuberculosis MEP (2C-methyl-d-erythritol 4-phosphate) pathway as a new drug target. Tuberculosis (Edinb). 2009;89(1):1-11.
109. Hunter WN. The non-mevalonate pathway of isoprenoid precursor biosynthesis. J Biol Chem. 2007;282(30):21573-7.

110. Hill RE, Himmeldirk K, Kennedy IA, Pauloski RM, Sayer BG, Wolf E, Spenser ID. The biogenetic anatomy of vitamin B6. A 13C NMR investigation of the biosynthesis of pyridoxol in Escherichia coli. J Biol Chem. 1996;271(48):30426-35.
111. Begley TP, Downs DM, Ealick SE, McLafferty FW, Van Loon AP, Taylor S, et al. Thiamin biosynthesis in prokaryotes. Arch Microbiol. 1999;171(5):293-300.
112. Brown AC, Eberl M, Crick DC, Jomaa H, Parish T. The nonmevalonate pathway of isoprenoid biosynthesis in Mycobacterium tuberculosis is essential and transcriptionally regulated by Dxs. J Bacteriol. 2010;192(9):2424-33.
113. Jansson AM, Wieckowska A, Bjorkelid C, Yahiaoui S, Sooriyaarachchi S, Lindh M, et al. DXR inhibition by potent mono- and disubstituted fosmidomycin analogues. J Med Chem. 2013;56(15):6190-9.
114. Kunfermann A, Lienau C, Illarionov B, Held J, Grawert T, Behrendt CT, et al. IspC as target for antiinfective drug discovery: synthesis, enantiomeric separation, and structural biology of fosmidomycin thia isosters. J Med Chem. 2013;56(20):8151-62.
115. Umeda T, Tanaka N, Kusakabe Y, Nakanishi M, Kitade Y, Nakamura KT. Molecular basis of fosmidomycin's action on the human malaria parasite Plasmodium falciparum. Sci Rep. 2011;1:9.
116. Abrahams KA, Besra GS. Mycobacterial drug discovery. RSC Med Chem. 2020;11(12):1354-65.
117. Ginn J, Jiang X, Sun S, Michino M, Huggins DJ, Mbambo Z, et al. Whole Cell Active Inhibitors of Mycobacterial Lipoamide Dehydrogenase Afford Selectivity over the Human Enzyme through Tight Binding Interactions. ACS Infect Dis. 2021;7(2):435-44.
118. Warner DF, Mizrahi V. Approaches to target identification and validation for tuberculosis drug discovery: a UCT perspective. S Afr Med J. 2012;102(6):457-60.
119. Schnappinger D, Ehrt S. Regulated Expression Systems for Mycobacteria and Their Applications. Microbiol Spectr. 2014;2(1).
120. Wong AI, Rock JM. CRISPR Interference (CRISPRi) for Targeted Gene Silencing in Mycobacteria. Methods Mol Biol. 2021;2314:343-64.
121. Ehrt S, Schnappinger D. Controlling gene expression in mycobacteria. Future Microbiol. 2006;1(2):177-84.
122. Ehrt S, Guo XV, Hickey CM, Ryou M, Monteleone M, Riley LW, Schnappinger D. Controlling gene expression in mycobacteria with anhydrotetracycline and Tet repressor. Nucleic Acids Res. 2005;33(2):e21.
123. Abrahams GL, Kumar A, Savvi S, Hung AW, Wen S, Abell C, et al. Pathway-selective sensitization of Mycobacterium tuberculosis for target-based whole-cell screening. Chem Biol. 2012;19(7):844-54.
124. Rock JM, Hopkins FF, Chavez A, Diallo M, Chase MR, Gerrick ER, et al. Programmable transcriptional repression in mycobacteria using an orthogonal CRISPR interference platform. Nat Microbiol. 2017;2:16274.
125. Kolly GS, Boldrin F, Sala C, Dhar N, Hartkoorn RC, Ventura M, et al. Assessing the essentiality of the decaprenyl-phospho-d-arabinofuranose pathway in Mycobacterium tuberculosis using conditional mutants. Mol Microbiol. 2014;92(1):194-211.
126. Greendyke R, Rajagopalan M, Parish T, Madiraju M. Conditional expression of Mycobacterium smegmatis dnaA, an essential DNA replication gene. Microbiology (Reading). 2002;148(Pt 12):3887-900.
127. Carroll P, Faray-Kele MC, Parish T. Identifying vulnerable pathways in Mycobacterium tuberculosis by using a knockdown approach. Appl Environ Microbiol. 2011;77(14):5040-3.
128. Schnappinger D, O'Brien KM, Ehrt S. Construction of conditional knockdown mutants in mycobacteria. Methods Mol Biol. 2015;1285:151-75.
129. Guo XV, Monteleone M, Klotzsche M, Kamionka A, Hillen W, Braunstein M, et al. Silencing Mycobacterium smegmatis by using tetracycline repressors. J Bacteriol. 2007;189(13):4614-23.
130. Doudna JA, Charpentier E. Genome editing. The new frontier of genome engineering with CRISPR-Cas9. Science. 2014;346(6213):1258096.
131. Qi LS, Larson MH, Gilbert LA, Doudna JA, Weissman JS, Arkin AP, Lim WA. Repurposing CRISPR as an RNA-guided platform for sequence-specific control of gene expression. Cell. 2013;152(5):1173-83.

132. Gilbert LA, Horlbeck MA, Adamson B, Villalta JE, Chen Y, Whitehead EH, et al. Genome-Scale CRISPR-Mediated Control of Gene Repression and Activation. Cell. 2014;159(3):647-61.
133. McNeil MB, Cook GM. Utilization of CRISPR Interference To Validate MmpL3 as a Drug Target in Mycobacterium tuberculosis. Antimicrob Agents Chemother. 2019;63(8).
134. Brandenburg J, Marwitz S, Tazoll SC, Waldow F, Kalsdorf B, Vierbuchen T, et al. WNT6/ACC2-induced storage of triacylglycerols in macrophages is exploited by Mycobacterium tuberculosis. J Clin Invest. 2021;131(16).
135. Jumde RP, Guardigni M, Gierse RM, Alhayek A, Zhu D, Hamid Z, et al. Hit-optimization using target-directed dynamic combinatorial chemistry: development of inhibitors of the anti-infective target 1-deoxy-d-xylulose-5-phosphate synthase. Chem Sci. 2021;12(22):7775-85.
136. Kolbe K, Mockl L, Sohst V, Brandenburg J, Engel R, Malm S, et al. Azido Pentoses: A New Tool To Efficiently Label Mycobacterium tuberculosis Clinical Isolates. Chembiochem. 2017;18(13):1172-6.
137. Lee PY, Costumbrado J, Hsu CY, Kim YH. Agarose gel electrophoresis for the separation of DNA fragments. J Vis Exp. 2012(62).
138. Southern E. Southern blotting. Nat Protoc. 2006;1(2):518-25.
139. Baym M, Kryazhimskiy S, Lieberman TD, Chung H, Desai MM, Kishony R. Inexpensive multiplexed library preparation for megabase-sized genomes. PLoS One. 2015;10(5):e0128036.
140. Zuniga ES, Early J, Parish T. The future for early-stage tuberculosis drug discovery. Future Microbiol. 2015;10(2):217-29.
141. Ronald Kaminsky Cs, Reto Brun. An "In Vitro selectivity index" for evaluation of cytotoxicity of antitrypanosomal compounds. In vitro toxicology. 1996;9.
142. Lica JJ, Wieczor M, Grabe GJ, Heldt M, Jancz M, Misiak M, et al. Effective Drug Concentration and Selectivity Depends on Fraction of Primitive Cells. Int J Mol Sci. 2021;22(9).
143. Payne DJ, Gwynn MN, Holmes DJ, Pompliano DL. Drugs for bad bugs: confronting the challenges of antibacterial discovery. Nat Rev Drug Discov. 2007;6(1):29-40.
144. Heinrichs MT, May RJ, Heider F, Reimers T, SK BS, Peloquin CA, Derendorf H. Mycobacterium tuberculosis Strains H37ra and H37rv have equivalent minimum inhibitory concentrations to most antituberculosis drugs. Int J Mycobacteriol. 2018;7(2):156-61.
145. Ejalonibu MA, Ogundare SA, Elrashedy AA, Ejalonibu MA, Lawal MM, Mhlongo NN, Kumalo HM. Drug Discovery for Mycobacterium tuberculosis Using Structure-Based Computer-Aided Drug Design Approach. Int J Mol Sci. 2021;22(24).
146. Martini MC, Zhou Y, Sun H, Shell SS. Defining the Transcriptional and Post-transcriptional Landscapes of Mycobacterium smegmatis in Aerobic Growth and Hypoxia. Front Microbiol. 2019;10:591.
147. Shell SS, Wang J, Lapierre P, Mir M, Chase MR, Pyle MM, et al. Leaderless Transcripts and Small Proteins Are Common Features of the Mycobacterial Translational Landscape. PLoS Genet. 2015;11(11):e1005641.
148. Campbell EA, Korzheva N, Mustaev A, Murakami K, Nair S, Goldfarb A, Darst SA. Structural mechanism for rifampicin inhibition of bacterial rna polymerase. Cell. 2001;104(6):901-12.
149. Li MC, Lu J, Lu Y, Xiao TY, Liu HC, Lin SQ, et al. rpoB Mutations and Effects on Rifampin Resistance in Mycobacterium tuberculosis. Infect Drug Resist. 2021;14:4119-28.
150. Gleditzsch D, Pausch P, Muller-Esparza H, Ozcan A, Guo X, Bange G, Randau L. PAM identification by CRISPR-Cas effector complexes: diversified mechanisms and structures. RNA Biol. 2019;16(4):504-17.
151. Levitte S, Adams KN, Berg RD, Cosma CL, Urdahl KB, Ramakrishnan L. Mycobacterial Acid Tolerance Enables Phagolysosomal Survival and Establishment of Tuberculous Infection In Vivo. Cell Host Microbe. 2016;20(2):250-8.
152. Danilchanka O, Sun J, Pavlenok M, Maueroder C, Speer A, Siroy A, et al. An outer membrane channel protein of Mycobacterium tuberculosis with exotoxin activity. Proc Natl Acad Sci U S A. 2014;111(18):6750-5.
153. Cheung CY, McNeil MB, Cook GM. Utilization of CRISPR interference to investigate the contribution of genes to pathogenesis in a macrophage model of Mycobacterium tuberculosis infection. J Antimicrob Chemother. 2022;77(3):615-9.

154. Heilker R, Lessel U, Bischoff D. The power of combining phenotypic and target-focused drug discovery. Drug Discov Today. 2019;24(2):526-32.
155. Swinney DC. Phenotypic vs. target-based drug discovery for first-in-class medicines. Clin Pharmacol Ther. 2013;93(4):299-301.
156. Sadri A. Is Target-Based Drug Discovery Efficient? Discovery and "Off-Target" Mechanisms of All Drugs. J Med Chem. 2023;66(18):12651-77.
157. Miller CH, O'Toole RF. Navigating tuberculosis drug discovery with target-based screening. Expert Opin Drug Discov. 2011;6(8):839-54.
158. Bosch B, DeJesus MA, Schnappinger D, Rock JM. Weak links: Advancing target-based drug discovery by identifying the most vulnerable targets. Ann N Y Acad Sci. 2024.
159. Dalberto PF, de Souza EV, Abbadi BL, Neves CE, Rambo RS, Ramos AS, et al. Handling the Hurdles on the Way to Anti-tuberculosis Drug Development. Front Chem. 2020;8:586294.
160. van der Krift F, Zijlmans DW, Shukla R, Javed A, Koukos PI, Schwarz LL, et al. A novel antifolate suppresses growth of FPGS-deficient cells and overcomes methotrexate resistance. Life Sci Alliance. 2023;6(11).
161. Gleckman R, Blagg N, Joubert DW. Trimethoprim: mechanisms of action, antimicrobial activity, bacterial resistance, pharmacokinetics, adverse reactions, and therapeutic indications. Pharmacotherapy. 1981;1(1):14-20.
162. Nixon MR, Saionz KW, Koo MS, Szymonifka MJ, Jung H, Roberts JP, et al. Folate pathway disruption leads to critical disruption of methionine derivatives in Mycobacterium tuberculosis. Chem Biol. 2014;21(7):819-30.
163. Ogawa T, Uchida H, Kusumoto Y, Mori Y, Yamamura Y, Hamada S. Increase in tumor necrosis factor alpha- and interleukin-6-secreting cells in peripheral blood mononuclear cells from subjects infected with Mycobacterium tuberculosis. Infect Immun. 1991;59(9):3021-5.
164. Sharma S, Bose M. Role of cytokines in immune response to pulmonary tuberculosis. Asian Pac J Allergy Immunol. 2001;19(3):213-9.
165. Pagan AJ, Ramakrishnan L. Immunity and Immunopathology in the Tuberculous Granuloma. Cold Spring Harb Perspect Med. 2014;5(9).
166. Subbian S, Tsenova L, Holloway J, Peixoto B, O'Brien P, Dartois V, et al. Adjunctive Phosphodiesterase-4 Inhibitor Therapy Improves Antibiotic Response to Pulmonary Tuberculosis in a Rabbit Model. EBioMedicine. 2016;4:104-14.
167. Subbian S, Tsenova L, O'Brien P, Yang G, Koo MS, Peixoto B, et al. Phosphodiesterase-4 inhibition alters gene expression and improves isoniazid-mediated clearance of Mycobacterium tuberculosis in rabbit lungs. PLoS Pathog. 2011;7(9):e1002262.
168. Subbian S, Koo MS, Tsenova L, Khetani V, Zeldis JB, Fallows D, Kaplan G. Pharmacologic Inhibition of Host Phosphodiesterase-4 Improves Isoniazid-Mediated Clearance of Mycobacterium tuberculosis. Front Immunol. 2016;7:238.
169. Brennan PJ, Nikaido H. The envelope of mycobacteria. Annu Rev Biochem. 1995;64:29-63.
170. Singh A, Jain S, Gupta S, Das T, Tyagi AK. mymA operon of Mycobacterium tuberculosis: its regulation and importance in the cell envelope. FEMS Microbiol Lett. 2003;227(1):53-63.
171. Singh A, Gupta R, Vishwakarma RA, Narayanan PR, Paramasivan CN, Ramanathan VD, Tyagi AK. Requirement of the mymA operon for appropriate cell wall ultrastructure and persistence of Mycobacterium tuberculosis in the spleens of guinea pigs. J Bacteriol. 2005;187(12):4173-86.
172. Nguyen L, Thompson CJ. Foundations of antibiotic resistance in bacterial physiology: the mycobacterial paradigm. Trends Microbiol. 2006;14(7):304-12.
173. De Rossi E, Ainsa JA, Riccardi G. Role of mycobacterial efflux transporters in drug resistance: an unresolved question. FEMS Microbiol Rev. 2006;30(1):36-52.
174. Viveiros M, Leandro C, Amaral L. Mycobacterial efflux pumps and chemotherapeutic implications. Int J Antimicrob Agents. 2003;22(3):274-8.

175. da Silva PEA, Von Groll A, Martin A, Palomino JC. Efflux as a mechanism for drug resistance in Mycobacterium tuberculosis. FEMS Immunology & Medical Microbiology. 2011;63(1):1-9.
176. Omollo C, Singh V, Kigondu E, Wasuna A, Agarwal P, Moosa A, et al. Developing synergistic drug combinations to restore antibiotic sensitivity in drug-resistant Mycobacterium tuberculosis. Antimicrob Agents Chemother. 2023;65(5).
177. Wang Q, Boshoff HIM, Harrison JR, Ray PC, Green SR, Wyatt PG, Barry CE. PE/PPE proteins mediate nutrient transport across the outer membrane of Mycobacterium tuberculosis. Science. 2020;367(6482):1147-51.
178. Cook GM, Berney M, Gebhard S, Heinemann M, Cox RA, Danilchanka O, Niederweis M. Physiology of mycobacteria. Adv Microb Physiol. 2009;55:81-182, 318-9.
179. Schaaf K, Hayley V, Speer A, Wolschendorf F, Niederweis M, Kutsch O, Sun J. A Macrophage Infection Model to Predict Drug Efficacy Against Mycobacterium Tuberculosis. Assay Drug Dev Technol. 2016;14(6):345-54.
180. Liang T, Zhang R, Liu X, Ding Q, Wu S, Li C, et al. Recent Advances in Macrophage-Mediated Drug Delivery Systems. Int J Nanomedicine. 2021;16:2703-14.
181. Gordon S, Martinez-Pomares L. Physiological roles of macrophages. Pflugers Arch. 2017;469(3-4):365-74.
182. Schnappinger D, Ehrt S, Voskuil MI, Liu Y, Mangan JA, Monahan IM, et al. Transcriptional Adaptation of Mycobacterium tuberculosis within Macrophages: Insights into the Phagosomal Environment. J Exp Med. 2003;198(5):693-704.
183. Tan S, Sukumar N, Abramovitch RB, Parish T, Russell DG. Mycobacterium tuberculosis responds to chloride and pH as synergistic cues to the immune status of its host cell. PLoS Pathog. 2013;9(4):e1003282.
184. Larrouy-Maumus G, Marino LB, Madduri AV, Ragan TJ, Hunt DM, Bassano L, et al. Cell-Envelope Remodeling as a Determinant of Phenotypic Antibacterial Tolerance in Mycobacterium tuberculosis. ACS Infect Dis. 2016;2(5):352-60.
185. Prideaux B, Via LE, Zimmerman MD, Eum S, Sarathy J, O'Brien P, et al. The association between sterilizing activity and drug distribution into tuberculosis lesions. Nat Med. 2015;21(10):1223-7.
186. Pisu D, Huang L, Grenier JK, Russell DG. Dual RNA-Seq of Mtb-Infected Macrophages In Vivo Reveals Ontologically Distinct Host-Pathogen Interactions. Cell Rep. 2020;30(2):335-50 e4.
187. Via LE, Lin PL, Ray SM, Carrillo J, Allen SS, Eum SY, et al. Tuberculous granulomas are hypoxic in guinea pigs, rabbits, and nonhuman primates. Infect Immun. 2008;76(6):2333-40.
188. Marakalala MJ, Raju RM, Sharma K, Zhang YJ, Eugenin EA, Prideaux B, et al. Inflammatory signaling in human tuberculosis granulomas is spatially organized. Nat Med. 2016;22(5):531-8.
189. Kjellsson MC, Via LE, Goh A, Weiner D, Low KM, Kern S, et al. Pharmacokinetic evaluation of the penetration of antituberculosis agents in rabbit pulmonary lesions. Antimicrob Agents Chemother. 2012;56(1):446-57.
190. Ellard GA, Humphries MJ, Allen BW. Cerebrospinal fluid drug concentrations and the treatment of tuberculous meningitis. Am Rev Respir Dis. 1993;148(3):650-5.
191. Mendoza-Aguilar M, Almaguer-Villagran L, Jimenez-Arellanes A, Arce-Paredes P, Cid-Gutierrez JL, Rojas-Espinosa O. The use of the microplate alamar blue assay (MABA) to assess the susceptibility of Mycobacterium lepraemurium to anti-leprosy and other drugs. J Infect Chemother. 2012;18(5):652-61.
192. Arora K, Ochoa-Montano B, Tsang PS, Blundell TL, Dawes SS, Mizrahi V, et al. Respiratory flexibility in response to inhibition of cytochrome C oxidase in Mycobacterium tuberculosis. Antimicrob Agents Chemother. 2014;58(11):6962-5.
193. Wei JR, Krishnamoorthy V, Murphy K, Kim JH, Schnappinger D, Alber T, et al. Depletion of antibiotic targets has widely varying effects on growth. Proc Natl Acad Sci U S A. 2011;108(10):4176-81.
194. Lakshminarayana SB, Huat TB, Ho PC, Manjunatha UH, Dartois V, Dick T, Rao SP. Comprehensive physicochemical, pharmacokinetic and activity profiling of anti-TB agents. J Antimicrob Chemother. 2015;70(3):857-67.
195. Blumenthal A, Trujillo C, Ehrt S, Schnappinger D. Simultaneous analysis of multiple Mycobacterium tuberculosis knockdown mutants in vitro and in vivo. PLoS One. 2010;5(12):e15667.

196. Woong Park S, Klotzsche M, Wilson DJ, Boshoff HI, Eoh H, Manjunatha U, et al. Evaluating the sensitivity of Mycobacterium tuberculosis to biotin deprivation using regulated gene expression. PLoS Pathog. 2011;7(9):e1002264.
197. Leblanc C, Prudhomme T, Tabouret G, Ray A, Burbaud S, Cabantous S, et al. 4'-Phosphopantetheinyl transferase PptT, a new drug target required for Mycobacterium tuberculosis growth and persistence in vivo. PLoS Pathog. 2012;8(12):e1003097.
198. Gandotra S, Schnappinger D, Monteleone M, Hillen W, Ehrt S. In vivo gene silencing identifies the Mycobacterium tuberculosis proteasome as essential for the bacteria to persist in mice. Nat Med. 2007;13(12):1515-20.
199. Shi F, Luan M, Li Y. Ribosomal binding site sequences and promoters for expressing glutamate decarboxylase and producing gamma-aminobutyrate in Corynebacterium glutamicum. AMB Express. 2018;8(1):61.
200. Khare G, Kar R, Tyagi AK. Identification of inhibitors against Mycobacterium tuberculosis thiamin phosphate synthase, an important target for the development of anti-TB drugs. PLoS One. 2011;6(7):e22441.
201. Du Q, Wang H, Xie J. Thiamin (vitamin B1) biosynthesis and regulation: a rich source of antimicrobial drug targets? Int J Biol Sci. 2011;7(1):41-52.
202. Park Y, Pacitto A, Bayliss T, Cleghorn LA, Wang Z, Hartman T, et al. Essential but Not Vulnerable: Indazole Sulfonamides Targeting Inosine Monophosphate Dehydrogenase as Potential Leads against Mycobacterium tuberculosis. ACS Infect Dis. 2017;3(1):18-33.
203. Cui L, Vigouroux A, Rousset F, Varet H, Khanna V, Bikard D. A CRISPRi screen in E. coli reveals sequence-specific toxicity of dCas9. Nat Commun. 2018;9(1):1912.
204. Fu Y, Foden JA, Khayter C, Maeder ML, Reyon D, Joung JK, Sander JD. High-frequency off-target mutagenesis induced by CRISPR-Cas nucleases in human cells. Nat Biotechnol. 2013;31(9):822-6.
205. Hsu PD, Scott DA, Weinstein JA, Ran FA, Konermann S, Agarwala V, et al. DNA targeting specificity of RNA-guided Cas9 nucleases. Nat Biotechnol. 2013;31(9):827-32.
206. Wang H, La Russa M, Qi LS. CRISPR/Cas9 in Genome Editing and Beyond. Annu Rev Biochem. 2016;85:227-64.
207. Richter MF, Zhao KT, Eton E, Lapinaite A, Newby GA, Thuronyi BW, et al. Phage-assisted evolution of an adenine base editor with improved Cas domain compatibility and activity. Nat Biotechnol. 2020;38(7):883-91.
208. O'Geen H, Henry IM, Bhakta MS, Meckler JF, Segal DJ. A genome-wide analysis of Cas9 binding specificity using ChIP-seq and targeted sequence capture. Nucleic Acids Res. 2015;43(6):3389-404.
209. Naeem M, Majeed S, Hoque MZ, Ahmad I. Latest Developed Strategies to Minimize the Off-Target Effects in CRISPR-Cas-Mediated Genome Editing. Cells. 2020;9(7).
210. Lo HP, Lim YW, Xiong Z, Martel N, Ferguson C, Ariotti N, et al. Cavin4 interacts with Bin1 to promote T-tubule formation and stability in developing skeletal muscle. J Cell Biol. 2021;220(12).

List of abbreviations

Abbreviation	Name
approx.	approximately
Atc	Anhydrotetracycline
ATCase	Aspartate transcarbamoylase
ATCC	American Type Culture Collection
BBQ	BlackBerry quencher
BCG	bacille Calmette-Guérin
BD	Becton Dickinson
bp	base pairs
BS	Blocking solution
BSA	Bovine serum albumin
BSL-3	Biosafety level-3
CC90	Cytotoxic Concentration 90
CCE	counterflow centrifugal elutriation
CFU	Colony Forming Units
CP	Carbamoyl phosphate
CP-ASP	Carbamoyl-aspartate
CRISPRi	Clustered Regularly Interspaced Short Palindromic Repeats interference
CSS	Colour substrate solution
DCR	derived count rate
DHFR	Dihydrofolate Reductase
DMAPP	Dimethylallyl diphosphate
DMSO	Dimethyl sulfoxide
DNA	Deoxyribonucleic acid
DprE1	decaprenyl-phosphoribose epimerase
DS-LB	Double strength Luria-Bertani
DTT	Dithiothreitol
DXP	1-deoxy-D-xylulose 5-phosphate
DXR	1-Deoxy-D-xylulose-5-phosphate Reductoisomerase
DXS	1-Deoxy-D-xylulose-5-phosphate Synthase
EMB	ethambutol
FAM	Carboxyfluorescein
FDA	Food and Drug Administration

G3P	Glyceraldehyde 3-phosphate
HBSS	Hanks' Balanced Salt Solution
HIPS	Helmholtz-Institut für Pharmazeutische Forschung Saarland
HMdM	Human Monocyte-derived Macrophages
hyg	hygromycin
IC50	Inhibition concentration 50
i.e	That is
IL-6	Interleukin 6
iMIC90	Intracellular Minimum inhibitory concentration 90
INH	isoniazid
IPP	Isopentenyl diphosphate
Kan	kanamycin
kb	kilobase
L-ASP	L-aspartate
LB	Luria-Bertani
LSB	low stringency buffer
LTBI	latent TB infections
M-CSF	macrophage colony-stimulating factor
MDR-TB	Multidrug-resistant tuberculosis
MEP	Methylerythritol phosphate
MIC	Minimum Inhibitory Concentration
min	minutes
MOI	Multiplicity of infection
mRNA	messenger Ribonucleic acid
MVA	Mevalonate
Mtb	*Mycobacterium tuberculosis*
NADH	Nicotinamide adenine dinucleotide hydrogen
NCBI	National Center for Biotechnology Information
NF	Nuclease free
NGS	Next-Generation sequencing
NT	nontargeting
OADC	oleic acid-albumin-dextrose-catalase
OD	Optical Density
PAM	protospacer adjacent motif
PBMC	peripheral blood mononuclear cell
PBS	Phosphate Buffered Saline
PCR	Polymerase chain reaction

PES	polyethersulfone
Pf	*Plasmodium falciparum*
PYZ	pyrazinamide
QFT	QuantiFERON-TB Gold
rcf	relative centrifugal force
RED	Restriction enzyme digestion
Rev	reverse
RIF	rifampicin
RLU	Relative light units
RNA	Ribonucleic acid
ROS	Reactive oxygen species
rpm	Revolutions per minute
RPMI	Roswell Park Memorial Institute Medium
RR-TB	Rifampicin-resistant tuberculosis
RTCA	Real-Time Cell Analyzer
RT-qPCR	Real-Time Quantitative Reverse Transcription PCR
SCO	Single Crossover organisms
SD	Standard Deviation
SET	Sucrose EDTA Tris
sgRNA	small guide RNA
SNPs	single nucleotide polymorphisms
SP	Single Plate
SSC	Saline-sodium citrate
TAE	Tris-acetate-EDTA
TB	Tuberculosis
tetO	tet operator
TetR	tet repressor
TNF-α	Tumor necrosis factor-alpha
ul	microliter
ug	microgram
USA/US	United States of America
VI	Vulnerability Index
w/wo	with and without
WHO	World Health Organization
WT	Wild Type
XDR	Extensively drug-resistant tuberculosis

List of Figures

List of Tables

List of supplementary figures

List of supplementary tables

Acknowledgements

First and foremost, I would like to express my deepest gratitude to my supervisor, **PD Dr. Norbert Reiling**. His unwavering support, motivation, and open-door policy have been invaluable throughout my PhD journey. His belief in my abilities, along with his insightful advice and ideas, have been instrumental to the success of this project. Moreover, his friendly attitude always made me comfortable approaching him whenever needed, which greatly contributed to my ability to persevere through my PhD.

I would like to extend my gratitude to my practical supervisor, **Dr. Gareth Prosser**. Without his expertise and guidance, especially with molecular biology, this project would not have taken a positive turn. I've learned so much from him, and his out-of-the-box thinking has shaped my practical and professional development. His motivation always reminded me why I love science in the first place. Plus, the fun lab songs we created never failed to keep me motivated.

I would also like to extend my sincere thanks to my co-supervisor, **Prof. Dr Matthias Merker**. His constant availability and support, especially during challenging times, have been immensely helpful.

Big thanks to my awesome lab group: **Dr Julius Brandenburg**, **Svenja Goldenbaum, Lisa Niwinski, Caro Moller,** (the fun size) **Linda Zemke, and Simone Tazoll**. You guys have been amazing, from dealing with all the little lab annoyances to listening to me vent about Mtb. Your support made the lab a positive and fun working space which definitely helped with the stress.

Thanks also to the **MepAnti consortium** for all the advice and support. **Prof. Dr. Anna Hirsch**, your leadership throughout the Mepanti project has been incredible. **Prof. Dr Pascal Maser**, thanks for guiding me during my time in Switzerland, and **Peter Maas**, for the chemistry guidance in The Netherlands. To my MepAnti colleagues/friends—**Patricia, Maria, Thibaut, and the rest**—meeting such amazing people has been one of the highlights of this journey. Thanks for supporting me through the tough times and for all the laughter and gossips.

A big thank you to my friends **Jessica, Emilie, Monica, Claire, Lindsay and Gishnu**. You all made Borstel so much more than just a place of work. Thanks for the laughs at the lunch table until my stomach hurt (not from the canteen food); And a special thanks to my best people—**Vibha, Pit and Alejo** for tolerating me and truly getting me through it all.

Lastly, I owe a debt of gratitude to my family—**Mom, Dad, Bhaiya, and San**. Your endless love, support, and encouragement have been my foundation throughout my PhD and my career. Thank you for reminding me every day that I am not alone. I miss you all dearly and cannot thank you enough for being my forever support system throughout this journey. "Mom, I did it!"

Publications, conference presentations and awards

List of publications:

Du X, **Sonawane V**, Zhang B, Wang C, de Ruijter B, Domling ASS, et al. Inhibitors of Aspartate Transcarbamoylase Inhibit *Mycobacterium tuberculosis* Growth. ChemMedChem. 2023;18(17): e202300279. DOI: 10.1002/cmdc.202300279

Nesterkina M, **Sonawane V,** Latta L, Kany A, Rasheed S, Neu T, Reiling N, Vashchenko O, Lisetski L, Kravchenko I, Müller R, Lehr CM, Hirsch A. Terpenoid-based isoniazid derivatives against *Mycobacterium tuberculosis:* eutectic mixture-mediated synthesis, *in vitro* activity, and mechanistic insights.
Manuscript Status: in writing

Braun-Cornejo M; Ornago C; **Sonawane V**; Haupenthal J; Kany A; Diamanti E; Jézéquel G; Reiling N; Blankenfeldt W; Maas P; Hirsch A. Target-Directed Dynamic Combinatorial Chemistry Affords Binders of *Mycobacterium Tuberculosis* IspE
Manuscript Status: Submitted

Braun-Cornejo, Maria; Platteschorre, Mitchell; Vries, Vincent; Bravo, Patricia; **Sonawane V**; Hamed M.; Reiling N; Rottmann M; Haupenthal J; Piet D; Diamanti E; Maas P; Hirsch A. A Positive Charge in an Antimalarial Compound Unlocks Broad-spectrum Antibacterial Activity
Manuscript Status: Accepted

Awards:

- 2nd price winner at FameLab Karlsruhe, Germany, Science Communication Competition and selected for national level Famelab competition
- Best oral presenter award: MepAnti conference Saarbrucken, Germany
- Best oral presenter award: LCI summer school, Germany

Conference presentation:

- Clinical Tuberculosis 2024 symposium, DZIF, Borstel Germany
  20/06/2024 to 21/06/2024. **Oral Presentation**

- Tuberculosis: The Host-Pathogen Interface, Keystone, Colorado, Germany
  25/03/2024 to 28/03/2024. **POSTER**

- ECCMID 2022, Portugal, Lisbon
  23/04/2022 to 27/04/2022. **POSTER**

- Leibniz Conference on Bioactive Compounds, CSSB, Hamburg
  5/5/2022 to 6/5/2022. **POSTER**

- DZIF Conference, Stuttgart, Germany
  1/6/2022 to 3/6/2022. **POSTER**

- EMBO Workshop on Tuberculosis 2022, Paris, France
  12/10/2022 to 16/10/2022. **POSTER**

Curriculum vitae

Personal details:

Vidhisha Sonawane
Bramfelder strasse 38, Hamburg,
Contact: +4917674978434
Email: vsonawane@fz-borstel.de

Academic qualifications:

Nov 2020-July 2024	PhD candidate, Research Center Borstel, Germany (PD Dr Norbert Reiling)
Oct 2018 to July 2020	MSc. Microbiology, Radboud University, The Netherlands
Aug 2015 to Aug 2018	BSc Microbiology Fergusson, University Pune, India

Research experience:

Nov 2020-July 2024	Doctoral candidate at Research Centre Borstel/University of Lübeck, Germany, Group of PD. Dr Norbert Reiling
June 2022-July 2022	Visiting Researcher at Swiss Tropical Public Health Institute, Switzerland, Group of Prof. Dr Pascal Mäser
Oct 2023 to Nov 2023	Visiting Researcher at Specs-e-molecules, The Netherlands Reference: Peter Maas
Oct 2018 to Aug 2020	Master's projects at Radboud University, The Netherlands, Group of Dr. Jakko van Ingen Group of Prof. Dr. Mihai Netea

AREA OF EXPERTISE

- *In vitro* drug discovery/screening
- Working with *Mycobacterium* in BSL-3 laboratory
- Host-pathogen interactions using cell-based assays
- Molecular biology: Cloning, PCR, qPCR, Southern blotting etc.
- Target Validation with CRISPRi
- Bioinformatics with genomics, NGS, PacBio, DNA/RNA isolation

Awards

- Winner at FameLab Karlsruhe, Germany: Science Communication Competition
- Best oral communicator at MepAnti conference Saarbrucken, Germany
- Best oral communicator at LCI summer school, Germany
- Best oral communicator at Masters Symposium at Radboud University, The Netherlands